ISSN 2300-5599

ACTA INNOVATIONS

CENTRUM
BADAŃ I INNOWACJI
PRO - AKADEMIA
RESEARCH AND INNOVATION CENTRE

no. 26

January 2018

Acta Innovations

quarterly

no. 26

Konstantynów Łódzki, Poland, January 2018

ISSN 2300-5599

Original version: online journal

Online open access: www.proakademia.eu/en/acta-innovations

Articles published in this journal are peer-reviewed

Publisher:

Research and Innovation Centre Pro-Akademia
9/11 Innowacyjna Street
95-050 Konstantynów Łódzki
Poland

The tasks “Creation of the English versions of the *Acta Innovations* articles”, “Selection & contracting of the renowned foreign reviewers for the assessment of received manuscripts”, “Digitalisation of the Acta Innovations journal in order to provide the open access by the Internet” and “Maintenance of the anti-plagiarism system” are financed by an agreement 605/P-DUN/2018from the resources of Polish Ministry of Science and Higher Education dedicated to the activity popularising the science.

Zadania „Stworzenie anglojęzycznych wersji artykułów w Acta Innovations”, „Dobór i kontraktacja uznanych zagranicznych recenzentów do oceny zgłaszanych manuskryptów”, „Digitalizacja Acta Innovations w celu zapewnienia otwartego dostępu przez sieć Internet” i „Utrzymanie systemu antyplagiatowego” finansowane w ramach umowy 605/P-DUN/2018 ze środków Ministra Nauki i Szkolnictwa Wyższego przeznaczonych na działalność upowszechniającą naukę.

Ministerstwo Nauki
i Szkolnictwa Wyższego

ACTA INNOVATIONS

no. 26

January 2018

Contents

Henryk Grajek, Justyna Jonik, Leszek Rutkowski, Marcin Purchała, Tomasz Wawer
Military University of Technology, Institute of Chemistry
ul. Kaliskiego 2, 00-908 Warszawa, hgrajek5819@wp.pl

THE OPTIMISATION OF CHROMATOGRAPHIC CONDITIONS FOR THE DETERMINATION OF ACCEPTOR-DONOR PROPERTIES OF GRAPHENE OXIDE AND REDUCED GRAPHENE OXIDE

Abstract
The oxidised and reduced graphene samples (having different surface functionalities) were studied by inverse gas chromatography to characterise their acceptor-donor properties. The DN values denoting the donor number in the Gutmann scale and the AN* values denoting the acceptor number in the Riddle-Fowkes scale have been chosen in the estimation of the electron-acceptor parameter K_A and electron-donor parameter K_D values.

Key words
Inverse gas chromatography, reduced and oxidized graphene, acceptor-donor properties.

Introduction

Throughout the history of mankind, each period has taken its name from the material that was commonly in use at the time, such as stone, bronze and iron. Already in 1962, Boehm et al. described a method of synthesis a carbon foil of 100 Å thickness [1]. But only in 2004, the two-dimensional materials period began a new phase of material engineering [2,3]. The material is graphene, which can change the contemporary electronic industry because of its unique properties. Since the first isolation from graphite, graphene became a very popular material. By 2012, 8000 articles were published on the subject [4].

Graphene is a one-atom-thick planar sheet of sp^2-bonded carbon atoms that are densely packed in a honeycomb crystal lattice. Apart from that it is the main part of the other allotropic forms of carbon, such as fullerenes or nanotubes [5,6].

Many unusual properties of graphene have been disclosed since its isolation. For example, researchers have observed a high mobility of charges (electrons and positive holes), c.a. 230000 $cm^2/V*s$ [7], a thermal conductivity, c.a. 5000 W/m*K [8], Young's modulus value, c.a. 1 TPa [9], and an ultimate tensile (and bending) strength, c.a. 130 GPa [9].

It is worth mention that graphene has many surface functionalities, such as carboxylic and ketone groups, which covalently attach many biological molecules and determines the possibilities in biodetectors. Moreover, chemically modified graphene (CMG) is a promising material for energy storage. Graphene oxide can be employed in environmental protection. Thanks to its surface, it can adsorb radionuclides from water and improve its quality. Because graphene preserves spin polarization, it can be used to create low-strength spin contacts, which could be compatible with ferromagnetic metal and a semiconductor. High catalytic activity and exceptional electrical conductivity make graphene possible for use in photovoltaic cells. Graphene batteries can convert up to 7.8 % of solar energy into electricity [10]. It has been proven that the deposition of graphene from the gas phase on a metal surface causes corrosion processes to proceed much slower. Therefore, graphene can be employed to make anti-corrosion coatings [11,12].

Materials and methods

The study was focused on the samples of oxidized (GO), PCode: 1001819253, Sigma Aldrich, and reduced (rGO) graphene, PCode: 1001888758, Sigma Aldrich. The inverse gas chromatography tests at infinite dilution (IGC-ID) were performed by means of the Unicam type 610 apparatus with a high sensitivity of flame ionization detector with the AC-DC converter. To accomplish the infinite dilution conditions, vapours of the testing substances were injected into a column by means of the Hamilton type 7000.5KH syringe. The chromatographic peaks were acquired at a sampling rate of 25 Hz. Chromatograph's software Unicam 4880, Microsoft Office Excel 2010, Syntat

Software TableCurve 2D v5.01 and Daniel G. Hyams CurveExpert Professional 2.0 were used for all calculations. The chromatographic conditions are collated in Table 1.

Table 1. Chromatographic conditions

Temperature of injector	155 °C
Temperatures of column	for GO: 150, 145, 140, 135, 130 °C
	for rGO: 150, 145, 140 °C
Temperature of detector	155 °C
Carrier gas used	helium N5.2, pure for analysis
Carrier gas flow-rate	20±0.5 cm^3/min
Mass of column filling	GO: 0.1251 g
	rGO: 0.0217 g
Detector's sensitivity	10 mV
Specific surface area S_{BET}	GO: 2 m^2/g
	rGO: 321 m^2/g
Testing substances	n-pentane, n-hexane, n-heptane, n-octane (only for GO), dichloromethane, chloroform, carbon tetrachloride, acetonitrile, ethyl acetate, diethyl ether, tetrahydrofuran

Source: Author's

The optimisation of the chromatographic conditions for elution of probes on graphene samples consists in such selection of them that all relevant properties of the tested graphene samples are thoroughly examined. Nevertheless, simultaneously with the aforesaid conditions to make up for the valuable observation and results received by Stankovich and his coworkers [13].

The resulting file contained all flow disturbance caused by the sample being injected into the carrier gas stream. The data obtained were loaded into the TableCurve 2D v5.01 software (prod. Syntat Corp.) that enables the description of the data set by a suitable mathematical function to obtain the highest value of the nonlinear correlation coefficient. The following mathematical functions were employed for the description of the primary elution data (Eq. 1 – the P4 function and Eq.2 – the ExtraVal4T function) [14].

$$c(t) = h_{max} \frac{\left[1+\frac{\left(t-\frac{ws_2}{2s_1}-t_R^{sc}\right)^2}{w^2}\right]^{-s_1} \exp\left[-s_2\left(tan^{-1}\left(\frac{t-\frac{ws_2}{2s_1}-t_R^{sc}}{w}\right)+tan^{-1}\left(\frac{s_2}{2s_1}\right)\right)\right]}{\left(1+\frac{s^2}{4s_1^2}\right)^{-s_1}} \quad (1)$$

$$c(t) = h_{max} * exp\left[\frac{-t+t_r^{sc}+w-ws*exp\left(\frac{-t+wlns-t_R^{sc}}{w}\right)}{ws}\right] \quad (2)$$

where:
c(t) – the time dependent concentration of the testing substance,
h_{max} – the height of the elution peak,
t – the elution time of the testing substance,
w – the width of the elution peak,
s – the parameter related to the symmetry of the elution peak,
t_R^{sc} – the retention time of the centre of gravity of the elution peak.

Based on the retention times of the centres of gravity of the elution peaks for the testing substances (which were calculated by applying the equations (1) and (2)), the values of the specific retention volumes, referred to 1 gram of the column filling and its specific surface area, were calculated. The values of the specific retention volumes calculated in this way are the physicochemical constants (Eqs 3, 4 and 5) [15].

$$V_g = \frac{V_N}{m} * \frac{T_C}{273{,}15} \quad (3)$$

$$V_N = j_3^2 \left(\frac{p_0 - p_{H_2O}}{p_0}\right) F_C (t_R - t_M) \frac{T_C}{T_0} \quad (4)$$

$$j = \frac{3}{2} \frac{\left[\left(\frac{p_i}{p_0}\right)^2 - 1\right]}{\left[\left(\frac{p_i}{p_0}\right)^3 - 1\right]} \quad (5)$$

where:
V_g – the specific retention volume,
V_N – the net retention volume,
m – the mass of column filling,
T_C – the column temperature,
j – James-Martin compressibility factor,
p_0 and T_0 – atmospheric pressure and temperature,
p_{H2O} – the pressure of water vapour at environment temperature,
F_C – the volumetric flow rate of the carrier gas through the column, measured by soap flow-meter at the constant column temperature,
t_R and t_M – the retention time of the centre of gravity of the probe and the hold-up time,
p_i – the inlet pressure at the column.

The molar differential enthalpy and entropy of adsorption can be estimated from the temperature dependencies of the specific retention volumes referred to 1 gram of the tested material and its specific surface area or the adsorption virial coefficients. The following equation can be employed for the aforementioned calculations [15]:

$$ln \frac{V_{g(T_C)}^{1g}}{T_C} = \frac{-\Delta H_{ADS}}{R} \frac{1}{T_C} + \frac{\Delta S_{ADS}}{R} + \ln(R * S_{BET} * m) \quad (6)$$

where:
$V_{g(T_C)}^{1g}$ – the specific retention volume referred to the centre of gravity of the elution peak and to 1g of column filling,
ΔH_{ADS} – the molar differential enthalpy of adsorption,
R – gas constant (8,314 J/mol*K),
ΔS_{ADS} – the molar differential entropy of adsorption,
S_{BET} – the specific surface area of GO and rGO.

Adsorption as a spontaneous process on the solid surface is accompanied by a decrease of the standard energy of the system tested. The value of the total free energy transfer of one mole of substance from the gas phase to the standard state on the graphene surface can be estimated by employing the following equation $\Delta G_{ADS} = -R * T_C * ln\left(\frac{p_{s,g}}{\pi_s S_{BET}} V_{g(Tc)}^{1g}\right)$ [15]. In this dependency $\Delta G_{ADS}$is the molar differential Gibbs free energy of adsorption, $p_{s,g}$ is the reference pressure of 1 atm (101325 N/m^2) and π_s is the two-dimensional pressure of the adsorbed state (0,338*10^{-3} N/m^2).

The molar differential Gibbs free energy of adsorption characterizes the interaction of adsorbate molecules in the mobile phase with the outermost atoms on the adsorbent surface and the interaction of adsorbate molecules in the mobile phase with the atoms on its surface. In the case of a well-defined chromatographic process, the increase in the free energy of adsorption referred to the methylene group in n-alkane chain can be estimated from the slope of the natural logarithm of the net retention volume by using the following equation $-\Delta G_{ADS}^{CH_2} = RT_C \ln\left(\frac{V_{N+1}^{(C_{n+1}H_{2n+4})}}{V_N^{(C_{n+1}H_{2n+2})}}\right)$ [15], where $\Delta G_{ADS}^{CH_2}$ is the molar differential Gibbs free energy of adsorption of a methylene group in an n-alkane molecule, $V_{N+1}^{(C_{n+1}H_{2n+4})}$ and $V_N^{(C_{n+1}H_{2n+2})}$ are the net retention volumes of consecutive n-alkanes having n+1 and n methylene groups in their molecules, respectively.

The $\Delta G_{ADS}^{CH_2}$ values allow us to estimate the magnitude needed for surface energetic characteristics, i.e., the dispersive component of the surface free energy, γ_S^D. The aforesaid dependency is based on the $\Delta G_{ADS}^{CH_2}$ increment per methylene group for subsequent n-alkanes consecutive. The values of the dispersion component of the surface free energy were determined by employing the following dependency (Eq.7) [16,17,18].

$$\gamma_S^D = \frac{1}{4\gamma_{CH_2}} \left(\frac{\Delta G_{ADS}^{CH_2}}{N_A \omega_{CH_2}} \right)^2 \quad (7)$$

where:
γ_S^D – the dispersive component of the free energy of the liquid or testing substance injected,
γ_{CH_2} – the surface energy of polyethylene-type polymers with a finite molecular weight, suggested by Voelkel ($\gamma_{CH_2} = 35{,}6 + 0{,}058[293 - Tc(K)]$)[16],
N_A – Avogadro constant,
ω_{CH_2} – the sitting area of methylene group.

The chromatographic tests of the acid-base interactions are only possible by testing substances having nucleophilic and electrophilic groups or atoms. In the case of the IGC tests, if the adsorbate used exhibits acidic properties, it is possible to estimate the basic properties of the graphene samples. The characteristic of the acceptor-donor properties of any system require the estimation of the total free energy of adsorption ΔG_{ADS}, which is sum of the component for the specific interactions ΔG_{ADS}^{SP} and other interactions than specific ΔG_{ADS}^{vdW} [16].

The specific interactions:
- acceptor-donor interactions,
- interactions between permanent dipoles,
- induced dipole-permanent dipole,
- hydrogen bonds interactions.

For chromatographic evaluation of the acceptor-donor properties of the adsorbent, the testing substances with strictly defined acid-base properties, which behave:
- as donor, i.e., they are donating an electron, or
- as acceptor, i.e., they are taking an electron.

To perform the acid-base characterization of the solid surface, it is necessary to determine the magnitude of the effects for the system: testing substance-adsorbent. Considering all the predetermined values of the retention times or the free energy of adsorption values, all testing substances can be classified on the basis of their interactions with the surface functionalities present on both sample surfaces:
- adsorbates molecules interacting with weak force: n-alkanes,
- adsorbates molecules interacting with middle force: dichloromethane, chloroform, carbon tetrachloride,
- adsorbates molecules strongly interacting: acetonitrile, ethyl acetate, diethyl ether, tetrahydrofuran.

The surface properties of a different adsorbent can be characterized using the K_A (characterizing the acceptor properties) and K_D (characterizing the donor properties) parameters estimated on the thermodynamic functions (Eq.8) [19].

$$\Delta H_{ADS}^{SP} = K_A * DN + K_D * AN^* \quad (8)$$

where:
ΔH_{ADS}^{SP} – the value of the specific component of the molar differential enthalpy of adsorption described by the following equation $\frac{\Delta G_{ADS}^{SP}}{Tc} = \frac{\Delta H_{ADS}^{SP}}{Tc} + const$[15], DN is the Gutmann donor number [20], K_A is the parameter characterizing the acceptor properties, AN^* is the Riddle-Fowkes acceptor number [21] and K_D is the parameter characterizing the donor properties.

The application the DN and AN* parameters in the physicochemical calculations based on the IGC results is mandatory because their empirical values unambiguously illustrate their fundamental source in the interaction strength of lone and shared electron pairs, and they treat each functionality (or molecule) as being either an acid or a base [22].

Voelkel has proposed a method of determining the values of the K_A and K_D parameters based on the values of the specific component of the free energy of adsorption that contain the entropy factor (Eqs 9 and 10) [19].

$$\Delta G_{ADS}^{SP} = \Delta H_{ADS}^{SP} + T_C * \Delta S_{ADS}^{SP} \quad (9)$$

$$\Delta G_{ADS}^{SP} \cong K_A * DN + K_D * AN^* \quad (10)$$

where:
ΔS_{ADS}^{SP} – the value of the molar differential entropy of adsorption of specific interactions.

The K_A and K_D values have been calculated for the graphene samples tested [19]:
a) without taking into account the entropic effect (Eq. 11):

$$\frac{\left(-\Delta H_{ADS}^{SP}\right)_i}{AN_i^*} = K_A \frac{DN_i}{AN_i^*} + K_D \quad (11)$$

b) with accounting for the entropic effect (Eq. 12):

$$\frac{(-\Delta G_{ADS}^{SP})_i}{AN_i^*} \cong K_A \frac{DN_i}{AN_i^*} + K_D \quad (12)$$

where:
i – subscript denoting the adsorbate used.

Results and discussion

Based on the acquired elution data performed at ideal, nonlinear chromatographic conditions, the values of the specific retention volume have been determined by using equations (3), (4) and (5). Based on the retention data obtained by using the ExtraVal4T function for the description of peak profiles, the ln(Vg/Tc)=f(1/Tc) dependencies for the GO sample have been prepared and presented in Figs 1, 2 and 3.The column temperature increase causes the decrease of the specific retention volume. However, the increase of the molecular mass causes an increase of the specific retention volume. The ln(Vg/Tc)=f(1/Tc) dependency is commonly employed for the determination of the molar differential enthalpy and entropy of adsorption.

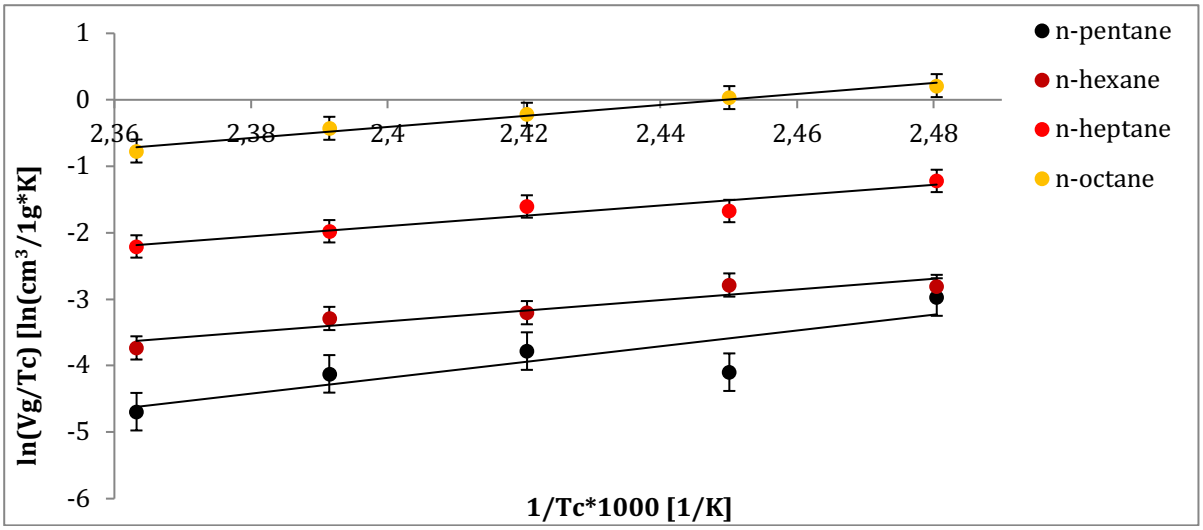

Fig. 1. The ln(Vg/Tc)=f(1/Tc) dependencies for the GO (n-alkanes)
Source: Author's

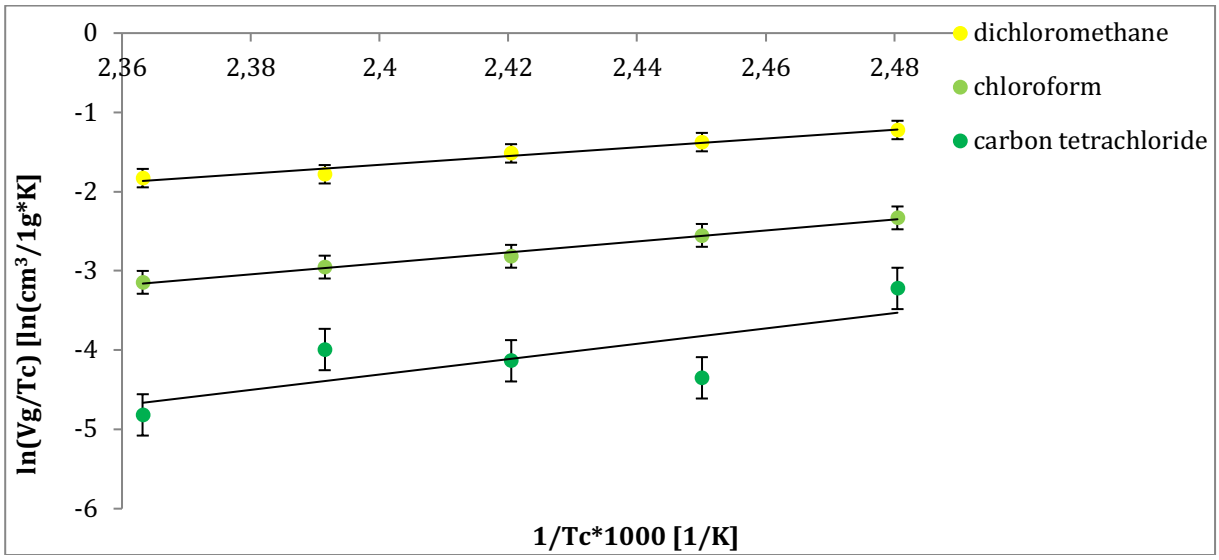

Fig. 2. The ln(Vg/Tc)=f(1/Tc) dependencies for the GO (dichloromethane, chloroform, carbon tetrachloride)
Source: Author's

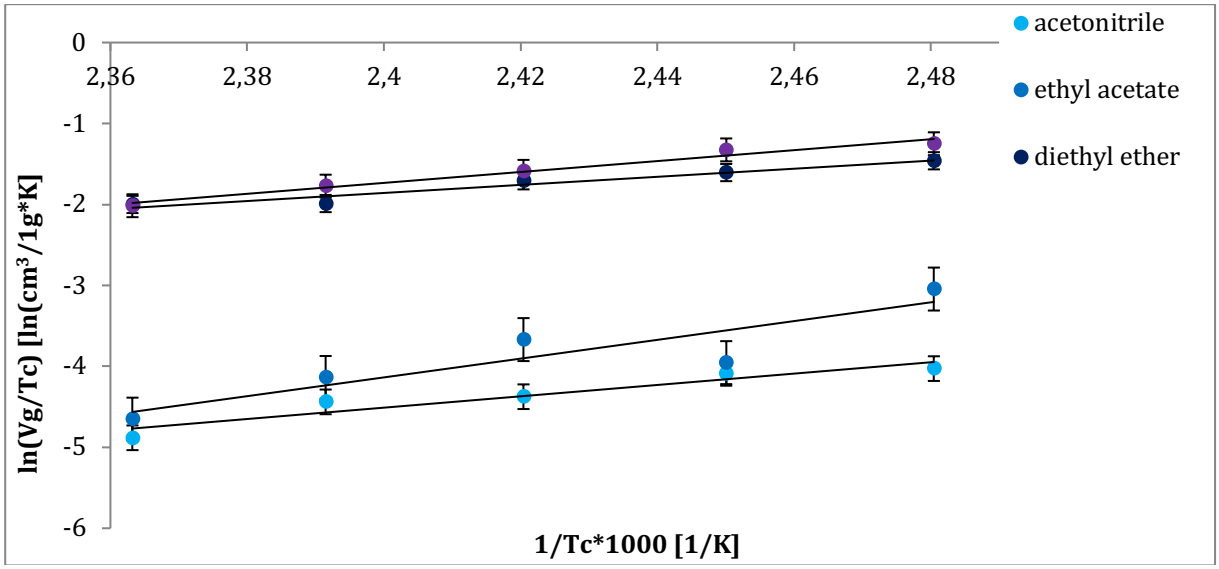

Fig. 3. The ln(Vg/Tc)=f(1/Tc) dependencies for the GO (acetonitrile, ethyl acetate, diethyl ether, tetrahydrofuran)
Source: Author's

The determined(by using equation (6)) values of the molar differential enthalpy and entropy of adsorption (vide collated in Table 2)which increase with the number of methylene groups in n-alkane chain. The existence of the linear dependencies between the molar differential entropy and enthalpy of adsorption confirm that during the elution processes the ideal, nonlinear conditions have been attained (Figs. 4 and 5).

Table 2. The values of the molar differential entropy and enthalpy of adsorption for GO and rGO (the P4 function).

Testing substances	GO			rGO		
	ΔH_{ADS} [kJ/mol]	ΔS_{ADS} [J/mol*K]	SD*10^{-2}	ΔH_{ADS} [kJ/mol]	ΔS_{ADS} [J/mol*K]	SD*10^{-2}
n-pentane	-74.03	-242.73	0.97	-67.64	-146.24	0.05
n-hexane	-69.96	-229.00	0.34	-64.74	-120.71	1.24
n-heptane	-60.27	-193.77	2.41	-60.28	-98.73	2.25
n-octane	-51.90	-189.24	1.27	-	-	-
dichloromethane	-28.97	-115.30	0.79	-67.60	-144.41	2.12
chloroform	-40.99	-168.69	1.55	-76.01	-164.42	2.33
carbon tetrachloride	-76.83	-250.10	0.28	-83.55	-188.90	0.27
acetonitrile	-3.28	-73.69	0.46	-55.46	-116.24	1.87
ethyl acetate	-133.18	-386.10	0.59	-62.47	-134.96	0.57
diethyl ether	-5.61	-57.03	0.57	-68.37	-136.74	0.49
tetrahydrofuran	-51.83	-170.70	2.07	-50.41	-47.87	0.04

Source: Author's

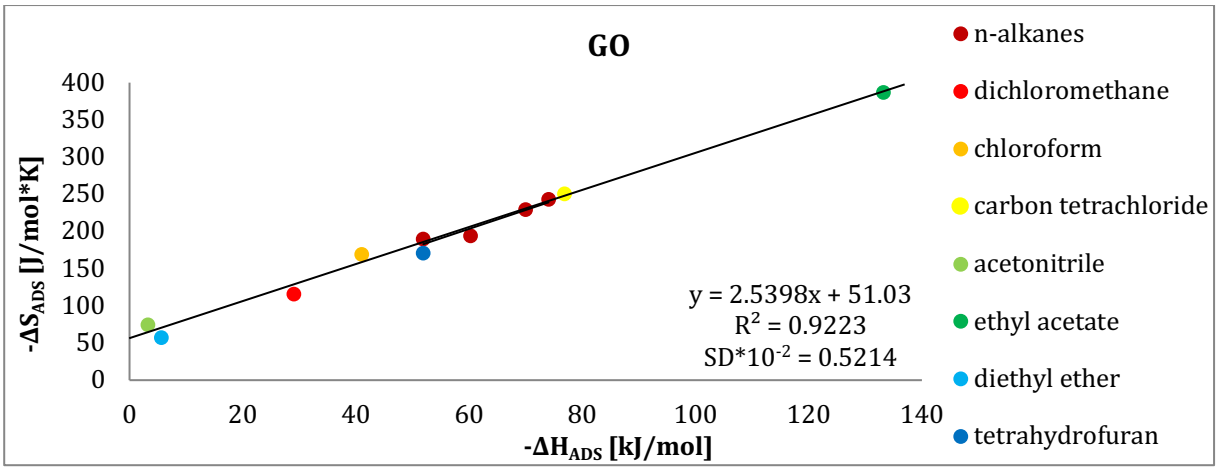

Fig. 4. The $-\Delta S_{ADS}=f(-\Delta H_{ADS})$ dependency for GO (the P4 function)
Source: Author's

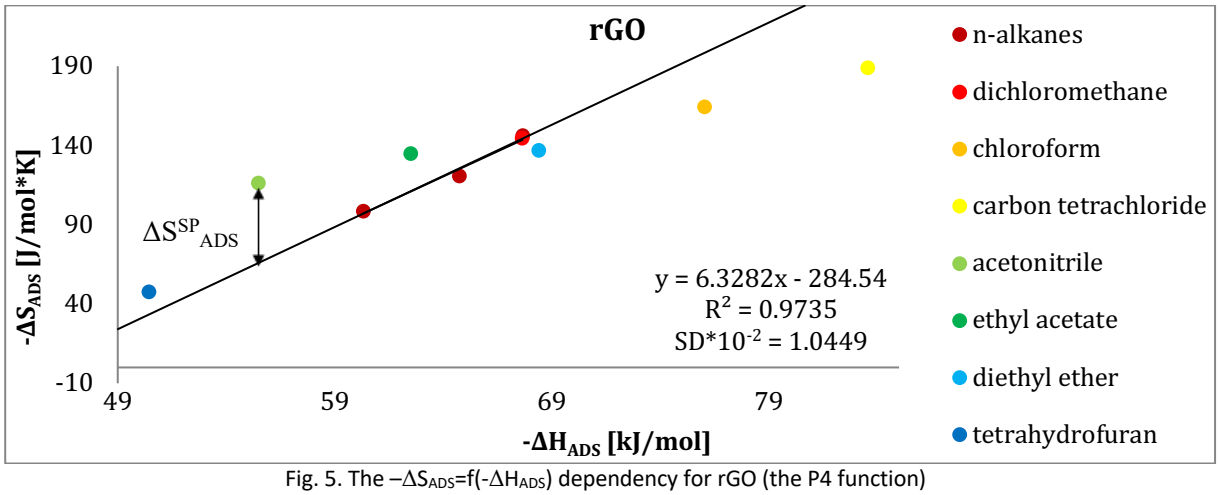

Fig. 5. The $-\Delta S_{ADS}=f(-\Delta H_{ADS})$ dependency for rGO (the P4 function)
Source: Author's

The interpretation of the interactions between the graphene samples tested and the molecules of the testing substances can be interpreted as specific and nonspecific. The specific interactions are caused by the polar groups and nonspecific interactions are involved by methyl and methylene groups. Analysing Figs. 6 and 7, we

can state that the specific interactions are stronger with the rGO sample.The dispersive component of the free energy of the liquid or testing substance injected was calculated by using equation 7.

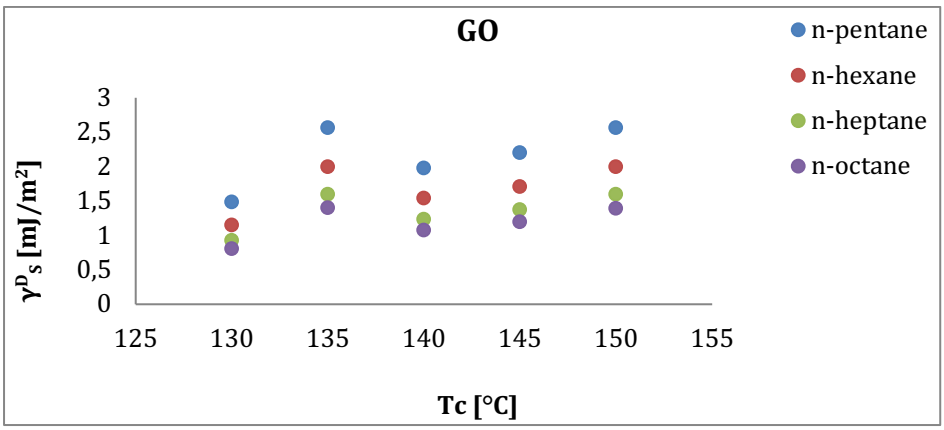

Fig. 6. The γ^{D}_{S}=f(Tc) dependency for GO (the ExtraVal4T function)
Source: Author's

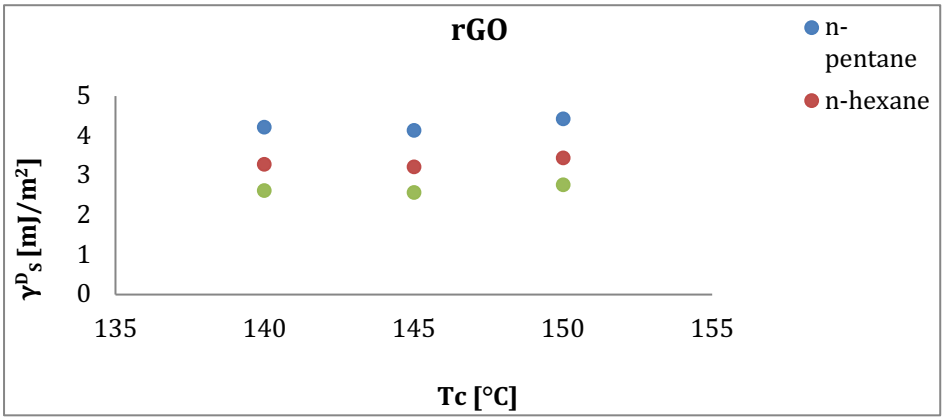

Fig. 7. The γ^{D}_{S}=f(Tc) dependency for rGO (the ExtraVal4T function)
Source: Author's

As it was mentioned previously, the specific interaction effects occur when the hydrogen bond, acid-base interactions and π-orbitals interactions are created. To estimate the specific component of the Gibbs free energy of adsorption, ΔG^{SP}_{ADS}, it is necessary to determine the following dependencies $\Delta G_{ADS} = f(Tc)$ (Figs 8, 9 and 10), $\Delta G_{ADS} = f(\omega * \sqrt{\gamma_L^{vdW}})$ (Fig. 11, where ω is the sitting area for adsorbate molecule and γ_L^{vdW} is the surface free energy of the pure phase [23]), $\Delta G_{ADS} = f(P_D)$ (Fig. 12, where P_D is the molar deformation polarisation [17]) and $\Delta G_{ADS} = f(\Delta H_{VAP})$ (Fig. 13, where ΔH_{VAP} is the enthalpy of vapourisation [17]), which must provide good linearity. The values of the specific component of the ΔG^{SP}_{ADS} magnitude are collated in Table 3.

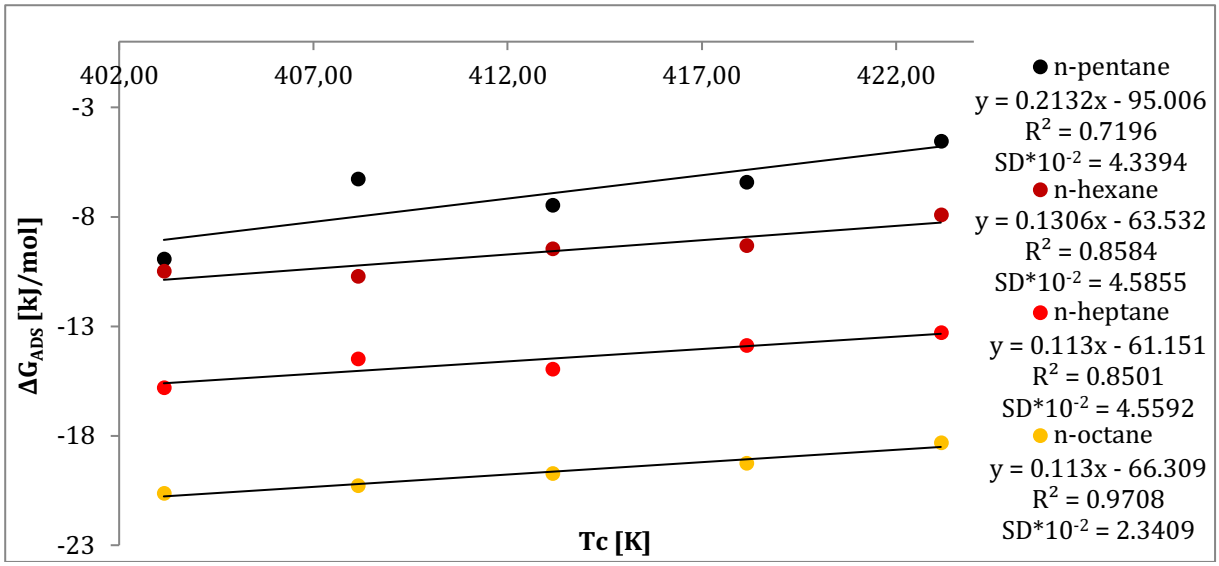

Fig. 8. The $-\Delta G_{ADS}$=f(Tc) dependency for GO (n-alkanes; the ExtraVal4T function)
Source: Author's

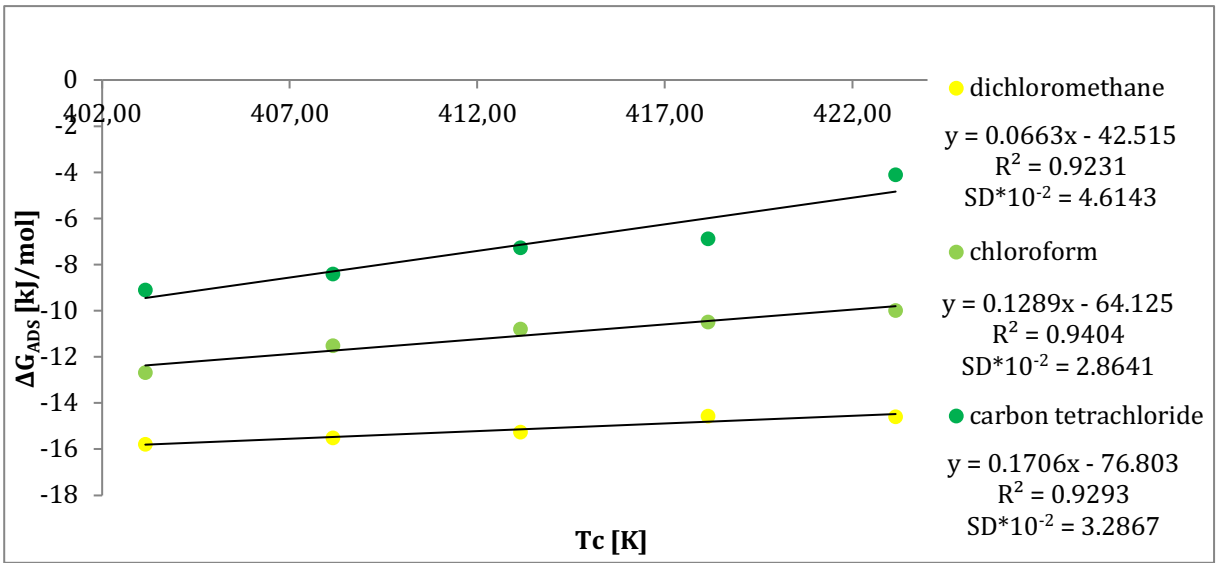

Fig. 9. The $-\Delta G_{ADS}$=f(Tc) dependency for GO (dichloromethane, chloroform, carbon tetrachloride; the ExtraVal4T function)
Source: Author's

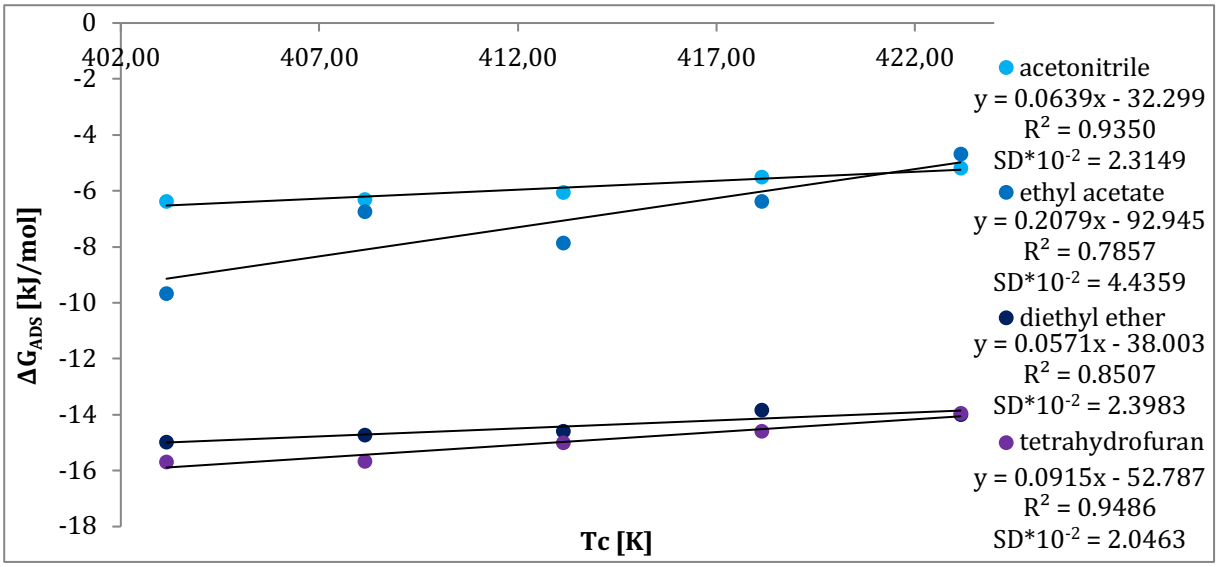

Fig. 10. The $-\Delta G_{ADS}$=f(Tc) dependency for GO (acetonitrile, ethyl acetate, diethyl ether, tetrahydrofuran; the ExtraVal4T function)

Source: Author's

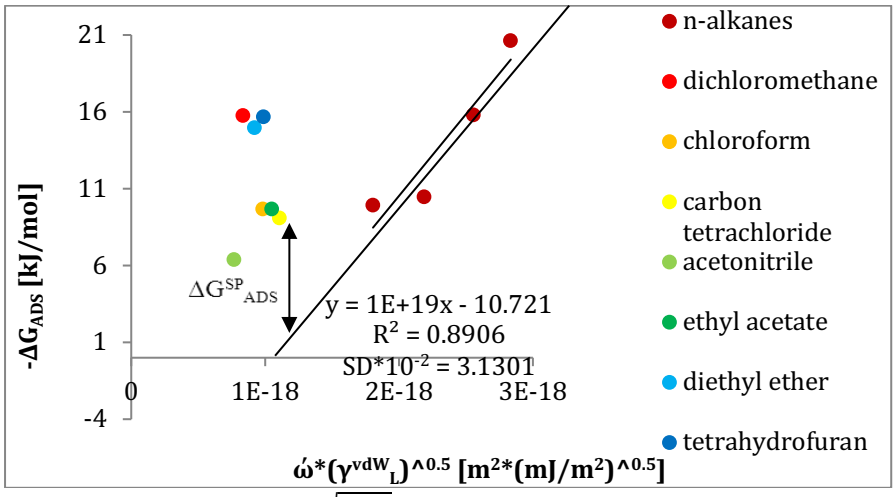

Fig. 11. The $\Delta G_{ADS} = f(\omega * \sqrt{\gamma_L^{vdW}})$ dependency for GO (the ExtraVal4T function)

Source: Author's

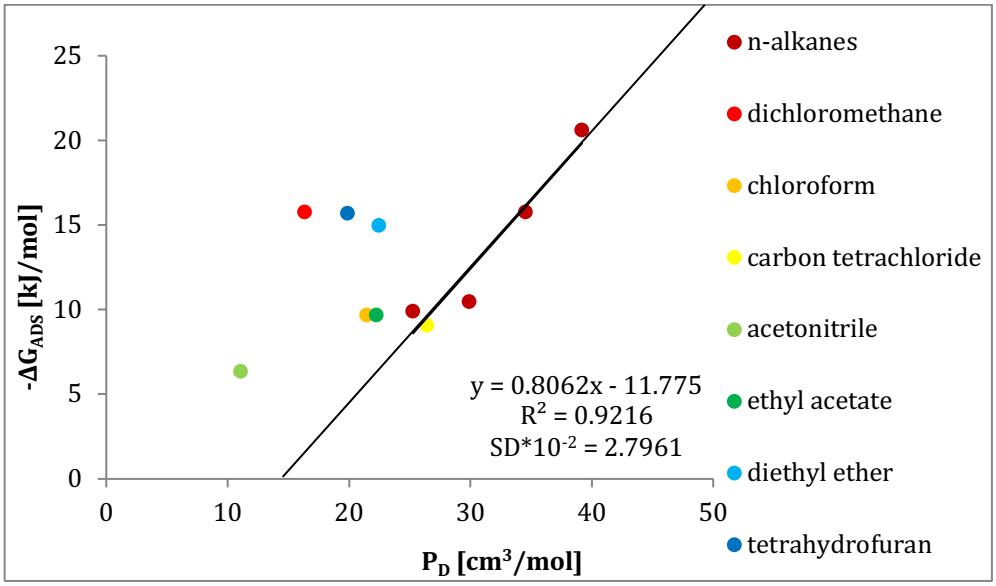

Fig. 12. The $\Delta G_{ADS} = f(P_D)$ dependency for GO (the ExtraVal4T function)
Source: Author's

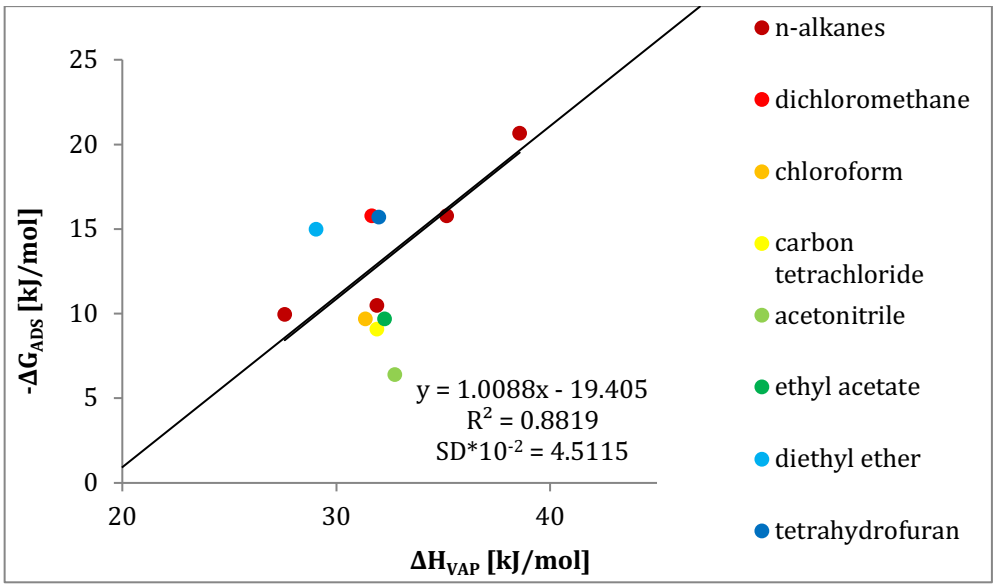

Fig. 13. The $\Delta G_{ADS} = f(\Delta H_{VAP})$ dependency for GO (the ExtraVal4T function)
Source: Author's

Table 3.The values of the specific component of the ΔG_{ADS}^{SP} for GO and rGO.

ΔG_{ADS}^{SP} [kJ/mol]				
$\omega * \sqrt{\gamma_L^{vdW}} \left[m^2 * \sqrt{\left(\frac{mJ}{m^2}\right)} \right]$				
Testing substances	**GO**		**rGO**	
	ExtraVal4T	**P4**	**ExtraVal4T**	**P4**
dichloromethane	22.28	21.07	12.36	13.63
chloroform	16.34	14.89	1.57	2.92
carbon tetrachloride	10.58	9.14	4.16	5.42
acetonitrile	15.77	14.25	13.09	14.39
ethyl acetate	12.75	11.23	6.58	7.98
diethyl ether	20.77	20.63	14.46	15.82
tetrahydrofuran	20.49	19.09	-18.80	-17.10
P_D [cm^3/mol]				
dichloromethane	16.79	16.35	11.69	12.30
chloroform	7.68	7.23	-2.68	-2.25
carbon tetrachloride	-1.37	-1.58	-4.01	-3.92
acetonitrile	14.40	13.40	17.83	18.74
ethyl acetate	4.02	3.55	2.62	3.06
diethyl ether	10.54	11.45	7.63	8.01
tetrahydrofuran	13.32	12.86	-20.92	-20.07
ΔH_{VAP} [kJ/mol]				
dichloromethane	4.23	4.42	-5.86	-5.94
chloroform	0.11	0.04	-13.21	-13.19
carbon tetrachloride	-5.03	-5.05	-9.01	-9.10
acetonitrile	-4.18	-4.23	-8.17	-8.27
ethyl acetate	-3.83	-3.90	-8.27	-8.25
diethyl ether	6.57	7.67	2.08	2.24
tetrahydrofuran	3.61	3.63	-34.45	-34.12

Source: Author's

As was mentioned previously, in the characterization of the acceptor-donor properties of the materials, the identification of the component of the specific effects must be separated from all interactions.

It is possible on the basis of the thermodynamic data estimated for two groups of the testing substances, namely characterizing by acceptor (a Lewis acid, AN) and donor (a Lewis base, DN) properties. Gutmann's background developed by Riddle and Fowkes (i.e., the AN* and DN numbers) are very useful in the IGC tests of the aforementioned parameters. The values of the AN* and DN parameters needed for the calculations are collated in Table 4.

Table 4. The Gutmann donor numbers and the Riddle-Fowkes acceptor numbers [20,21]

Testing substances	DN [kJ/mol]	AN* [kJ/mol]
dichloromethane	0.0	16.3
chloroform	0.0	22.6
carbon tetrachloride	0.0	2.9
acetonitrile	59.0	19.7
ethyl acetate	71.5	7.5
diethyl ether	80,3	5.9
tetrahydrofuran	83.7	2.1

Source: Author's

By applying the equations (8), (10) and also (11) and (12) it is possible to determine the values of the K_A and K_D parameters, which directly characterise the acceptor-donor properties of the tested column fillings.

The obtained results are collated in Table 5 and the exemplary plot for $\frac{(-\Delta H_{ADS}^{SP})_i}{AN_i^*} = f\left(\frac{DN_i}{AN_i^*}\right)$ dependency is depicted in Fig. 14.

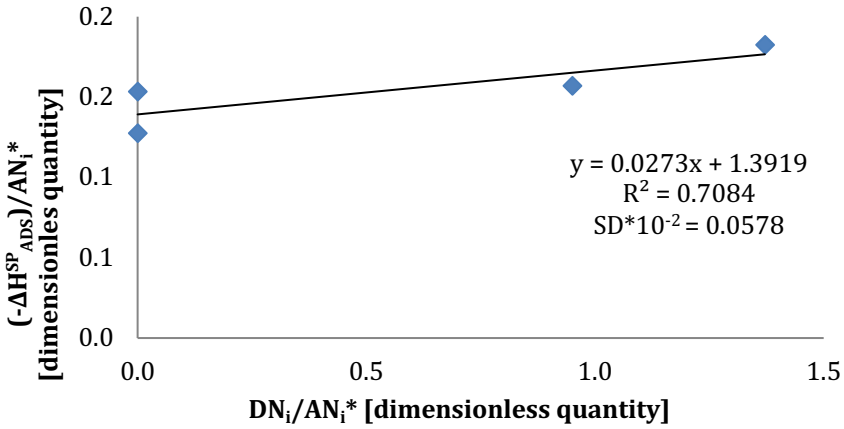

Fig. 14. The $\frac{(-\Delta H_{ADS}^{SP})_i}{AN_i^*} = f\left(\frac{DN_i}{AN_i^*}\right)$ dependence (the ExtraVal4T function)

Source: Author's

Table 5. The obtained results of the K_A and K_D parameters and K_A/K_D ratio for the description by the ExtraVal4T function.

Parameter	GO		rGO	
	Equation 16	Equation 17	Equation 16	Equation 17
$\omega * \sqrt{\gamma_L^{vdW}} \left[m^2 * \sqrt{\left(\frac{mJ}{m^2}\right)} \right]$				
K_A	0.032	0.038	0.119	0.048
K_D	1.619	1.260	0.485	0.524
K_A/K_D	0.020	0.030	0.246	0.091
P_D [cm³/mol]				
K_A	0.025	0.031	0.107	0.037
K_D	1.428	1.074	0.319	0.358
K_A/K_D	0.017	0.029	0.338	0.103
ΔH_{VAP} [kJ/mol]				
K_A	0.027	0.036	0.112	0.042
K_D	1.391	1.041	0.358	0.396
K_A/K_D	0.019	0.034	0.314	0.107

Source: Author's

It can be easily recognized that the values of the K_A and K_D can be influenced by many factors, including the properties of the attached functional groups.

The aforementioned parameters expressed as the K_A/K_D quotients allow relative characteristics of the surface properties of the materials tested [24]:
a) a surface with acidic properties:

$$\frac{K_A}{K_D} \geq 1.1$$

b) a surface with neutral properties:

$$0.9 < \frac{K_A}{K_D} < 1.1$$

c) a surface with basic properties:

$$\frac{K_A}{K_D} \leq 0.9$$

Analysing the K_A/K_D values it is necessary to state that both oxidized and reduced graphene surfaces have donor properties. It can be caused by the method of synthesis of the samples.

Summary and conclusions

The optimisation of the chromatographic conditions revealed that the sets of the K_A, K_D and K_A/K_D values obtained by the IGC method enable a deeper characteristic of the acceptor-donor properties of graphene samples. In our studies we confirmed that the intermolecular interactions of the probes with graphene materials were governed by acceptor-donor interactions as evidenced by Drago's studies. It also showed that the 'thermodynamic compensation effect' [$-\Delta S_{ADS}=f(-\Delta H_{ADS})$] can be accomplished for the ideal, nonlinear chromatographic conditions. In addition, it demonstrated that the tested samples of graphene, both oxidized and reduced, have donor properties, although the GO surface has stronger basic properties due the lone electron pairs of oxygen atoms.

The optimisation of the acceptor-donor tests for the graphene samples in this paper produce a wide range of information on the one hand, and as many adsorption tests, they are highly sensitive to the chromatographic condition on the other. Nevertheless, the way in which electrons are exchanged between the functionalities located in the structure of the graphene samples and the active sites of testing substances, now is not possible to elucidate. Thus, the exact description of the electron transfer mechanism is still a matter of methodical and thorough scientific debate.

References

[1] H.P. Boehm, A. Clauss, G.O. Fischer, U. Hofmann, Dünnste Kohlenstoff-Folien, Zeitsdirift für Naturforschung 17 b, Seite 150-153, 1961 (in German).
[2] A.K. Geim, K.S. Novoselov, The rise of graphene, Nature Materials 6 (2007)183-191.
[3] S. Mikhailov, Z. Koinov, Physics and applications of graphene theory, InTech, New York, 2011.
[4] D. Jiang, Z. Chen, Graphene chemistry: theoretical perspectives, John Wiley & Sons Inc, United Kingdom, 2013.
[5] A.K. Geim, Graphene prehistory, Phys. Scr. T146 (2012) 014003 (4pp).
[6] S. Alwarappan, A. Kumar, Graphene-based nanomaterials: science and technology, CRC Press, 2013.
[7] K.I. Bolotin, K.J. Sikes, Z. Jianga, M. Klima, G. Fudenberg, J. Hone, P. Kim, H.L. Stormer, Ultrahigh electron mobility in suspended graphene, Solid State Communications 146, 9 (2008) 351-355.
[8] A.A. Balandin, S. Ghosh, W. Bao, I. Calizo, D. Teweldebrhan, F. Miao, C.N. Lau, Superior Thermal Conductivity of Single-Layer Graphene, Nano Lett. 8, 3(2008) 902-907.
[9] C. Lee, X. Wei, J.W. Kysar, J. Hone, Measurement of the Elastic Properties and Intrinsic Strength of Monolayer Graphene, Science 321, 5887 (2008) 385-388.
[10] S. Chowdhury, R. Balasubramanian, Three-dimensional graphene-based macrostructures for sustainable energy applications and climate change mitigation, Progress in Materials Science 90 (2017) 224-275.
[11] L.E.F. Foà Torres, S. Roche, J.-C. Charlier, Introduction to graphene-based nanomaterials: from electronic structure to quantum transport, Cambridge University Press, New York, 2014.
[12] W. Choi, J. Lee, Graphene synthesis and applications, CRC Press, Boca Raton, 2012.
[13] S. Stankovich, D.A. Dikin, R.D. Piner, K.A. Kohlhaas, A. Kleinhammes, Y. Jia, Y. Wu, S.T. Nguyen, R. S. Ruoff, Synthesis of graphene-based nanosheets via chemical reduction of exfoliated graphite oxide, Carbon 45 (2007) 1558-1565.
[14] TableCurve 2D: Automated curve fitting and equation discovery: version 5.01 for windows; user's manual. Richmond, CA: SYSTAT, 2002.
[15] Ł. Farczak, Chromatograficzne badania zredukowanego i utlenionego grafenu, WAT, Warszawa, 2015.
[16] H. Grajek, J. Paciura-Zadrożna, Z. Witkiewcz, Chromatographic characterisation of ordered mesoporous silicas. Part I. Surface free energy of adsorption, J. Chromatogr. A 1217 (2010) 3105-3115.
[17] M.C. Gutiérrez, S. Osuna, I. Baráibar, Solid surface mapping by inverse gas chromatography, J. Chromatogr. A 1087, 1-2 (2005) 142-149.
[18] M.C. Gutierrez, J. Rubio, F. Rubio, J.L. Oteo, Inverse gas chromatography: a new approach to the estimation of specific interactions, J. Chromatogr. A 845, 1-2 (1999) 53-66.
[19] H. Grajek, Ł. Farczak, T. Wawer, P. Jabłoński, M. Purchała, The characteristic of the adsorption and energetic properties of the oxidised and reduced graphene, Aparatura Badawcza I Dydaktyczna, 3 (2015) 224-233.
[20] V. Gutmann, The donor-acceptor approach to molecular interactions, Plenum Press, New York, 1978.
[21] F.L. Riddle, F.M. Fowkes, Spectral shifts in acid-base chemistry. 1. van der Waals contributions to acceptor numbers, J. Am. Chem. Soc. 112, 9 (1990) 3259-3264.
[22] R.S. Drago, G.C. Vogel, T.E. Needham, A Four-Parameter Equation for Predicting Enthalpies of Adduct Formation, Journal of the American Chemical Society 93, 23 (1971) 6014-6026.

[23] G.M. Dorris, D.G. Gray, Adsorption of n-alkanes at zero surface coverage on cellulose paper and wood fibers, J. Coll. Interface Sci. 77 (1980) 353.
[24] U. Panzer, H.P. Schreiber, On the Evaluation of Surface Interactions by Inverse Gas Chromatography, Macromolecules 25 (1992) 3633-3637.

Aleksandra Jastrzębska, Krzysztof Jastrzębski, Witold Jakubowski
Lodz University of Technology, Mechanical Faculty, Institute of Materials Science and Engineering
Stefanowskiego 1/15 St., 90-924 Lodz, aleksandra.jastrzebska@dokt.p.lodz.pl

CAN TITANIUM ANODIZATION LEAD TO THE FORMATION OF ANTIMICROBIAL SURFACES?

Abstract
In recent years, there has been observed a growing need for novel, multifunctional materials that would not only replace, but also heal the damaged tissues. In this paper, the titanium dioxide films manufactured by anodic oxidation method are investigated. The study of their structurization and antimicrobial properties of the coatings is presented. Samples anodized in water solutions of ethylene glycol exhibited various character - from structurized to porous ones. As the study revealed, all samples acted anti-adhesive in terms of bacterial (*Escherichia coli*) and fungal (*Candida albicans*) surface colonisation.

Keywords
Ti6Al4V, anodic oxidation, antimicrobial properties

Introduction

Biomaterials and medical devices market is growing every year, all the time introducing new technologies and materials leading to prevent post-implantation and post-treatment bacterial and fungal infections [1,2]. A great effort is put on designing not only materials that exhibit desired properties like haemocompatibility or enhancement of ossteointegration, but most importantly – having antimicrobial properties[3-5]. Bacterial and fungal infections are a very serious problem concerning implants – it affects every type of surfaces, no matter if they are made of metal, polymer or biological tissues[6]. In case of microbial colonization on biomaterials by pathogenic microorganisms, one of the best solutions seem to be the replacement of the whole implant to the new one. However, the risk of recurrent infection is very high [7]. According to literature, a relatively high percentage of reimplantation due to microbial infections takes place. Based on literature review and own experience, this work assesses the material properties that can influence the microbial biofilm formation – both bacterial and fungal.

Microbial biofilm is a microorganisms-based structure in which microbes are attached to each other and surrounded by extracellular matrix (made of polysaccharides, proteins and DNA), that is attached to biological or artificial surface [8, 9]. This structure has been recognized as the basic form in which microorganisms can live on the surfaces, while the endospores and planktonic forms only serve to move and inhabit new places [10,11]. Biofilm formation is a complex process, with its duration dependent on environmental conditions and type of microbes that create it. It can be divided into 4 consecutive processes[12], presented in the diagram on the Fig.1.

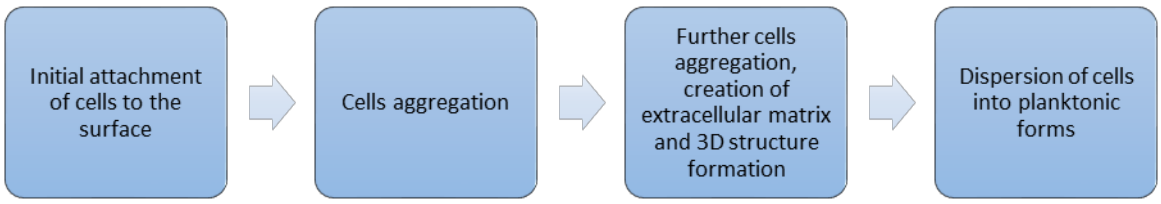

Fig. 1. Biofilm formation steps
Source: Author's

All these stages lead to the formation of a drug-resistant, complex structure that, when untreated, can cause the infection spreading around the whole human organism.

There are many factors that influence the formation of biofilms on biomaterials. Surface topography of the material, i.e. its roughness and presence of irregularities like scratches, cavities etc., can have a great influence on the adhesion of microorganisms[13]. One of the main suggestion when preparing the surface of biomaterial

is that all the imperfections of the surface should be at least one order of magnitude smaller than the size of microorganisms that can inhabit the material. That is, the higher is the roughness of the surface, the higher will be the adhesion of microorganisms because of the fact that they will find 'a shelter' between the irregularities [14-16]. However, there exist theoretical models that do not agree completely with those statements. According to Seigismund et al., calculating the interaction energy between microorganisms and surface, it was seen that with the increasing Ra parameter, the distance between bacteria and surface is increased, thus reducing the interaction between microbe and material [17]. All published data suggest though, that the dependence between surface topography and microbial attachment is non-linear, and only when surface irregularities are on comparable level to adhered microbes, the contact between cells and material increases as well as the risk of increased microbial adhesion [18-20]. Chemical composition of the surface onto with microorganisms are about to attach plays a crucial role in determining microbial biofilm formation. Since decades, scientists are proposing new materials and coatings that can deal with inhibition of attachment of microorganisms. The most popular approach is ion implantation to the surfaces of materials. Those ions must exhibit desired properties like causing microbial apoptosis or reducing the amount of cells attachment. Very similar is deposition of coatings that would repel microorganisms or prevent them from colonization. Such materials involve e.g. diamond-like carbon coatings, titanium dioxide and coatings doped with antimicrobial agents like silver, copper, zinc, fluoride, silicon etc. [21-26].

One of the biomaterials that is frequently used in manufacturing of the implants and prosthesis is titanium. Its excellent mechanical properties combined with biocompatibility make this material very promising in the development of new solutions in biomaterials and surface engineering. One of the very interesting features of the titanium is that it has the possibility to form in an environment where oxygen is present, a very thin, oxide passive layer – titanium dioxide [27-30]. However, this layer is formed spontaneously and it can easily be removed from the material surface. Many coatings deposition technologies were tested, so that the more durable titanium dioxide coating could be formed. One of them – anodic oxidation, is a fast, non-expensive coatings manufacturing methods that allows to obtain the TiO_2 of the desired properties simply by changing the process parameters or electrolyte composition [31-35].

Anodic oxidation (also called anodization) is a method of electrolytic passivation of metals in the electrolytes, in presence of electric current. During the process, the material being coated serves as an anode, and the electrolytes are most often the water-based solutions of acids (very frequently these are sulfuric, phosphoric or hydrofluoric acid). While the voltage is applied to the system, the dissolved oxygen reacts with the metal immersed in the electrolyte, which forms a thin oxide layer on the anode surface [36-40].

This work is devoted to the analysis of titanium anodized in viscous electrolytes in terms of the layers structurization and their microbiological properties.

Materials and methods

Samples of titanium alloy Ti6Al4V (Bibus Metals Sp. z o.o.) were used as a substrate material. All samples were disks of ϕ = 16 mm. Prior to anodization processes all disks were washed with deionized water and acetone to remove all the contamination. Anodization of titanium was performed in a bath containing different concentrations of ethylene glycol (Chempur) in aqueous solutions. Each electrolyte had an addition of 2% vol. of hydrofluoric acid (Chempur). All electrochemical processes were conducted in constant voltage of 20V with 20 minutes deposition time. Voltage was controlled by the digital multimeter and devoted software. Prepared coatings list is presented in table 1.

Table 1. List of deposited TiO2 coatings

Sample	Water concentration [% vol.]	Ethylene glycol concentration [% vol.]
G1	50 %	50 %
G2	40 %	60 %
G3	30 %	70 %
G4	20 %	80 %
G5	10 %	90 %

Source: Author's

The topography of the prepared coatings was investigated with the use of Scanning Electron Microscopy (SEM) [41,42]. The observations were performed in high vacuum, under the accelerating voltage of 20 kV and magnification 5000x. What is more, the roughness of surfaces was evaluated by mechanical profilometer. For all samples, the values of Ra parameter were calculated.

The antimicrobial character of the coatings was analysed with 2 strains – bacteria *Escherichia coli* (gram negative) and fungi *Candida albicans* (yeasts). *E.coli* was grown in Luria-Bertani medium, while *C.albicans* in YPG. All samples were incubated in culture medium for 24 hours at temperature 37C. When the samples were taken out from the growth medium, the specimens were rinsed with deionized water so the not-adhered microorganisms were removed from the surface. The observations were conducted under the fluorescent microscope Olympus GX 71, and the visualization of both live and dead cells was possible due to the use of two fluorescent dyes – propidium iodide and bis-benzamide. After 5 minutes incubation in dark, samples were observed. For the purpose of comparison of the samples, stainless steel (Medgal sp. z o.o.) substrate was used as a control. The number of adhered cells being the % of the cells attached to the control samples was calculated.

Results and discussion

Figure 2 presents the images from the scanning electron microscope, revealing the topography of the obtained coatings. Water to ethylene glycol ratio marked below.

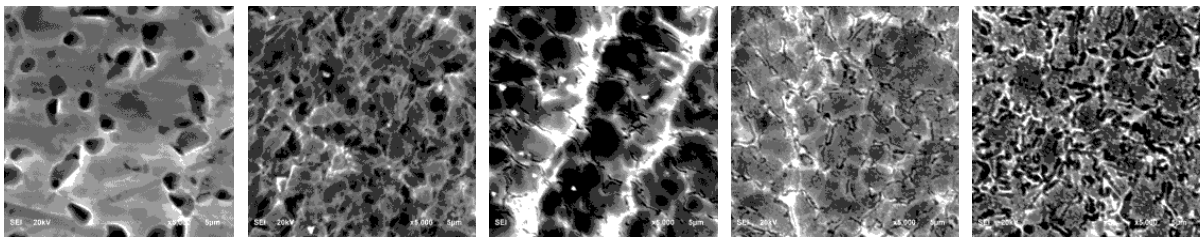

10:90 20:80 30:70 40:60 50:50

Fig. 2. Topographical SEM images of the deposited coatings in 5000x magnification
Source: Author's

In the electrochemical processes involving viscous electrolytes, the general trend is that the reduction of amount of water in the electrolyte may cause help the formation of longer tubular structures [43-45]. That is due to the fact that that in organic electrolytes the donation of oxygen to the formed layer is more difficult. What is more, the anodic oxidation processes performed in viscous electrolytes may result in the formation of much different shapes than are observed for aqueous oxidizing baths[46-48]. However, in this study, as the scanning electron microscope examination revealed, the samples prepared in ethylene glycol electrolytes (see fig. 2) did not exhibit tubular structures.

For the sample being prepared in the electrolyte containing 70% vol. of ethylene glycol and 30% vol. of water, a nearly tubular but not very deep structures were observed. Surprisingly, for the electrolyte with the highest concentration of ethylene glycol (90% vol. of ethylene glycol and 10% vol. of water), a porous character rather than rough and tubular is observed.

Also, the roughness measurements showed that porous surfaces had an average roughness Ra being almost 3 times higher than for structurized samples, as it is presented in the Table 2.

Table 2. Average roughness (Ra) measurements.

Water to ethylene glycol ratio				
50:50	**40:60**	**30:70**	**20:80**	**10:90**
0.28 ± 0.06 µm	0.26 ± 0.07 µm	0.18 ± 0.06 µm	0.06 ± 0.01 µm	0.06 ± 0.01 µm

Source: Author's

Antimicrobial performance of the coatings was assessed in terms of bacterial and fungal adherence to the formed layers. Figure 3 and 4 present the microbial adhesion being expressed by the total area occupied by microorganisms being the % of the control sample. In this investigation, the number of cells adhered to the control sample is expressed as 100%.

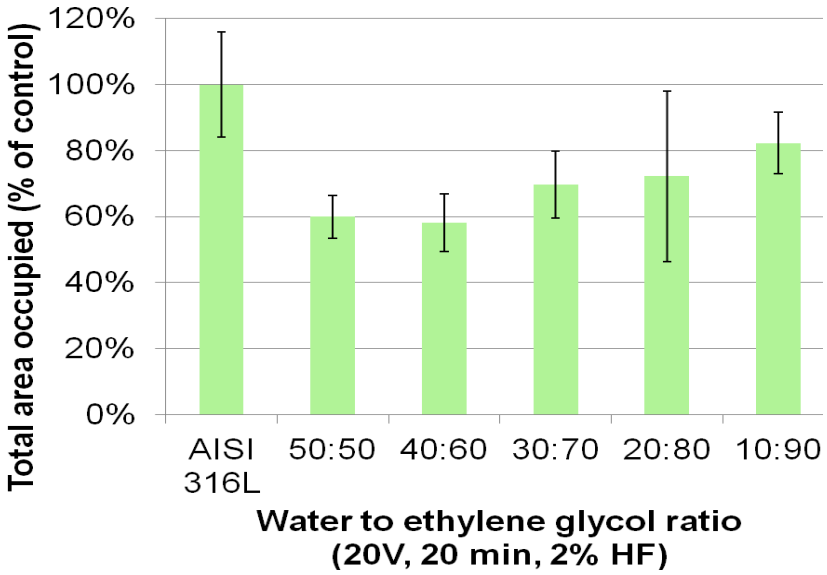

Fig. 3. Bacterial adhesion to anodized surfaces expressed by percentage of control
Source: Author's

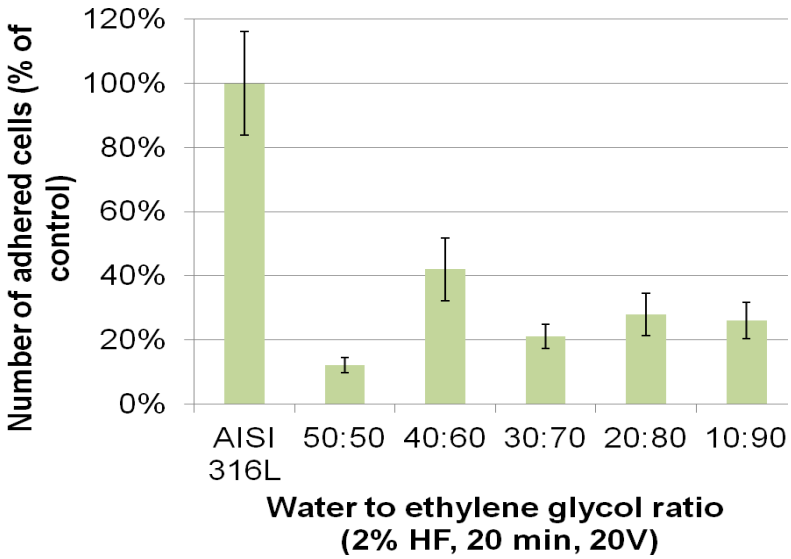

Fig. 4. Fungal adhesion to anodized surfaces expressed by percentage of control
Source: Author's

Numerous publications show that depending on the type of model organism selected for the experimental procedure, the obtained biological answer may differ. Presented researches were conducted on microorganisms belonging to different model groups: gram negative bacteria (*E coli*) and yeasts (*C albicans*). Those models are divergent for example on the basis of their physiology - like structure and composition of cell walls and in that way presence of different proteins, like integrins, responsible for adhesion to abiotic surfaces. Gram negative bacteria are characterised by three-component cell wall: two outer lipopolysaccharidic membranes and thin layer of peptidoglycan in the periplasmic space between them. Such structure results in for example low permeability for lipophilic molecules. In case of yeasts, the cell wall consists mostly of various glucans, with chitin dominating in inert part and mannoproteins in outer one [49]. Considering the above the type of the model organism might affect how the bacteria and yeasts were interacting with surfaces of various roughness.

When studying the bacterial colonisation on the manufactured surfaces, when the ethylene glycol content in the electrolyte was increasing, the almost linear growth of the total area occupied by bacteria in comparison to control sample was observed. However, considering fungal adhesion, for *Candida albicans* no linear dependence between the electrolyte composition and fungal surface colonisation was observed. The number of fungal cells occupying the surface was similar in all cases, with one exception. For the sample that was deposited in the electrolyte containing water to ethylene glycol ratio being 40:60, the number of *Candida* cells attached was much higher in comparison to others.

Conclusions

The study performed proved that the anodization process of titanium alloys can be possible when viscous electrolytes are used. However, as the most general trend should be that the reduction of water content in electrolyte help the formation of more tubular and longer titanium dioxide structures, no such dependence was observed . Each of the samples however, exhibited different character and structure. The anti-adhesive character of the obtained TiO_2 surfaces was maintained in terms of bacterial and fungal biofilm formation (the biological model employed in this manuscript were gram negative bacteria and yeasts) - all samples exhibited the antimicrobial character in comparison to the control sample.

References

[1] A. Colas, J. Curtis, Silicone Biomaterials: History and Chemistry & Medical Applications of silicones, Biomaterials Science, 2nd edition

[2] A. Tathe, M. Ghodke, A.P. Nikalje, A brief review: biomaterials and their applications, International Journal of Pharmacy and Pharmaceutical Sciences 2, 2010, 19-23

[3] A.Robin, M. Bernardes de Almeida Ribeiro, J.L. Rosa, R.Z. Nakazato, M.B. Silva, Formation of TiO2 nanotube layer by anodization of titanium in ethylene glycol-H2O electrolyte, Journal of Surface Engineered Materials and Advanced Technology 4, 2014, 123-130

[4] L. Sun, S. Zhang, X. Sun, X. He, Effect of the geometry of the anodized titania nanotube array on the performance of dye-sensitized solar cells, Journal of Nanoscience and Nanotechnology 10, 2010, 4551-4561

[5] Y-C. Lim, Z. Zainal, W-T. Tan, M.Z. Hussein, Anodization Parameters Influencing the growth of titania nanotubes and their photoelectrochemical response, International Journal of Photoenergy, 2012, 1-9

[6] S.R. Shah, A.M. Tatara, R.N. D'Souza, A.G. Mikos, F.K. Kasper, Evolving strategies for preventing biofilm on implantable materials, Materials Today 15, 2013, 177-182

[7] P. Went, M. Krismer, B. Frischut, Recurrence of infection after revision of infected hip arthroplasties, Journal of bones and joints surgery 77, 1995, 307-309

[8] R.M. Donlan, J. W. Costerton, Biofilms: survival mechanisms of clinically relevant microorganisms, Clinical Microbiology Revision 15, 2002, 167-193

[9] C.R. Kokare, S. Chakraborty, A,N, Khopade, K.R. Mahadik, Biofilm: Importance and applications, Indian Journal of Biotechnology 8, 2009, 159-168

[10] J.S. Webb, M. Giskov, S. Kjelleberg, Bacterial biofilms: prokaryotic adventures in multicellularity, Current Opinion in Microbiology 6, 2003, 578-585

[11] C. Desrousseaux, V. Sautou, S. Descamps, O. Traore, Modification of the surfaces of medical devices to prevent microbial adhesion and biofilm formation, Journal of Hospital Infection 85, 2013, 87-93

[12] C. R. Arciola, D. Campoccia, P. Speziale, L. Montanaro, J. W. Costerton, Biofilm formation in Staphyloccocus, implant infections. A review of molecular mechanisms and implications for biofilm-resistant materials, Biomaterials 33, 2012, 5967-5982

[13] D.B. Schlisselberg, S. Yaron, The effects of stainless steel finish on Salmonella Typhimurim attachment, biofilm formation and sensitivity to chlorine, Food Microbiology 35, 2013, 65-72

[14] J. Li, K. Hirota, T. Goto, H. Yumoto, Y. Mikaye, T. Ichikawa, Biofilm formation of Candida albicans on implant overdenture materials and its removal, Journal of dentistry 40, 2012, 686-692

[15] S.H. Flint, J.D. Brook, P.J. Bremer, Properties of the stainless steel substrate, influencing the adhesion of thermo-resistant Streptococci, Journal of Food Engineering 43, 2000, 235-242

[16] A.S.D. Al-Radha, D. Dymock, C. Younes, D. O'Sullivan, Surface properties of titanium and zirconia dental implant materials and their effect on bacterial adhesion, Journal of dentistry 40, 2012, 146-153

[17] D. Seigsmund, A. Undisz, S. Germerodt, S. Schuster, M. Rettenmayr, Quantification of the interaction between biomaterial surfaces and bacteria by 3D modelling, Acta Biomaterialia 10, 2014, 267-275

[18] K.A. Whitehead, J. Verran, The effect of surface topography on the retention of microorganisms, Food and Bioproducts Processing 84, 2006, 253-259
[19] K. Bazaka, R.J. Crawford, E.P. Ivanova, Do bacteria differentiate between degrees of nanoscale surface roughness?, Biotechnology Journal 6, 2011, 1103-1114
[20] R.J. Crawford, H.K. Webb, V.K. Truong, J. Hasan, E.P. Ivanova, Surface topographical factors influencing bacgterial attachment, Advances in Colloid and Interface Science 179-182, 2012, 142-149
[21] M. Medeiros Ronsani, A. Ulbrich Mores Rymovicz, T. Martins Meira, A. M. Trindade Gregio, O. Guariza Filho, O. Motohiro Tanaka, E. A. Ribeiro Rosa, Virulence modulation of Candida albicans biofilms by metal ions commonly released from orthodontic devices, Microbial Pathogenesis 51 (2011), s: 421-425
[22] K. Bazaka, M. V. Jacob, R. J. Crawford, E. P. Ivanova, Efficient surface modification of biomaterial to prevent biofilm formation and the attachment of microorganisms, Applied Microbiology and Biotechnology 95 (2012), s: 299-311
[23] C.E. ZoBell. The influence of solid surface on the physiological activities of bacteria in sea water, Journal of Bacteriology (1943), s:33-86
[24] Q. Zhao, Y. Liu, C. Wang, S. Wang, N. Peng, C. Jeynes, Reduction of bacterial adhesion on ion-implanted stainless steel surfaces, Medical Engineering & Physics 30, 2008, 341-349
[25] A. Atay, B. Piskin, H. Akin, C. Sipahi, A. Karakas, M. A. Saracli, Evaluation of Candida albicans adherence on the surface of various maxillofacial silicone materials, Journal de Mycologie Medicale 23, 2013, 27-32
[26] D. Campoccia, L. Montanaro, C. R. Arciola, A review of the biomaterials technologies for infection-resistant surfaces, Biomaterials 34, 2013, 8533-8554
[27] S.M. Dizaj, F. Loftipour, M.Barzegar-Jalali, M.H. Zarrintan, K. Adibkia, Antimicrobial activity of the metals and metal oxide nanoparticles, Materials Science and Engineering C 44, 2014, 278-284
[28] Z. Huang, P-C. Maness, D.M. Blake, E.J. Wolfrum, S.L. Smolinski, W.A. Jacoby, Bactericidal mode of titanium dioxide photocatalysis, Journal of Photochemistry and Photobiology A: Chemistry 130, 2000, 163-170
[29] U. Diebold, The surface science of titanium dioxide, Surface Science Reports 48, 2003, 53-229
[30] J.M. Macak, H. Tsuchiya, A. Ghicov, K. Yasuda, R. Hahn, S. Bauer, P. Shmuki, TiO2 nanotubes: Self-organized electrochemical formation, properties and applications, Current Opinion in Solid State and Materials Science 11, 2007, 3-18
[31] X. Liu, P.K. Chu, C. Ding, Surface modification of titanium, titanium alloys and related materials for biomedical applications, Materials Science and Engineering R 47, 2004, 49-121
[32] D.M. Brunette, P. Tengvall, M. Textor, P. Thomsen, Titanium in Medicine: material science, surface science, engineering, biological responses and medical applications, In: Engineering Materials, Springer 2001
[33] N. Ohtsu, S. Komiya, K. Kodama, Effect of electrolytes on anodic oxidation of titanium for fabricating titanium dioxide photocatalyst, Thin Solid Films 534, 2013, 70-75
[34] X. Zhu, J. Chen, L. Scheidler, R. Reichl, J. Geis-Gerstofer, Effects of topography and composition of titanium surface oxides on osteoblast responses, Biomaterials 25, 2004, 4087-4103
[35] L. Wu, J. Liu, M. Yu, S. Li, H. Liang, M. Zhu, Effect of anodization time on morphology and electrochemical impedance of anodic oxide films on titanium alloy in tartrate solution, International Journal of Electrochemical Science 9, 2014, 5012-5024
[36] G.K. Mor, O.K. Varghese, M. Paulose, K. Shankar, C.A. Grimes, A review of highly ordered, vertically oriented TiO2 nanotube arrays: Fabrication, material properties, and solar energy applications, Solar energy Materials & Solar Cells 90, 2006, 2011-2075
[37] A. Haring, A. Morris, M. Hu, Controlling morphological parameters of anodized titania nanotubes for optimized solar energy applications, Materials 5, 2012, 1890-1909
[38] V. Galstyan, E. Comini, G. Faglia, G. Sberveglieri, TiO2 nanotubes: recent advances in synthesis and gas sensing properties, Sensors 13, 2013, 14813-14838
[39] K.Das, S. Bose, A. Bandyopadhyay, Surface modifications and cell-materials interactions with anodized Ti, Acta Biomaterialia 3, 2007, 573-585
[40] P. Mandracci, F. Mussano, P. Rivolo, S. Carossa, Surface treatments and functional coatings for biocompartibility improvement and bacterial adhesion reduction in dental implantology, Coatings 6, 2016, 1-22
[41] J.Yao, H.Wang, Preparation of mesoporous titania using furfuryl alcohol and polymerizable solvent, Industrial & Engineering Chemistry Research 46, 2007, 6264--6268

[42] S. Peglow, M-M. Pohl, A. Kruth, V. Bruser, Plasma basedsynthesis, electron microscopy, and optical characterization of Au-, Ag-,and Ag/Au-Core-Shell nanoparticles, The Journal of Physical Chemistry C 119, 2015,563-572
[43] K. Lee, A. Mazare, P. Schmuki, One-dimensional titanium dioxide nanomaterials: nanotubes, Chemical Reviews 114, 2014, 9385-9454
[44] D. Fattakhova-Rohlfing, A. Zaleska, T. Bein, Three-dimensional titanium dioxide nanomaterials, Chemical Reviews 114, 2014, 9487-9558
[45] K.S. Raja, M. Misra, K. Paramguru, Formation of self-ordered nano-tubular structure of anodic oxide layer on titanium, Electrochimica Acta 51, 2005, 154-165
[46] J.M. Macak, P. Schmuki, Anodic growth of self-organized anodic TiO_2 nanotubes in viscous electrolytes, Electrochimica Acta 52, 2006, 1258-1264
[47] B. Vijayan, N.M. Dimitrijevic, T. Rajh, K. Gray, Effect of calcination temperature on the photocatalytic reduction and oxidation processes of hydrothermally synthesized titania nanotubes, The Journal of Physical Chemistry 114, 2010, 12994-13002
[48] X. Quan, S. Yang, X. Ruan, H. Zhao, Preparation of titania nanotubes and their environmental applications as electrode, Environmental Science&Technology 39, 2005, 3770-3775
[49] W.L. Chaffin, J.L. Lopez-Ribot, M. Casanova, D. Gozalbo, J.P. Martinez, Cell wall and secreted proteins of Candida albicans: identification, function and expression, Microbiology and Molecular Biology Reviews 62, 1998, 130-180

Piotr Pacholski, Jerzy Sęk
Lodz University of Technology, Faculty of Process Engineering and Environmental Protection, Department of Chemical Engineering
Wolczanska str.#213, 90-924 Lodz, Poland, piotr.pacholski@edu.p.lodz.pl

EXPERIMENTAL ANALYSIS OF CHEMICAL DEMULSIFICATION OF CUTTING OIL

Abstract
The wastewater produced by the metal industry is often present in the form of oil-in-water (O/W) or water-in-oil (W/O) emulsions. These fluids contain a certain amount of valuable oil that can be recovered in the recycling process. Therefore, the development of novel, efficient, and low cost processes for the treatment of metalworking fluid is necessary. Demulsification to separate oil/water mixtures is a very interesting option because it allows the recovery and reuse of the lubricant oil and effects in cleaner, easily treatable wastewater.Chemical destabilization is the most common way of demulsification of metalworking fluids. As an example, inorganic salts can be used as demulsifiers. In the presented work the efficiency of treatment of cutting emulsions with chemical demulsification with usage of aluminum sulfate (IV) is described. The emulsion was prepared with Emulgol-ES12 self-emulsyfing oil delivered by Orlen S.A. In the research the feasibility of the demulsifier was checked.The novel in this paper is determination of the optimal dosage of emulsifier using the TurbiscanLab® apparatus. It is relatively quick and precise method that can be applied in the industry.

Key words
demulsification, emulsion, TurbiscanLab, cutting oil

Introduction

Emulsions of cutting fluids are metalworking fluids (MWFs) that are being used in metal-mechanical industries to aid cutting processes, to prevent corrosion, and to improve lubrication, cooling, surface cleaning, and tool life. When used in machining processes, these emulsions lose their properties and effectiveness due to thermal degradation and contamination[1]. The replacement of these fluids leads to the occurrence of stable waste emulsions that can be hazardous to the environment [2,3,4,5].Cutting fluids are usually composed of mineral oil (40-80 *wt.*%), a surfactant, and additives. The additives are present in the mixture to meet the specifications for commercial concentrates, such as resistance to bacterial growth and low corrosion capacity. Additionally, some cutting fluids may contain water in their composition [2,5,6].

The lifecycle of cutting fluids in a machining facility involves four stages [7]:

- storage and handling
- mixing with water
- process using
- disposal

After the using stage, cutting oils, normally in the form of oil-in-water emulsion, will consist of different contaminants, such particles, heavy metals, and organic matters. These rejected oils are typically handled by two methods. The first one is recycling, during which contaminants are separated from the rejected oil, and then purified before returning to use in the manufacture process. Separation process can be operated by a variety of physical processes: separation by magnetic or centrifugal force, filtration or sedimentation. After this stage, the oils are purified to adjust their properties. As an example, oil can be heated to reduce viscosity. Sterilization is also significant process for protecting against infection to eliminate bacteria, which might be present in the oil. Another process used with rejected oil is disposal. This method is applied when oil recovery is not possible or difficult. This can happen when emulsion presents high water content or inadequate quality in the recovered oil. The disposal process is in two stages. First, the oil emulsions are destabilized into oil and water, normally by chemical processes. According to Rios et al. [5], inorganic salts can be employed as coagulants to demulsify the emulsion, leading to the coalescence of oil droplets. The separated oil is then used as an alternative fuel. However, biodegradation is another interesting alternative. Cheng et al. [3] reviewed that the biological degradation, both aerobic and anaerobic, and stated that it can effectively remove COD and turbidity, which

represent the amount of cutting oil in water. Electro-coagulation is another process that can be applied for treatment of metalworking fluid as well [8,9].Methods of demulsification of oil in water emulsion are presented in Table 1.

Table 1. Demulsification methods of metalworking fluids

Demulsification method	**Described by**
1.With inorganic salts	Rios et al.(1998)
2.Biodegradation	Cheng et al.(2005)
3.Electrocoagulation	Bensadok et al.(2007)

Source: Author's

Residual cutting fluids have a high carcinogenic potential due to the presence of products derived from the degradation of additives, polycyclic aromatic hydrocarbon (PAH), nitrosamines, among others [10]. According to Soković and Mijanović [11], secondary substances that are formed using cutting fluids include reaction products, foreign bodies, and microorganisms. It is essential to treat the cutting fluid wastewaters before its disposal in the environment considering the risks and the presence of strict environmental regulations. For example, the directive 2000/76/EC of the European Union defines a limit on the amount of used metalworking fluids that can be disposed of by incineration. Therefore, the development of novel, efficient, and low cost processes for the treatment of metalworking fluid is necessary[3, 12,13,28].

As it was mentioned, there are many methods of utilization of used cutting fluids. In chemical methods, it is possible to use salts such as alum or ferric salts[5,14]. The advantages of this method are low investment costs and the possibility of a wide range of applications. The measurement necessary for demulsification consists of a tank filled with emulsion, a stir and a pump for demulsifier. Operation costs depends mainly on the price of demulsifiers. The disadvantage of this method is fact that it is difficult to adjust the type and amount of used demulsifier [15].Therefore, in this article we also focused on the determination of the optimal dosage of the emulsion breaking agent.

Chemicals that are generally used to for destabilization of cutting oils emulsions are described below[16]:

- Monovalent electrolytes
- Bivalent electrolytes
- Multivalent electrolytes
- Surfactants with opposite charge

In experiments, the TurbiscanLab® was used. It is an optical measurement device that allows to monitor the emulsion behaviour in real time. The apparatus uses a multiple light scattering analysis technique [18,19,20]. TurbiscanLab® can be used to monitor the reversible degradation processes such as creaming and sedimentation and irreversible ones such as coalescence and aggregation. This apparatus can detect the changes in structure of fluid before they can be visible to human eye [20]. Analysis of transmittance signal and back scattering signal is recorded in time. This allows to monitor the real time stability of fluid. This device is used in the chemical industry [18] as well as in the pharmaceutical industry [20]. Up to now, not many articles present the analysis of demulsification with a TurbiscanLab® device. However, it is possible that this apparatus can be used to conduct a precise analysis of the emulsion degradation processes [21,23,26,27].

The aim of this work is to analyse the degradation mechanisms of 4% and 8% oil in water emulsion based on EMULGOL ES 12 oil delivered by Orlen S.A. This concentration has been chosen since they are most popular in industry. During the analysis, we used aluminium sulphate with a concentration of 8g/l to conduct demulsification. To analyse kinetics of phase separation the TurbiscanLab® apparatus was used. The method uses novel equipment to correctly determine the amount of necessary demulsifier for emulsion breakage. It is quick and simple method that can be broadly introduced in the industry. The conducted experiments are very important for metal-mechanical employees. As an example, presented research can be used as a short guide in demulsification of metalworking emulsions.

Materials and methods

In a 250ml baker we prepared 100ml emulsion based on emulsifying oil EMULGOL ES-12 delivered by Orlen S.A, by mixing mentioned oil and water with a hand homogenizer for 120 seconds. In Table 2we present the type of emulsion prepared, Table 3 shows the percentage composition of the emulsion system, and Table 4 represents the used demulsifier.

Tab.2. Specification of used emulsion

Emulsion type	Dispersed phase	Continuous phase
oil-in-water (O/W)	Emulsyfing oil Emulgol ES-12	Tap water

Source: Author's

Tab.3. The concentration of used emulsion

Water amount	Oil amount	Concentration of emulsion
96ml	4ml	4%
92ml	8ml	8%

Source: Author's

Tab.4. Type and amount of used demulsifier

Demulsifier type	Demulsifier concentration	The amount of used demulsifier
aluminium sulfate $Al_2(SO_4)_3$	8g/l	4ml/10ml emulsion 4% 6ml/10ml emulsion 4% 6ml/10ml emulsion 8% 8ml/10ml emulsji 8% 10ml/10ml emulsji 8%

Source: Author's

In Fig. 1 we present the picture of Turbiscan Lab scanning device with measuring principle.

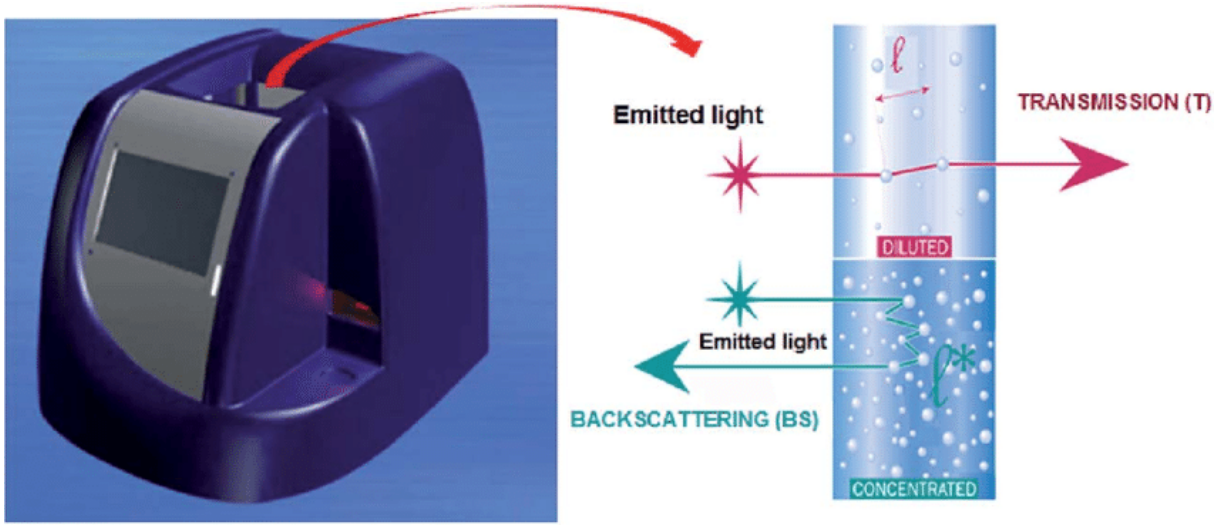

Fig. 1. Turbiscan Lab and its measuring method
Source: [17]

In order to separate phases in previously prepared systems, we placed 10ml of emulsion in a measuring cell of the TurbiscanLab® device. After this, we added to it certain amount of demulsifier-4ml, 6ml, or 8ml with a syringe and mixed the system with a magnetic stirrer for 20 seconds. Then we inserted the measuring cell in the TurbiscanLab® apparatus and started the measurement. We set the device to scan a measurement cell every 1

minute for the first hour, then every 5 minutes for two hours, and then every hour. The total time of a single experiment was 24 hours. To better understand the results of the experiment we also made visual observations of the samples.

Results and discussion

In Fig.2 we presented the results of demulsification of 4% emulsion based on emulsifying oil Emulgol ES-12 after addition of 4ml of aluminum sulfate with concentration of 8g/l for 10ml of emulsion. In the picture, transmittance and back-scattering signal is presented. The time of measurement was 24 hours. It can be observed that the fastest changes are present in first three hours of the process. The lowering of the back scattering signal at that time means that coalescence occurred. It can also be noted that close to the bottom of the measurement cell the water layer is present just after a couple minutes. Therefore, the measurements need to be conducted just after the addition of demulsifier. It can be also noted that after 24 hours the demulsification process was not finished- the transmittance at cell height 20mm-28mm was still very little.

Our demulsification results are in common with the observations of Rios et al. [5], however we monitored emulsion for a longer period of time. Another deviation is that instead of nefelometric measuring device, we used more advanced turbidimetric technique. Our method is also more simple than electrocoagulation used by Bensadok et al. [2] and Kobya et al. [25]. Compared to work of Cheng et al. [3], who studied biological degradation, our approach eliminate significant difficulties in operating bioreactors, such as maintenance of the stability of the microbial communities present in activated sludge plants. Demirbas and Kobya [28] investigated processes of metalworking fluid wastewater chemical coagulation and electrocoagulation, however they focused mainly on operation costs. They also used emulsion based on Castrol oil, while we are using the one based on Emulgol, which is more popular in Europe.

In Fig. 3 we present the visual observations of the demulsification process. On the left side, we present the sample after ten minutes of demulsifier addition, and on the right side we show the same sample after 180 minutes of process. It can be observed that the clarity of the sample increased and at the top the oil layer is present. However, the visual analysis does not allow one to follow the mechanism of demulsification. Therefore, we state that turbidimetric analysis is more precise than visual observation and it allows to us to better understand the nature of demulsification.

In Fig. 4 we presented the results for the same emulsion as in Fig. 2, but in this case we added 6ml of aluminum sulfate for 10 ml of emulsion. As it can be observed, the transmittance signal increment is bigger than in Fig. 1. Also, the final signal is higher, which means that the separation process finished and oil is fully separated from water. During analysis of the back-scattering signal it is possible to observe the separation of the oil phase at the top of the sample, which results in a decrease of signal at this height.

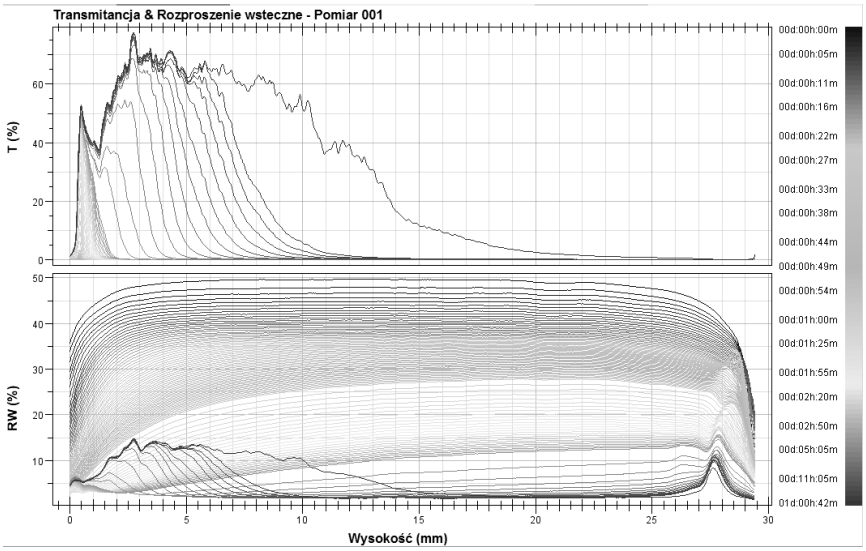

Fig. 2. Transmittance and back-scattering signal change in time versus height of the sample for 4ml of demulsifier addition for 10ml of 4% emulsion

Source: Author's

Fig. 3. On left- sample after 10 minutes of demulsifier addition. On right- sample after 180 minutes of demulsifier addition.
Source: Author's

Full separation of phases in the case of Fig. 2 was observed after 72 hours of demulsifier addition. In the case of Fig. 3, it took 24 hours to separate the water from the oil, which means that by that time all oil droplets moved to the top of measurement cell.

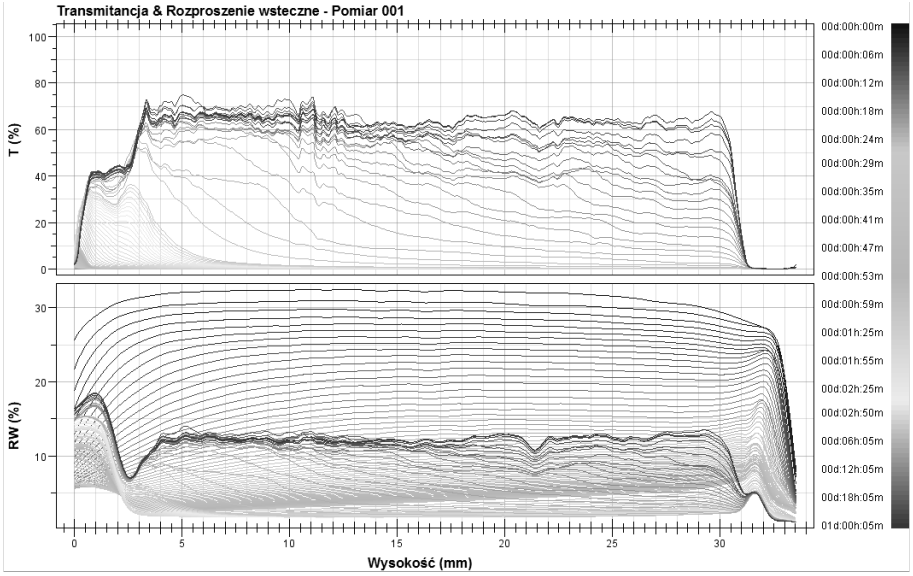

Fig. 4. Transmittance and back-scattering signal change in time versus height of the sample for 6ml addition of demulsifier for 10ml of 4% emulsion
Source: Author's

In Fig. 5 we presented the increment of transmittance in time for addition of 4ml and 6ml of aluminum sulfate for 10ml of 4% emulsion at 25mm height of measuring cell. As can be seen, the increase is gradual for the addition of 6ml. The sample reaches 70% of transmittance after 24 hours, which means that there is no oil left in water phase.

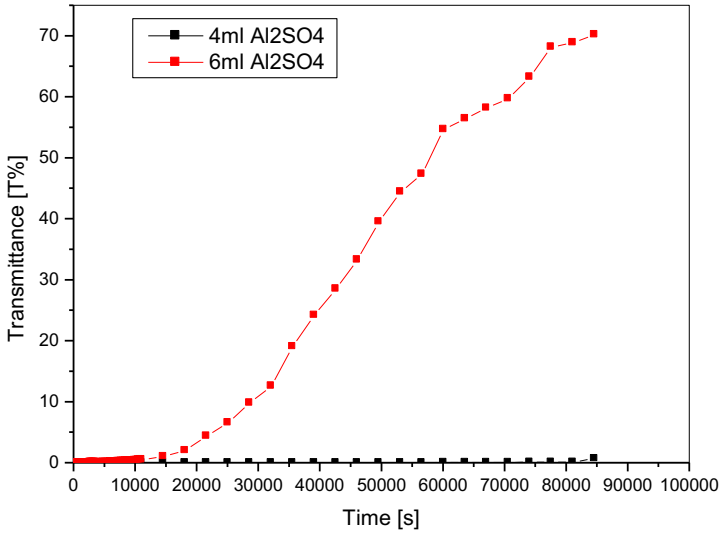

Fig. 5. Increment of transmittance for 4ml and 6ml addition of demulsifier for 10ml of 4% oil-in-water emulsion
Source: Author's

In Fig. 6 we presented the change of the back-scattering signal over time for 6ml demulsifier addition for 10ml of emulsion with 4% oil concentration. It was read for 25mm height. As can be seen, the signal decreased and then increased. During first two hours, the signal value lowers, which is related to the coalescence of droplets. Then phases separate, and only tiny oil droplets are left in water phase. After three hours of process the signal increased again, which can be explained with Mie theory, according to which the increment of this signal is present when the oil droplets are very small- in case of TurbiscanLab® below 0,6µm [24].

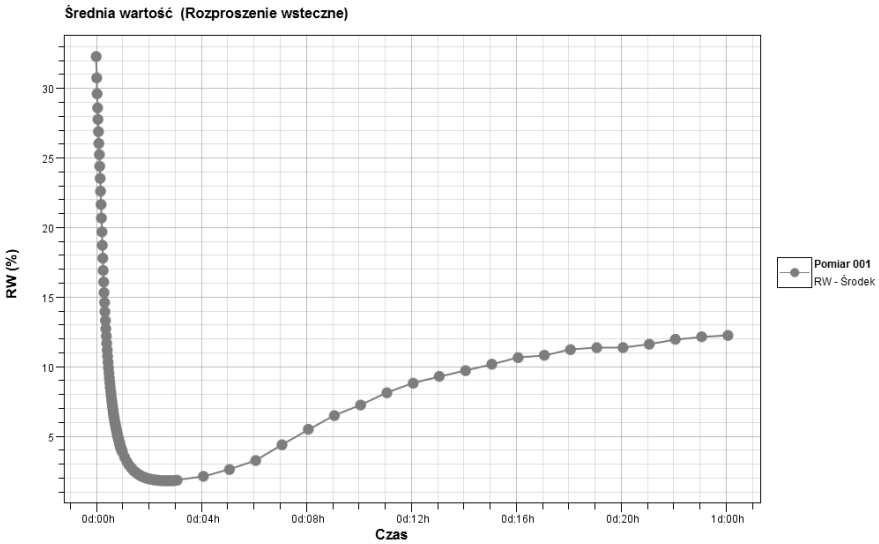

Fig. 6. Change of back-scattering signal at the middle of sample for 24 hours of process for 6ml demulsifier addition for 10ml of 4% emulsion
Source: Author's

In Fig. 7 we presented results for analysis of separation of emulsion with 8% concentration, reading two times higher than before. For this experiment, we added 10ml of sample 6ml of aluminum sulfate with 8g/l concentration. As can be seen, the increment in transmittance is observed only at the bottom of the sample. It means that 24 hours was not enough time for the complete separation for this amount of demulsifier addition.

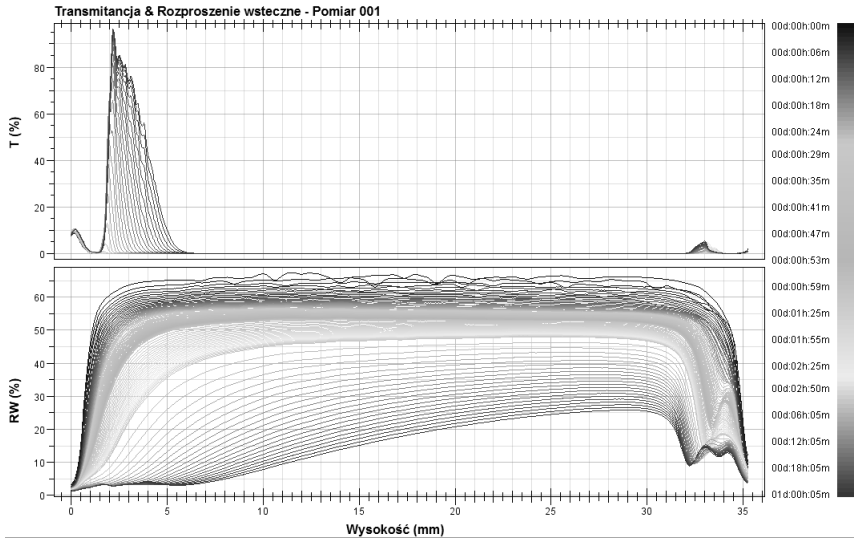

Fig. 7. Transmittance and back-scattering signal change in time versus height of the sample for 6ml addition of demulsifier for 10ml of 8% emulsion

Source: Author's

In Fig. 8 we presented the transmittance and the back-scattering signal change for 8% emulsion overtime after the addition of 8ml demulsifier for 10ml of emulsion. From transmittance, it can be observed that the water phase was bigger than in the case of Fig. 7. However, the small value of this signal at a height of 25mm to 33mm suggests that the process did not complete in 24 hours. Probably a few more hours would be needed to finish the phase separation.

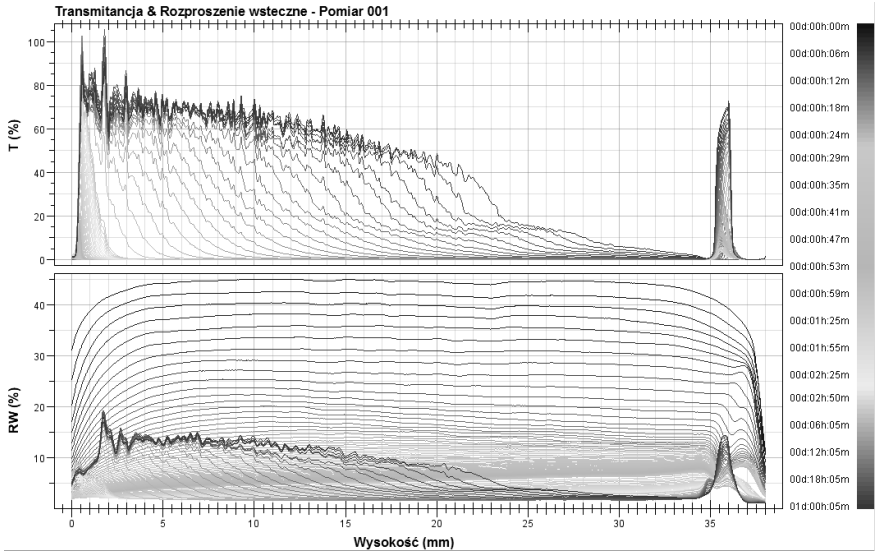

Fig. 8. Transmittance and back-scattering signal change in time versus height of the sample for 8ml addition of demulsifier for 10ml of 8% emulsion

Source: Author's

In Fig. 9 we presented the transmittance and the back-scattering signal change for 8% emulsion overtime after the addition of 10ml demulsifier for 10ml of emulsion. In this case, the transmittance signal was smaller than after 8ml the addition of demulsifier. It means that the time needed for demulsification will be longer than for 8ml of additional emulsion breaker. Therefore, we state that 8ml addition of aluminum sulfate with 8g/l concentration is the optimal dosage for break 8% oil-in-water emulsion based on Emulgol ES-12.

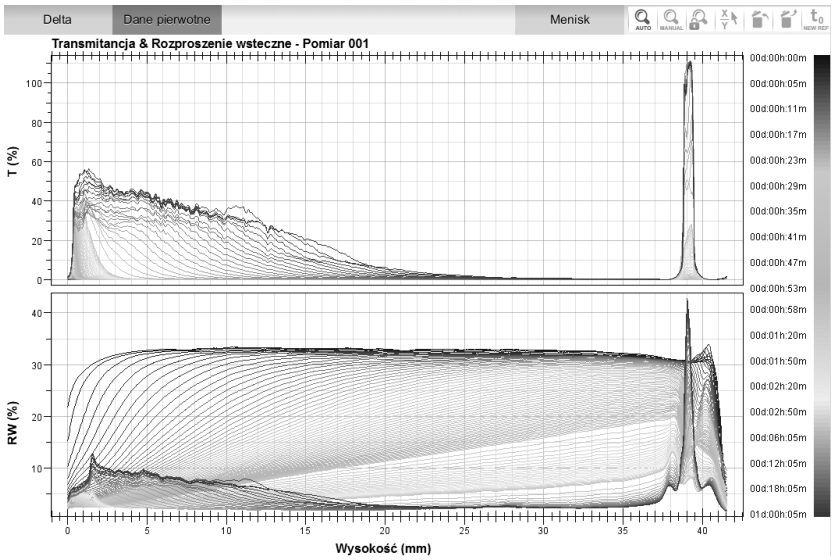

Fig. 9. Transmittance and back-scattering signal change in time versus height of the sample for 10ml addition of demulsifier for 10ml of 8% emulsion

Source: Author's

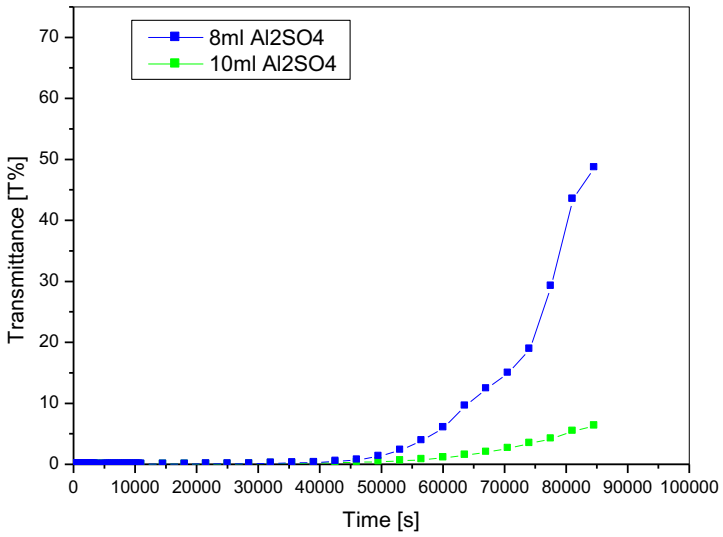

Fig. 10. Increment of transmittance for 8ml and 10ml addition of demulsifier for 10ml of 8% oil-in-water emulsion

Source: Author's

In Fig. 10 we presented the transmittance increment overtime for an addition of 8ml and 10ml demulsifier for 10ml of 8% emulsion. This parameter was obtained for a height of 15mm of the sample, since at 25mm of the sample the oil phase was present. As can be seen, the value varies for different amounts of additional demulsifiers. A bigger increment is observed for 8ml addition of emulsion breaker. It confirms our statement that this addition was optimal to separate phases in 8% emulsion.

Summary and conclusions

The used cutting oils are considered to be hazardous waste that can be dangerous for the environment. One method of its disposal is separation of oil and water. Demulsification with aluminum sulfate appears to be a simple and efficient method of phase separation for the fluids. During analysis of process it is possible to notice the increment of transmittance signal varies over time. It is related to coalescence and phase migration during process. At the beginning the coalescence of droplets occurs, which can be observed by a rapid decrease in the back-scattering signal. Then the phase separates which can be noticed as the increment of transmittance signals

at the bottom of a measuring cell. The amount of 6ml aluminum sulfate with a concentration of 8g/l for 10ml of emulsion allowed the separation of phases in 4% emulsion completely in 24 hours, while the amount of 4ml of demulsifier needed 72hours to complete demulsification for this emulsion concentration. In the case of 8% emulsion, the most effective appeared to be 8ml additional aluminum sulfate for 10ml of emulsion. After the addition of 6ml the phase separation was not observed, while for 10ml addition the process was slower than for 8ml of demulsifier. Therefore, we concluded that the addition of 8ml of aluminum sulfate with a concentration of 8g/l for 10ml of 8% cutting oil emulsion is optimal dosage for phase separation.

References

[1] Polowski W., Musiałek K., Nowak D. Badania cieczy obróbkowych stosowanych w procesie skrawania metali oraz postępowanie z emulsjami zużytymi,Materiały Konferencyjne Ecofirm, IV Symp. IOS Kraków: (2000)111-115

[2] Bensadok, K.; Belkacem, M.; Nezzal, G. Treatment of cutting oil/water emulsion by coupling coagulation and dissolved air flotation. Desalination(2007) 206: 440-448

[3] Cheng, C., Phipps, D., Alkhaddar, R.M. Review treatment of spent metalworking fluids. Water research (2005) 39: 4051-4063

[4] Komorowicz T., Janusz M., Marta P., Luiza P.Badania rozdziału emulsji olej-woda z zastosowaniem deemulgatorów, Czasopismo Techniczne Wydawnictwo Politechniki Krakowskiej (2007) :48-58

[5] Rios, G., Pazos, C., Coca, J. Destabilization of cutting oil emulsions using inorganic salts as coagulants. Physicochemical and Engineering Aspects (1998) 138: 383-389

[6] Bataller, H.; Lamaallam, S.; Lachaise, J.; Gracia, A.; Dicharry, C. Cutting fluid emulsions produced by dilution of a cutting fluid concentrate containing a cationic/nonionic surfactant mixture. Journal of Materials Processing Technology,(2004) 152 : 215-220.

[7] Grzesik, W. Cutting fluids. Advanced machining processes of metallic materials:Theory, modeling, and application. US: Elsevier (2008)

[8] Bensadok, K., Benammar, S., Lapicque, F., Nezzal, G. Electrocoagulation of cutting oil emulsions using aluminium plate electrodes. Journal of hazardous materials (2008) 152: 423-430

[9] Kobya ,M., et al, Treatment of potato chips manufacturing wastewater by electro coagulation, Desalination, (2006)190: 201-211.

[10] Occupational safety and health administration (OSHA), Metalworking fluids standardadvisory committee (MWFSAC). Metalworking fluids: safety and health bestpractices manual.(1999)

[11] Soković, M.; Mijanović, K. Ecological aspects of the cutting fluids and its influence on quantifiable parameters of the cutting processes. Journal of Materials Processing Technology (2001) 109:181-189

[12] El Baradie, M.A. Cutting fluids: part II. Recycling and clean machining. Journal of Material Processing Technology (1996) 56: 798-806

[13] Feldman, D. G.; Kessler, M. Fluid qualification tests – evaluation of the lubricating properties of biodegradable fluids. Industrial Lubrication and Tribology, (2002)54,3: 117-129,

[14] Gierżatowicz R., Pawłowski L., Sposób demulgacji emulsji wodno-olejowych zwłaszcza przepracowanych chłodziw obrabiarkowych, opis patentowy (1994) 165104

[15] Komorowicz T. Kupiec K., Mółka A. Zastosowanie nowych demulgatorów organicznych do rozdziału emulsji olej-woda (2014) 1/14 1-10

[16] Chawaloesphonsiya, Nattawin, Séparation d'émulsions par flottation et coalescence pour le traitement d'eaux uses (2015)PhD thesis

[17] Yang, Hongbin & Kang, Wanli & Wu, Hairong & Yu, Yang & Zhu, Zhou & Wang, Pengxiang & Zhang, Xiangfeng & Sarsenbekuly, Bauyrzhan. Stability, rheological property and oil-displacement mechanism of a dispersed low-elastic microsphere system for enhanced oil recovery. RSC Adv.. 7. 8118-8130 (2017)

[18] Barad J.M., Chakraborty M., Bart H.J. Stability and performance study of water-in-oil-in-water emulsion: extraction of aromatic amines, Ind. Eng. Chem. Res.(2010) 49: 5808-5815

[19] Lemarchand C.,Couvreur P., Vauthier C., Costantini D., Gref R. Study of emulsion stabilization by graft copolymers Rusing the optical analyzer Turbiscan, Int. J.Pharm. (2003)254: 77-82

[20] Celia C., Trapasso E., Cosco D., Paolino D., Fresta M. TurbiscanLab® Expert analysis of the stability of ethosomes and ultradeformable liposomes containing a bialyer fluidizing agent, Colloid Surf.B (2009) 72:155-160

[21] Buron H. Mengual O. Meunier G. Cayre I. Snabre P. Optical characterization of concentrated dispersions: applications to laboratory analyses an on-line process monitoring and control, Polym. Int. (2004)53:1205-1209
[22] Mengual O. Meunier G. Cayre I., Snabre P. Characterization of instability of concentrated dispersions by a New optical analyser: the TURBISCAN MA 1000, Colloid Surf. A (1999) 152 111-123
[23] Liu J. Huang X.,LuL.,Li M., Xu J. Deng H. TurbiscanLab® Expert analysis of the biological demulsification of water-in-oil emulsion by two biodemulsifiers Journal of Hazardous Materials (2011) 190:214-221
[24] Hergert W., Wriedt T.,Mie Theory 1908-2008, Present developments and Interdisciplinary aspects of light scattering, Universität Bremen, Bremen –presentation (2008)
[25] M. Kobya, C. Ciftci, M. Bayramoglu and M. T. Sensoy, Study on the Treatment of Waste Metal Cutting Fluids Using Electrocoagulation, Separation and Purification Technology, Vol. 60, No. 3, (2008)285-291
[26] Lesaint C., Glomm W, Lundgaard L., Sjöblom J., Dehydration efficiency of AC electrical fields on water-in-model-oil emulsions, Colloids and Surfaces A: Physicochemical and Engineering Aspects, Volume 352, Issues 1–3, (2009), 63-69
[27] Li Z., Wu H., Yang M., Xu D., Chen J., Feng H., Lu Y., Zhang L., Yu Y., Kang W., Stability mechanism of O/W Pickering emulsions stabilized with regenerated cellulose, Carbohydrate Polymers (2017)
[28] Demirbas E., Kobya M., Operating cost and treatment of metalworking fluid wastewater by chemical coagulation and electrocoagulation processes, Process Safety and Environmental Protection, Volume 105, (2017) 79-90,

Olga Shtyka, Łukasz Przybysz, Jerzy Sęk
Institution Faculty of Process and Environmental Engineering, Technical University of Lodz
Wolczanska 177, 90-924 Lodz, Poland, olga.shtyka@edu.p.lodz.pl

TRANSPORT OF EMULSIONS IN GRANULAR POROUS MEDIA DRIVEN BY CAPILLARY FORCE

Abstract
The transport of liquids driven by capillary suction-pressure and balanced by both viscous drag force and gravity acceleration is known as spontaneous imbibition. The prediction of spontaneous imbibition in porous media is of importance due to its relevance as a fundamental phenomenon in numerous industrial technologies as well as in nature. A vast majority of the experimental results and mathematical models concerning the imbibition process of single-phase liquids are considered and analyzed in the literature. The present research focuses on two-phase liquids transport in porous medium driven by capillary force. The penetrating liquids were surfactant-stabilized emulsions with the different dispersed phase concentrations. The discussed issues are the influence of porous bed composition and inner phase concentration on the height of an emulsion penetration, which allows to predict the velocity of imbibition process. From a practical point of view, the experimental results give the possibility to evaluate: productivity of granular sorbents applied to recover the environment, efficiency of building materials wetting with multiphase liquids, process of oil-derived pollutants migration in porous media, e.g. soil and other rock structures, etc.

Key words
emulsion, imbibition, kinetics, granular media, pore radius

Introduction

The liquids transport driven by capillary force and counterbalanced by viscous drag force and gravity acceleration is referred in literature as spontaneous imbibition or wicking [1-4]. The imbibition as a physical phenomenon occurs in porous structures on the condition that adhesion predominates a mutual force of attraction between molecules in a permeating liquid [3-5]. The prediction of the spontaneous imbibition in porous media remains of importance due to its relevance as a fundamental phenomenon in a variety of industrial technologies and in nature: oil recovery and removal of different oil-derivative products from the environment, paper coating, ink penetration process, drug delivery systems, hydrological regime of soil layers, and measuring of contact angle in surface chemistry [1, 2, 6].

The process of porous media imbibition with such single-phase liquids as water [1, 4, 7], and different inorganic substances, i.e. dimethyl silicone oil, dodecane, hexadecane, diethyl ether, was experimentally investigated and described in the literature [3, 5, 8]. There are numerous approaches used to describe the single-phase liquids wicking in various porous structures. A great deal of the discussed mathematical models considers the effect of a dynamic contact angle on capillary rise [4, 8, 9]. Another group predicts the spontaneous imbibition in the porous media regarding structural parameters, i.e. porosity, tortuosity and shape of pores [2, 10-12]. A lot of approaches confiders both factors: structure of voids and medium saturation [11, 13, 14]. This allows for the characterization of the imbibition process in a wide range of granular media such as sorbents, soil, silica glasses, and other rocks. The mentioned concepts are appropriate to predict imbibition process in case of various single-phase liquids, while there is lack of experimental results and mathematical models, which predict wicking of multiphase liquids in granular beds.

This research work focuses on the study of the imbibition process in case of oil-in-water emulsions as two-phase dispersions differed by wettability and viscosity. The experiments reported in the paper were undertaken to investigate the kinetics of imbibition in different granular beds in terms of the changes of penetration height as a function of time, i.e. $h_{im} = f(t_{im})$. The influence of the dispersed phase concentration and the composition of granular media on the kinetics of imbibition, velocity of this process, its instantaneous velocity as well as the maximal height of an emulsion front rise were also considered and discussed.

Materials and Methods

In these experiments, the spontaneous imbibition process was investigated experimentally using the wicking test, as described in details in the publication [6, 15]. The used experimental set-up is schematically represented in Figure 1. A sample of a granular medium (*2*) was directly immersed with one end into a reservoir with an emulsion (*1*) with a contact area of 0.00096 m^2. The changes of the emulsion mass m_{im} in a reservoir (*1*) were registered versus time t_{im} using an analytical balance (*3*) as well as the height of its penetration h_{im} by means of a ruler (*4*). The time when the mass of the emulsion in a reservoir (*1*) became steady was assumed as the final time of imbibition process t_{max}. The achieved height of the liquid front at t_{max} was denoted as the equilibrium height, denoted as $h_{max.}$

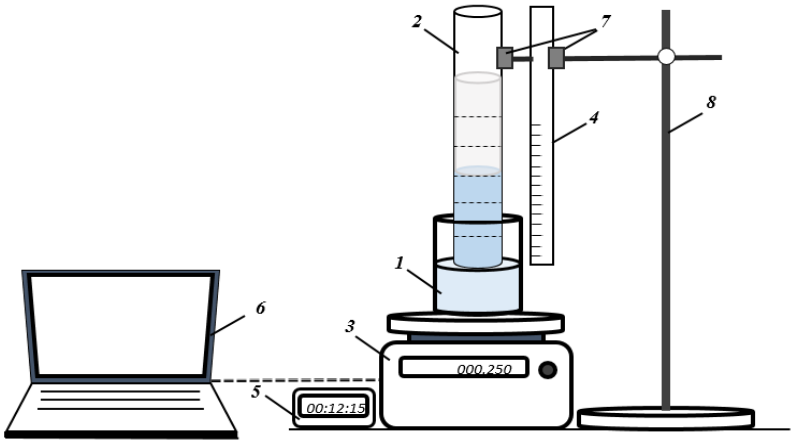

Fig. 1. Schematic illustration of the used experimental set-up for a granular medium: 1 – reservoir with an emulsion; 2 – granular bed; 3 – analytical balance; 4 – ruler; 5 – timer CDN TM15; 6 – computer to register data; 7 – fixators; and 8 – stand. The camera Nikon Coolpix L120 was used to record the changes of the height.
Source: Author's

Three types of oil-in-water emulsions were used in the current experiments. The emulsions were prepared according to the standard procedure. The dispersions differed by the inner phase concentration, which was equal to 10 vol.%, 30 vol.%, and 50 vol.%. They were stabilized with 2 vol.% of a non-ionic surfactant composed of ethoxylated oleic acid (commercial name Rokacet O7), obtained from PCC Exol SA (Poland). The defined volume of the distilled water, as a continuous phase, was mixed with the emulsifier and dispersed phase in a 500 ml beaker with a diameter d_{bk} of 0.08 m. The immiscible phases and surfactant were mixed by means of a high shear laboratory homogenizer with revolution of 12000 min^{-1} during 600 s.

Microscopic images analysis of the prepared emulsions was carried out by means of Microscope Leica DMI3000B with a Lumenera Infinity1 camera. The distribution of the dispersed droplet size in emulsions is shown in Fig. 2. According to the results, the diameters of dispersed oil droplets in the prepared emulsions were in the range 1–20 µm, while a majority of them (75–80%) had a size of 2–10 µm.

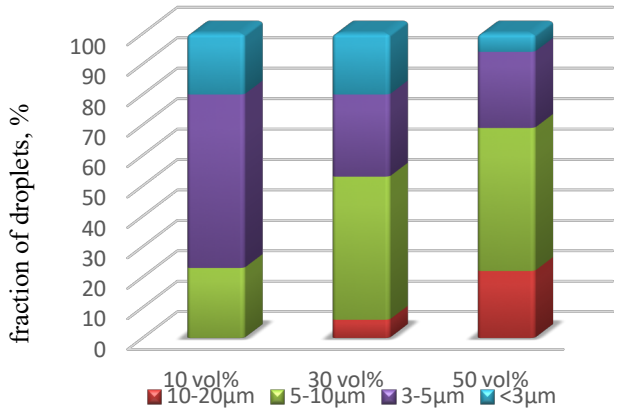

Fig. 2. Distribution of the dispersed droplet size in emulsions stabilized by the surfactant in concentration φ_s of 2 vol.%.
Source: Author's

The viscosity was measured using a shear rheometer Bohlin CVO120 (Malvern Instruments, UK). The density was determined using the picnometric method. The surface tension was measured using a tensiometer KRÜSS K12 (KRÜSS GmbH, Germany). The physicochemical properties of the emulsions components are shown in Table 1.

Table 1. Properties of emulsions components (T=23±1^{0}C)

Type of liquid	**Density (kg/m^3)**	**Viscosity (mPa·s)**	**Surface tension (mN/m)**	**HLB (-)**
Dispersed phase	922.1±0.6	53.12±1.44	32.2±1.7	-
Rokacet O7	908.0±2.7	50.21±0.62	36.2±1.8	10.6

Source: Author's

The porous medium was represented by a granular bed consisting of spherical granules, and characterized by the oleophilic/hydrophilic property. The beads were produced and obtained from "Alumetal-Technik" (Poland). The used porous media differed by a size of the particles, and their diameters ranged from 100–800 µm. The parameters of the granular media used are provided in Table 2.

Table 2. Parameters of the granular media

Type of medium	**Range of beads diameter (µm)**	**Average diameter of beads, d_a (µm)**	**Porosity, ε**
GS 100	100–200	180±10.9	0.35±0.010
GS 200	200–300	245±12.3	0.36±0.011
GS 600	600–800	650±9.2	0.37±0.013

Source: Author's

All experiments were conducted at 23±1^{0}C and atmospheric pressure. Three independent replications were carried out for each experiment, and results were presented as their mean values.

Result and Discussion

The results concerning the change of the emulsion penetration height h_{im} as a function of time t_{im} for the different granular beds are represented in Figure 3. The used granular beds were composed of spherical grains with sizes in the ranges of 100–200 µm, 200–300 µm, and 600–800 µm. The data were obtained for emulsions with the different dispersed phase concentrations of 10 vol%, 30 vol%, and 50 vol%.

As shown in Figure 3, the emulsions differ significantly by the height of penetration, thus a fraction of beads size and consequently, radii of pores in a granular bed causes the strong influence on the height of the emulsion front rise. The hydraulic radius of pores r_h was calculated according to Kozeny-Carman theory as a relation between medium porosity and average diameter of beads [16]. Thus, it was 16.2±0.16 µm for a medium with particles diameter d_b in a range of 100–200 µm, 23.0±0.38 and 63.6±0.18 µm for GS 200 and GS 600, respectively. To compare used granular beds, all emulsions tended to wick higher in case of medium with lower value of r_h. In contrast, the dispersed phase concentration is recognized initially as a less important factor.

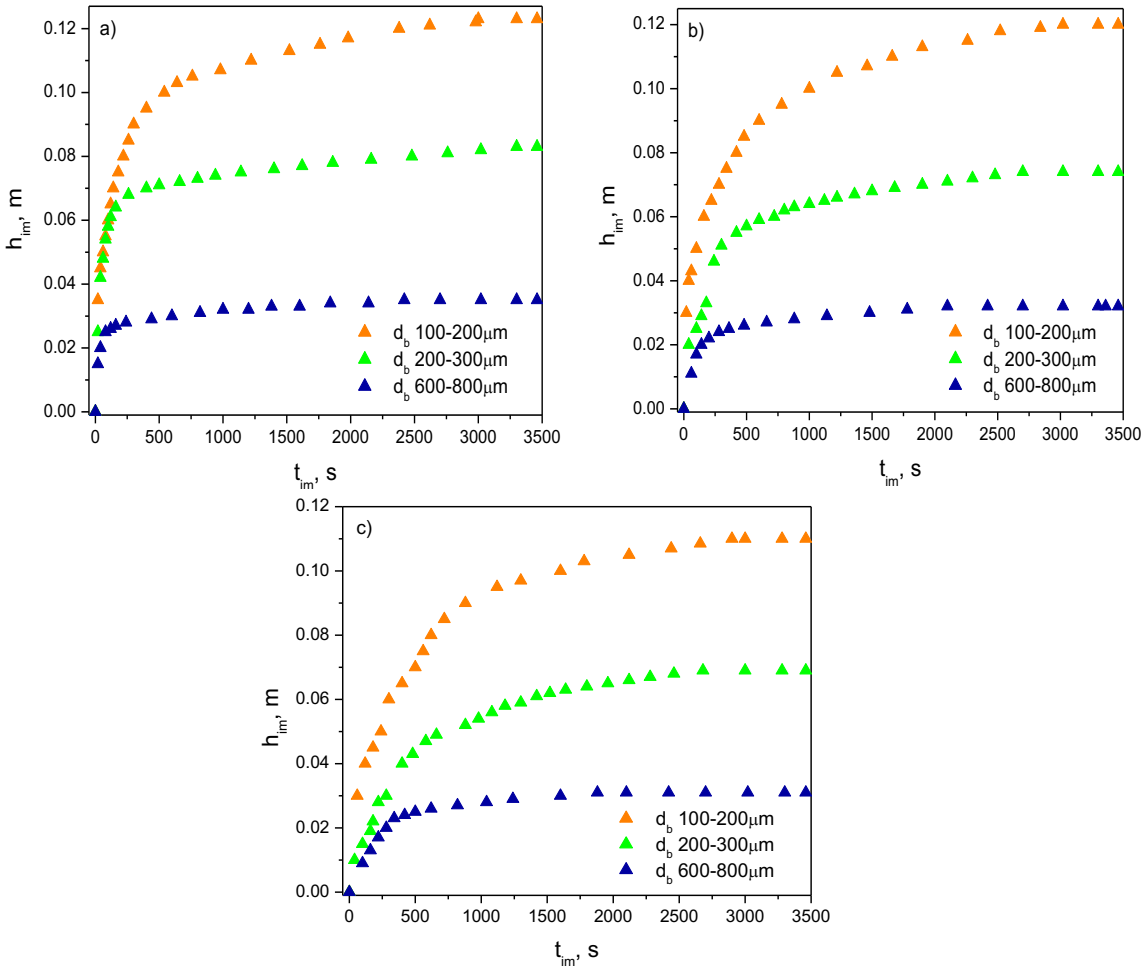

Fig. 3. Changes of emulsion front height h_{im} versus time t_{im} during the imbibition process in the different granular media in case of: a – 10% emulsions; b – 30% emulsions; c – 50% emulsions.
Source: Author's

The experimental data allowed to define the maximal height of emulsions penetration in the different granular media, and the results are shown in Table 3.

Table 3. The maximal height h_{max} of the imbibed emulsions

Type of medium	Dispersed phase fraction, φ_d		
	10 vol%	30 vol%	50 vol%
GS 100	0.123	0.120	0.110
GS 200	0.083	0.074	0.069
GS 600	0.035	0.032	0.031

Source: Author's

The maximal height tends to decrease slightly, i.e. maximum up to 17 %, with the enlarging of the dispersed phase concentration. Such tendency was observed for porous beds with different compositions. The experimental results shown that the highest values of h_{max} were obtained in case of the granular medium composed of beads with d_b in a range of 100–200 μm, i.e. 0.123, 0.12, and 0.11 m for 10%, 30%, and 50% emulsions, respectively. Consequently, the lowest values were derived for the spontaneous imbibition process in a granular medium with d_b of 600–800 μm.

The changes of the imbibition velocity as $v_{imh} = f(t_{im})$ on the base of height values in the used granular beds are shown in Figure 4.

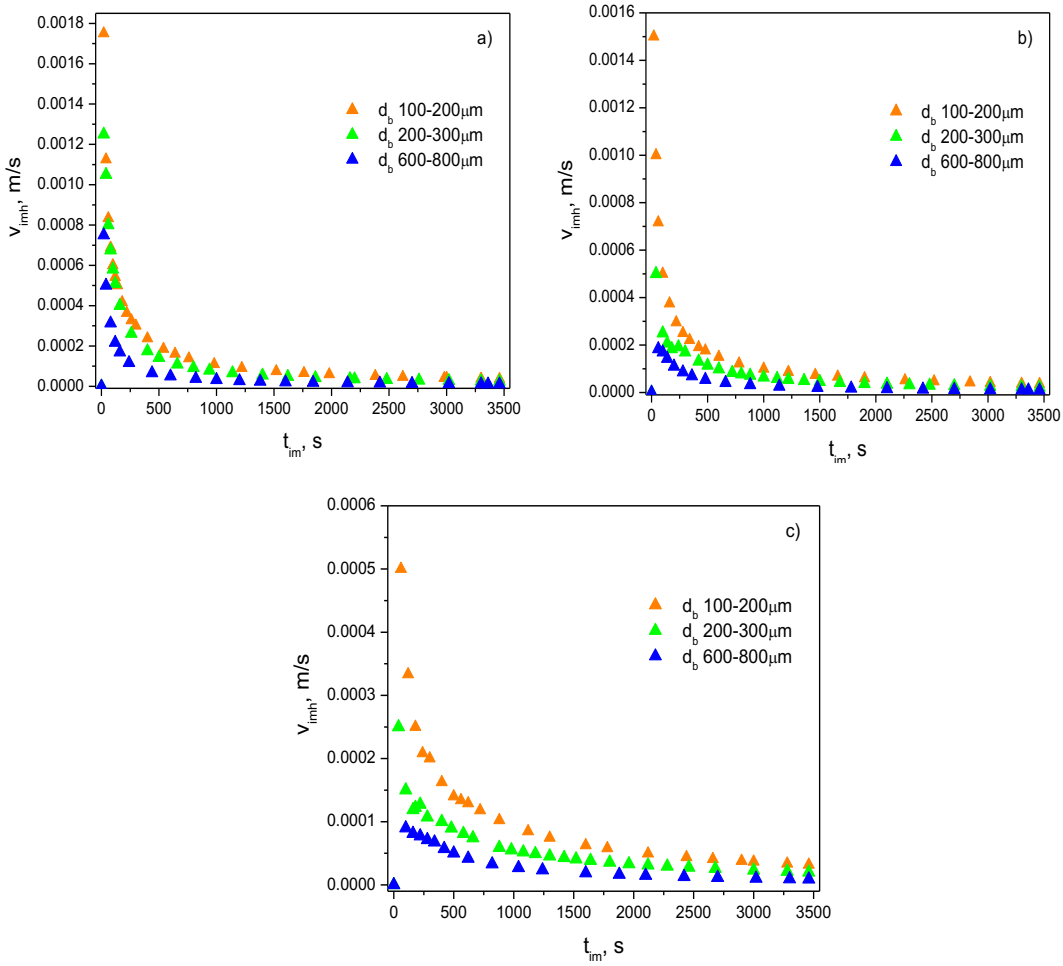

Fig. 4. Changes of the imbibition velocity v_{imh} versus time t_{im} for: a – 10% emulsions; b – 30% emulsions; c – 50% emulsions
Source: Author's

The imbibition velocity v_{imh} tends to rise rapid and after that decreases as shown on the graphs. It can be explained by growth of the counterbalancing force, i.e. gravity acceleration, due to increase of an imbibied emulsion mass. The values of the maximal velocity v_{max} of the wicking process and time $t(v_{max})$, when it was reached, are represented in Table 4.

Table 4. The maximal velocity v_{max} of the imbibition process

Dispersed phase concentration, φ_d	**GS 100**		**GS 200**		**GS 600**	
	v_{max}, m/s	**t (v_{max}), s**	**v_{max},m/s**	**t (v_{max}), s**	**v_{max},m/s**	**t (v_{max}), s**
10 vol%	0.00175	20	0.00125	20	0.00075	20
30 vol%	0.00150	20	0.00050	40	0.00018	60
50 vol%	0.00050	40	0.00025	40	0.00009	100

Source: Author's

In all investigated cases, the highest maximal velocity values were obtained in case of the dispersions with the lowest inner phase concentration. It can be explained by the difference in viscosity, and lower value is less influence of the viscous drag force. Thus, the prepared emulsions have the following viscosities: for 10% it was equal to 6.1 mPa·s, in case of 30% this parameter was near 14.8 mPa·s, and the largest value was obtained for 50% dispersion, i.e. 48.4 mPa·s.

As shown in Table 4, it is equal to 0.00175 m/s for the porous bed with d_b of 100–200 μm, 0.00125 m/s for 200–300 μm, and consequently, 0.00075 m/s for 600–800 μm. To compare, the lowest values of v_{imh} were observed for 50% emulsions in all used granular beds. The maximal velocity was registered at t_{im} = 20 s for 10% emulsions,

however it tends to growth with increase of the inner phase concentration. The enlargement of grains size and consequently, hydraulic radius of pores causes the increase of time needed to obtain the maximal velocity, i.e. up to 20 s ≤ t_{im} ≤ 100 s (Table 4).

The changes of instantaneous velocity v_{inh} with time t_{im} was additionally calculated relating to average velocity of the imbibition process. It represented as velocity of a liquid in motion at the specific point of time process. The results of the instantaneous velocity variations are performed in Figure 5.

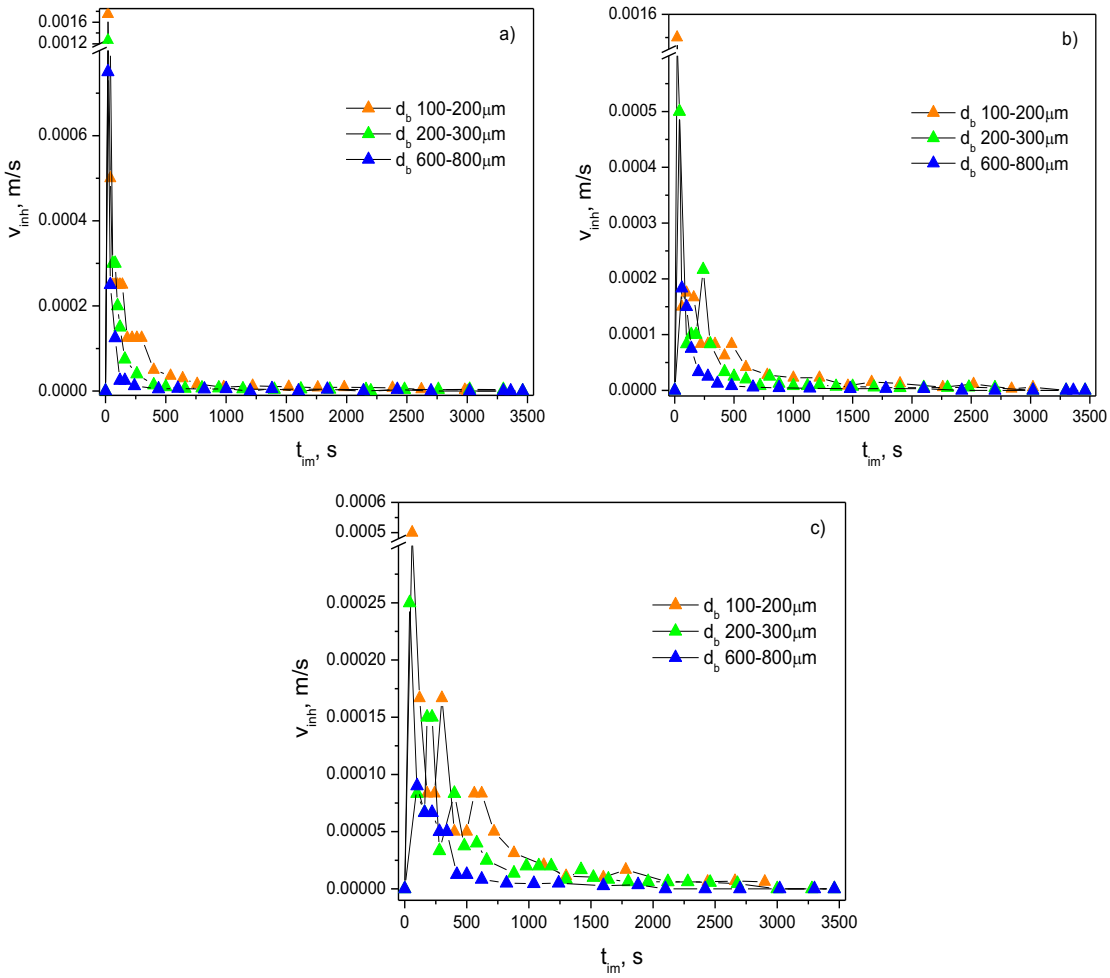

Fig. 5. Changes of the instantaneous imbibition velocity v_{inh} versus time t_{im} for: a – 10% emulsions; b – 30% emulsions; c – 50% emulsions.
Source: Author's

As show in Figure 5a, the higher instantaneous imbibition velocity was obtained for 10% emulsions in all granular beds investigated as in the case of the imbibition velocity v_{imh}. In contrast, the lowest values were derived for 50% dispersions. According to the results, the stronger influence of a bed composition is also observed for emulsions with the inner phase concentration of 50 vol%. In case of 10% emulsions, the instantaneous imbibition velocity becomes almost the same after t_{im} = 800 s (Fig. 5a).

To conclude, the emulsions imbibition in terms of the penetration height depends considerably on the composition of a granular bed. On the one hand, the dispersed phase concentration causes less significant influence on the height of an imbibed emulsion wicking in a granular media. On the other hand, the composition of the dispersed phase effects the imbibition velocity as well as instantaneous one.

Summary and conclusions

The discussed issues were the influence of porous bed composition and dispersed phase concentration on the height of emulsion penetration, which allows to predict velocity of the imbibition process and the maximal height

of dispersion rise in a granular bed. According to results, the height of an emulsion front permeation in a granular medium forced by the capillary pressure depends more strongly on the composition of this bed than on the initial concentration of the dispersed phase. However, the effect of a porous medium structure was more considerable in case of 50% dispersions. From a practical point of view, the experimental results give the possibility to predict the productivity of granular sorbents applied to recovery the environment, the building materials wetting with dispersions, i.e. paints, antifungal liquid, and pollutants migration in various porous media, i.e. soil layers, sands and other rock structures.

References

[1] R. Masoodi, K.M. Pillai, Darcy's law-based model for wicking in paper-like swelling porous media, AlChE Journal 56 (2010) 2257-2267.

[2] J. Cai, X. Hu, D. S. Standnes, L. You, An analytical model for spontaneous imbibition in fractal porous media including gravity, Colloids Surf., A 414 (2012) 228-233.

[3] R. Masoodi, K.M. Pillai, P.P. Varanasi, Darcy's law based models for liquid absorption in polymer wicks, AlChE Journal 53 (2007) 2769-2782.

[4] A. Hamraoui, T. Nylander, Analytical approach for the Lucas–Washburn equation, J. Colloid Interface Sci. 250 (2002) 415-421.

[5] B.V. Zhmud, F. Tiberg, K. Hallstensson, Dynamics of capillary rise, J. Colloid Interface Sci. 228 (2000) 263-269.

[6] O. S. Shtyka, M. M. Błaszczyk, J. P. Sęk, Analysis of emulsions concentration changes during imbibition in porous sorbents, IJEST 13 (2016) 2401-2414.

[7] H.T. Xue, Z.N. Fang, Y. Yang, J.P. Huang, L.W. Zhou, Contact angle determined by spontaneous dynamic capillary rises with hydrostatic effects: Experiment and theory, Chem. Phys. Lett. 432 (2006) 326-330.

[8] R.M. Digilov, Capillary rise of a non-Newtonian power law liquid: impact of the fluid rheology and dynamic contact angle, Langmuir 24 (2008)13663-13667.

[9] M. Hilpert, Liquid withdrawal from capillary tubes: explicit and implicit analytical solution for constant and dynamic contact angle, J. Colloid Interface Sci. 351 (2010) 267-276.

[10] H.Y. Zhao, K.W. Li, A fractal model of production by spontaneous water imbibition, Latin American and Caribbean Petroleum Engineering Conference (2009).

[11] J. Cai, E. Perfect, C.L. Cheng, X. Hu, Generalized Modeling of Spontaneous Imbibition Based on Hagen−Poiseuille Flow in Tortuous Capillaries with Variably Shaped Apertures, Langmuir 30 (2014) 5142-5151.

[12] C.L. Cheng, E. Perfect, B. Donnelly et al., Rapid imbibition of water in fractures within unsaturated sedimentary rock, Adv. Water Resour. 77 (2015) 82-89.

[13] K.W. Li, R.N. Horne, An analytical scaling method for spontaneous imbibition in gas-water-rock systems, SPE Journal 9 (2004) 322-329.

[14] K.W. Li, R.N. Horne, Generalized Scaling Approach for Spontaneous Imbibition: An Analytical Model, SPE Journal 9 (2006) doi.org/10.2118/77544-PA.

[15] O. Shtyka, J. Sęk, M. Błaszczyk, S. Kacprzak, Investigation into hydro- and oleophilic porous medium saturation with two-phase liquids during the imbibition process, Inż. Ap. Chem. 55 (2016) 36-374.

[16] J.S. Kowalski, Inżyneria materiałów porowatych, Wydawnictwo Politechniki Poznańskiej, Poznan (2004).

Paulina Pędziwiatr, Filip Mikołajczyk, Dawid Zawadzki, Kinga Mikołajczyk, Agnieszka Bedka
Studenckie Koło Naukowe Oktan, Faculty of Process Engineering and Environmental Protection, Lodz University of Technology
213 Wolczanska str., 90-924 Lodz, Poland, mikolajczyk.filip.pl@gmail.com

DECOMPOSITION OF HYDROGEN PERODIXE - KINETICS AND REVIEW OF CHOSEN CATALYSTS

Abstract
Hydrogen peroxide is a chemical used in oxidation reactions, treatment of various inorganic and organic pollutants, bleaching processes in pulp, paper and textile industries and for various disinfection applications. It is a monopropellant, which, when purified, is self-decomposing at high temperatures or when a catalyst is present. Decomposing to yield only oxygen and water(disproportionation), hydrogen peroxide is one of the cleanest, most versatile chemicals available. The catalytic decomposition of hydrogen peroxide allows the use of various catalysts that will increase the rate of decomposition. Comparison and description of the most commonly used catalysts were presented in this review.

Key words
decomposition, hydrogen peroxide, catalysis, catalysts, silver catalyst, photocatalysis

Introduction

Hydrogen peroxide is a commonly used chemical compound with the formula H_2O_2. In pure liquid form, it has a distinctive pale blue colour [1]. However, in a diluted solution, at room temperature, it appears as colourless mixture with a slightly sharp odour [2]. It doesn't ionise fully in water when it is dissolved. Solution of hydrogen peroxide is a weak acid, on the market it is usually offered in concentrations of 30, 50, and 70 percent by weight. Viscosity of H_2O_2 is slightly higher than water. Gaseous hydrogen peroxide is naturally present in the air in small amounts, which are created when ultraviolet rays strike oxygen in the presence of moisture [3]. Vapour of hydrogen peroxide is irritating to the respiratory tract and, what is more, it is corrosive to the skin and the eyes. Diluted solutions of H_2O_2 can be safely decomposed in the presence of proper enzymes known as catalase peroxidases, which are possessed by all aerobes.

Compounds with an oxygen–oxygen single bond are categorised as peroxides. Hydrogen peroxide represents the simplest type of this group of chemicals. It is characterized by its tendency to decompose, caused by the nature of its unstable peroxide bond. It must be stored with a stabilizer, such as acetanilide or similar organic materials. The solution is not flammable, regardless of its concentration. However, hydrogen peroxide is a strong oxidizing agent, due to its chemical structure and unpaired electrons [4].

Hydrogen peroxide can be used as a chemical intermediate, in the bleaching and deodorizing processes in pulp and the paper industry or in the textile industry[5]. H_2O_2 is also used in water treatment operations (substitute for chlorine in water and sewage treatment), exhaust air treatment, in production of foam rubber, organic chemicals (manufacture of glycerol) and in refining and cleaning metals. Concentrated hydrogen peroxide, or "high-test peroxide," has been also used to propel rockets [6]. In macroscale, it is known as a propellant of submarines and satellites. On the other hand, it is utilized for the propulsion of catalytic nanomotors in microscale [7]. In the food industry,H_2O_2 is applied in bleaching, oxidizing and neutralizing (in wine distillation) processes. It helps to control viscosity of starch and cellulose derivatives. In the form of carbamide peroxide it is commonly used for tooth whitening. At low concentrations (3-9%), hydrogen peroxide is found in many households as a hair and clothing bleach and for medical (anti-infective) applications. High reactivity gives H_2O_2 the ability to damage cellular macromolecules, including lipids, proteins and nucleic acids. Decomposing to only oxygen and water, hydrogen peroxide is said to be one of the most versatile and cleanest chemicals available.
Hydrogen peroxide was discovered in 1818 by Louis Jacques Thenard. He reacted barium peroxide with nitric acid and then with hydrochloric acid. He managed to obtain pure hydrogen peroxide, which was called "oxygenated water". The addition of different substances, including blood, caused the new compound to decompose with the release of oxygen. Thenard's process was used until the middle of the 20th century.

Nowadays, production of hydrogen peroxide is mostly conducted according to the anthraquinone-auto oxidation process, where H_2O_2 is produced from hydrogen and atmospheric oxygen. The post-reaction mixture is then purified and concentrated. After appropriate stabilization, it is distributed as an aqueous solution. Different methods of derivation are electrolytic processes (aqueous sulphuric acid or acidic ammonium bisulfate is converted electrolytic ally) and auto oxidation of isopropyl alcohol [8].

Decomposition of hydrogen peroxide

Hydrogen peroxide is a very unique substance due to its molecular structure. It consists atoms of oxygen in oxidation state of -1 unlike many substances, where oxygen occurs in oxidation state of 0 or -2. This means that this substance can be used as both an oxidizing and a reducing agent, depending of pH of its solution. Due to those properties, particles of hydrogen peroxide can decompose via reaction of disproportionation as shown on Pic.1 [9].

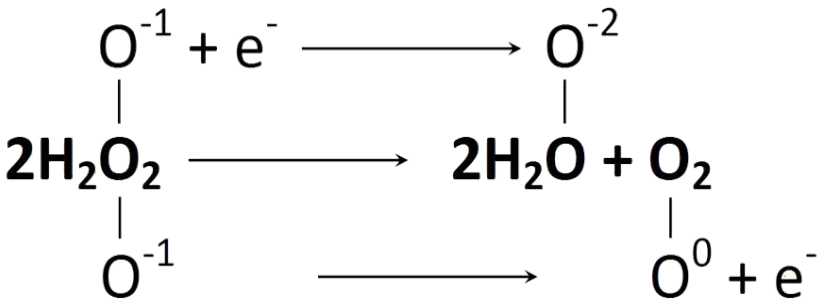

Fig. 1. Reaction of disproportionation of hydrogen peroxide
Source: Author's

Hydrogen peroxide is a quite stable substance in low and moderate pH. Although hydroxyl anions cannot trigger the reaction on their own [10], an increase of alkalinity in the environment of reaction up to a certain value may result in a rising rate of reaction. Unfortunately, the influence of pH on the rate of reaction is highly dependent on the purity of the solution. For example, in a low purity solution, pH may not affect it at all [11]. However, H_2O_2 easily decomposes when it is exposed to impurities or catalysts like metallic surfaces or yeast. Other factors that affect the rate of reaction are temperature, pressure, concentration of solution, type, activity and area of active catalytic surface of the catalyst, exposure to direct sunlight and presence of inhibitors [10].

Reaction of decomposition of hydrogen peroxide is very slow in moderate temperatures without the presence of a catalyst [11]. It can be sped up by increasing the temperature, which triggers the reaction of thermal decomposition. This reaction can be carried out in a liquid or vapour phase. Usually the rate of reaction is increased by adding catalysts to the reactor. Almost all types of catalyst can be used with this reaction: heterogeneous (e.g. silver, gold, iron), homogeneous (iodide or iron ions) and enzymes (catalase).

This reaction is exothermic. It produces large amount of heat (ΔH=-2884.5 kJ/kg H_2O_2 for pure compound), which further increases rate of reaction and makes reaction self-sustaining after phase of catalytic initiation [12]. The mechanism of reaction is dependent on the type of catalyst used. For example, for transition metal complexes two general types of mechanism have been postulated: radical mechanism proposed by Haber and Weiss and peroxide complex mechanism proposed by Kremer and Stein [13]. Some reaction mechanisms still need more research. For example, the exact mechanism of reaction catalysed by MnO_2 is still unknown. Thermal decomposition is a very complex reaction, one of the proposed models is based on 27 subordinate reactions [9]. Often the final mechanism of reaction is a combination of various other mechanisms, usually thermal decomposition in addition to the reaction with catalysts and impurities.

In many industries decomposition of hydrogen peroxide is used e.g.to produce sodium perborate and sodium percarbonate (bleaching agents in solid and liquid detergents). In textile industry hydrogen peroxide bleach and deodorize textiles, wood pulp, hair, fur, etc. The other applications of H_2O_2 are as source of organic and inorganic peroxides, rocket fuel, plasticizers, neutralizing agent in wine distillation, bleaching and oxidizing agent in foods, substitute for chlorine in water and sewage treatment, viscosity control for starch and cellulose derivatives [1]. Hydrogen peroxide is also present in pulp and paper industry, manufacture of glycerol, foam rubber, refining and

cleaning metals [2]. Because of antichlor, dyeing, electroplating, antiseptic epoxidation, hydroxylation, oxidation and reduction properties it is wide use in many industrial processes.

Silver catalyst

Silver is one of most effective heterogeneous catalysts for hydrogen peroxide decomposition. Due to the high influence of the catalytic active area on the rate of reaction usually only significantly modified geometric forms of silver are being used in this reaction. Generally, silver is used in metallic form or as an alloy. It is not used in ionic form, as it is prone to precipitation. The most popular forms used in industry or in laboratories are mesh and powder. Use of powder and nanoparticles is attractive due to their high surface area, but it may result in the necessity of using some additional process of separation of catalyst and solution. In other cases, a post reaction mixture may be contaminated [14]. Therefore, usually silver is used in the form of mesh or other geometric forms, which allows the forming of a bed. To restrain the cost of catalyst, sometimes silver is used in the form of a thin layer coating, instead of using pure silver. It does not affect rate of reaction, because reaction takes place only within the interphase layer.

Despite the fact that new catalysts for the reaction are developed every year, metallic catalyst based on silver are still very attractive. The main advantages of using silver are its high decomposition efficiency, compactness, uncomplicated process of fabrication, and multiple available form of catalyst [15]. Silver catalysts also have some disadvantages, like temperature limitations (melting temperature of silver – 961.8°C) and a complicated process of activation of catalyst. Another drawback of silver is catalyst loss of mass after several cycles of reaction. Mass loss is proportional to the squared area of catalyst [16]. This process is intensive for new and regenerated metal at the start of a process of decomposition. After some time, the concentration of ions of silver in the solution stabilizes due to the saturation of solution. These ions are inhibitors to silver degeneration. The most important disadvantage of silver is its vulnerability to surface poisoning. To counter that, the catalyst must be periodically regenerated, for example with nitric acid. Regeneration has one additional effect for the catalyst – it develops a surface of metal and increases the amount of active centres. It is crucial for new silver, where surface is undeveloped and smooth, which results in limited decomposition efficiency [17]. Silver is also quite expensive when compared to other catalysts, such as those based on iron.

During the reaction of hydrogen peroxide decomposition catalysed by silver, four different reaction zones can be noticed, each dominant for a range of bulk solution temperatures. In low temperature zones, the rate of reactions is chemically controlled by properties of the catalyst. In nuclear boiling zone, due to the contact between catalysts and boiling liquid temperature of catalyst does not exceed the boiling point of the solution. The next zone is the film boiling zone, where the vapour phase is formed. This results in significant limitation of area of contact between reactant and catalysts and a noticeable decrease of the rate of reaction. The last zone is called the high temperature reaction zone, where the rate of reaction of decomposition is more dependent on the reaction of homogeneous thermal decomposition rather than heterogeneous catalysed reaction [18]. Due to the heterogeneous nature of the process of decomposition of H_2O_2catalysed by silver exact mechanism of this reaction is still unknown, probably it is based on a radical mechanism.

Manganese compounds

Potassium permanganate ($KMnO_4$) in standard conditions is a solid with density 2.7 g/cm^3. It is not hydroscopic, in contrast to sodium permanganate. It has good water solubility, in 20°C it is 6,4g in 100cm^{3}of water. The colour of its solution is strictly dependent on its concentration; it varies from bright pink in diluted solutions to dark purple in saturated solutions. Solid $KMnO_4$ thermally decomposes in 240°C, as shown on following equation:

$$2KMnO_4 \rightarrow K_2MnO_4 + MnO_2 + O_2$$

This substance has strong oxidizing properties, but mechanism of this oxidation reaction is strongly dependent on pH of the environment of the reaction. In acid solutions $KMnO_4$ is reduced to Mn^{+2}, the solution changes colour to pale pink:

$$MnO_4^- + 8H^+ + 5e^- \rightarrow Mn^{+2} + 4H_2O$$

In a weak alkaline or inert solution permanganate ion is reduced to manganese oxide, which appears in the form of a brownish sediment:

$$MnO_4^- + 2H_2O + 3e^- \rightarrow MnO_2 + 4OH^-$$

However, in a strong alkaline environment, the solution changes its colour to green:

$$MnO_4^- + e^- \rightarrow MnO_4^{-2}$$

Potassium permanganate is being used in titration analysis - manganometry. It also has a strong bactericidal and fungicidal properties, diluted solution is used in oral rinsing.

The reaction of catalytic decomposition of hydrogen peroxide catalysed by potassium permanganate can be divided into three stages: a fast initial phase, an induction period and an autocatalytic step [25]. This reaction is autocatalytic, because product of reaction Mn^{+2} creates unstable complex with MnO_4^{-1}. Products of decomposition of this complex have better catalytic properties than the complex itself. Some studies are focused on obtaining porous cement slurry with the use of reaction decomposition of H_2O_2 with potassium based catalysts. Currently, aluminium powder is being used in this process, but the rate of reaction of producing gases is hard to control [22].

Manganese oxide (MnO_2) is widely used in heterogeneous reaction of decomposition of hydrogen peroxide thanks to its excellent catalytic efficiency in this reaction. It is usually used in the form of a powder thanks to its very high contact surface [21]. One of disadvantages of this catalyst is a necessity of immobilizing a manganese oxidize powder on solid base. The kinetics of catalytic decomposition hydrogen peroxide can be represented by pseudo first-order rate model [24]. Si-Hyun Do and the others [24] suggested a 15-tier mechanism of this reaction.

Potassium dichromate ($K_2Cr_2O_7$)

Potassium dichromate is an orange crystalline ionic solid. In water solutions, it is durable only in an acid environment, in alkali solutions its colour is changing from orange to yellow as a result of redox reaction of dichromate ion:

$$Cr_2O_7^{-2} + 2OH^- \rightarrow 2CrO_4^{-2} + H_2O$$

However, reverse reaction can occur when pH of solution changes back to acid:

$$2CrO_4^{-2} + 2H^+ \rightarrow Cr_2O_7^{-2} + H_2O$$

Potassium dichromate is used as an oxidizing agent in various reactions in chemical industry and laboratory preparation, such as dye production, electrolysis, pyrotechnics, glassware, glues, dyeing, photography, lithography and the ceramic industry. The solution of potassium dichromate in sulfuric acid is being used to clean laboratory glass, soiled organic compounds and other compounds susceptible to oxidation. Nowadays its use is very limited, due to problematic disposal of wastes containing chromium compounds. Potassium dichromate, as other Cr (VI) compounds, is toxic, mutagenic and carcinogenic. It is also extremely dangerous to the environment.

The mechanism of reaction of decomposition of hydrogen peroxide catalysed by potassium dichromate is complicated and a lot of research has been carried out over the last 100 years [1,2]. During those studies various Cr(VI)-peroxo complexes were observed at different pH and concentrations of solution, for example:

- at pH=4 - $Cr^{VI}(O)_5(H_2O)$ or$Cr^{VI}(O)(O_2)_2(OH_2)$. Their solution is called blue peroxochromatic acid,
- at pH between 4 and 7 -violet deprotonated from of "peroxochromic acid" $[Cr^{VI}(O)(O2)(OH)]^-$
- at least four Cr(V)-peroxocomplexes appearing at different pH and concentrations[19].

Potassium dichromate as a catalyst studied reaction has some advantages: it is easy to implement and the reaction rate can be controlled by H_2O_2 solution dilution [23].

Iron oxide

Another known reaction based on the decomposition of hydrogen peroxide is Fenton's reaction, where a hydroxyl radical is created by iron ions. This reaction was suggested by Haber and Weiss in 1932,however their investigation was not focused on oxidation. Thanks to Fenton's theories about oxidation this process is now named after him [29]. One of the forms of catalyst used in that type of reaction is goethite, a pure crystalline iron oxide in aqueous medium- α-FeOOH. Many key reactions of this process are based on the transition aqueous hydrogen peroxide to the anion form OH_2•.

$$H_2O_2 + Fe^{2+} \rightarrow Fe^{3+} + OH + OH\bullet$$
$$OH + H2O2 \rightarrow H2O + O2H$$
$$OH + H_2O_2 \rightarrow O_2 + H_2O + OH$$
$$OH + Fe^{2+} \rightarrow Fe^{3+} + OH\bullet$$

Profound research on that mineral was carried by Shu-Sung Lin and Mirat de Gurol[26]. It is worth mentioning that it is the most abundant crystalline iron oxide mineral in nature. However, this material is not the only one

used as the source of iron oxide. Equally popular are hematite (α-Fe_2O_3) and ferrihydrite ($(Fe^{3+})_2O_3$*$0.5H_2O$) [28]. The most efficient of these three minerals is ferrihydrite thanks to its large inner surface that is associated with an increased rate of diffusion process. It is also worth mentioning that the iron oxide in the form of aqueous goethite is suitable for catalysing hydrogen peroxide decomposition even in highly concentrated solutions (about 1-10 mM). Compounds containing ferric ions, for example ferric salts, are also regarded as good catalysts, due to their high selectivity. Nevertheless, they can cause many problems since reactions of decomposition of catalyst and hydrogen peroxide are highly exoenergetic [27]. Despite this fact, iron oxides are commonly used in our daily life, in metallurgy, as a colorants or thermite component. Thanks to their super magnetic properties and the ability to overcome the blood-brain barrier they can also be used in medicines, as a contrast in MRI (Magnetic Resonance Imaging) [30].Some scientists tried to overcome some of weaknesses of this reaction. About 20 years ago (Huston & Pignatello, 1999; Ruppert et al., 1993) it was found that combination of Fenton reaction and UV light radiation (nowadays it is called photo-Fenton process) has strongly accelerated the rate of degradation of a variety of pollutants, even if it is compared to the regular Fenton reaction. This is mainly due to the presence of photochemical reduction of Fe^{3+} back to Fe^{2+}. This reaction can be present as:

$$Fe^{3+}{}_{aqa} + H_2O + hv \rightarrow Fe^{2+}{}_{aqa} + HO\bullet + H^+ \quad [31]$$

This reaction shows some strong advantages in comparison with regular Fenton reaction. First of all, the main weakness of classical Fenton reaction - self-blocking through the increasing amount of sludge is not present in photo-Fenton reaction. Secondly, chemical consumption is significantly lower, what results in lower cost of the process. To add more, due to negligible formation of sludge, there is no need to remove it, what reduces operation costs even more. [32]

Photocatalytic decomposition on TiO Surface

The next type of reaction of decomposition of hydrogen peroxide is a reaction involving use of UV light and TiO_2 surface [33] that has some photo catalytic properties as in the case of iron compounds in the photo-Fenton reaction. In this type of reaction when TiO_2 is irradiated light which has photon energy equal to or higher than its band-gap, an electron (e−) can be excited from the valence band to the conduction band and leave a hole (h+) in the valence band:

$$TiO_2 + UV \rightarrow h^+ + e^-$$
$$h^+ + OH^-/H_2O \rightarrow \bullet OH/\bullet OH + H$$
$$e^- + h^+ \rightarrow heat$$

The presence of hydrogen peroxide in this reaction is essential, because as an electron acceptor it is responsible for the growth of photocatalytic efficiency and mineralization of losses of energy during UV radiation. Controlling the amount of H_2O_2 during this process is crucial. Although this process requires a large amount of hydrogen peroxide, too large of a dose may cause the accumulation of electrons on the hydrogen peroxide radicals and competitive adsorption of hydrogen peroxide instead of its decomposition [35]. In this type of process the amount of titanium dioxide is equally important because it can be used to control the rate of decomposition. Due to its vulnerability to fragmentation to the size of nanoparticles it has excellent photocatalytic properties, especially one of its catalytic form named anataz. However, that properties are highly dependent on the temperature and the specific surface area. Furthermore, TiO2 may also be used in rutile form, which has very good mechanical and catalytic properties thanks to high chemical resistance and high refractive index.

Photocatalytic reactions on TiO_2 surface in presence of hydrogen peroxide are useful in the oxidised degradation or transformation of a wide range of pollutants for the treatment of drinking water, groundwater, wastewater and contaminated soils. It is also useful to get rid of hazardous compounds present in dyes [34].However, most applications of titanium dioxide are still carried out at a laboratory rather than at industrial scales.

Hydrogen peroxide in living cells

Hydrogen peroxide naturally occurs in the human body as one of the by-products of biochemical metabolism of many different cells. For example, hydrogen peroxide is directly produced by some oxidise enzymes like glycolateoxidise or monoamine oxidise. Hydrogen peroxide is also created by the peroxisomal pathway for L-oxidation of fatty acids [36].

What is more, some popular beverages, including instant coffee, black tea and green tea, can contain hydrogen peroxide at low concentrations. Consumption of these beverages may conduct to diffusion of hydrogen peroxide

into the cells of the oral cavity and upper part of the gastrointestinal tract [36]. Another source of hydrogen peroxide in the gastrointestinal tract are oral bacteria which produce this substance [36].

Hydrogen peroxide could also be found in exhaled air of living organisms. It is uncertain whether the source of it is oral bacteria, phagocytes or other lung cells. People with lung diseases or cigarette smokers exhale more hydrogen peroxide than healthy ones[36].

Considering all the above it is not surprising that hydrogen peroxide is also present in the blood. But concentration of hydrogen peroxide in human blood has not been determined with satisfactory accuracy yet. There are some conventional methods of hydrogen peroxide detection but the absolute values remain uncertain [37]. The literature is full of data about the hydrogen peroxide level in blood but credibility of it is questionable due to the great variability of results [37].

To sum up, it seems that most human cells are exposed to hydrogen peroxide.H_2O_2 can have significant impact on aging processes. During decomposition of hydrogen peroxide with, for example, copper (I) and iron (II) ions as a catalyst, hydroxyl radical ($OH^{\bullet}$) is formed [38]. Free radicals are molecules, atoms or ions which have single, unpaired electron at the outer orbits. High activity individuals have this chemical and oxidize each compound with which they have contact in order to join or donate electrons. The objects of the attacks of free radicals in the human body are mainly compounds having double bonds in the molecules like proteins, DNA, polysaccharides, lipids (like cholesterol in the blood) or unsaturated fatty acids which are part of cell membranes [36].

Accumulation of hydrogen peroxide may have very bad influence on cells and can even kill them, so it has to be decomposed. The natural process of hydrogen peroxide decomposition is very slow. Therefore, in living organisms there has to be an acceleration mechanism for this reaction. It is widely known that reactions in cells are mostly accelerated by enzymes. In case of hydrogen peroxide decomposition, it occurs in the same way. One of such substance is an enzyme called Catalase, which lowers the energy of activation needed for decomposition [39].

Conclusion

Hydrogen peroxide is one of the cleanest, most versatile chemicals available. Due to its beneficial properties, it is used in a broad variety of application areas e.g.: in aseptic packaging as sterilizing agent, in cosmetics and medicine as an antimicrobial agent, in chemical synthesis as a powerful and environmentally benign oxidizing agent, in pulp, paper and textile industry as a versatile bleaching agent and also in transportation high concentrated, high purity hydrogen peroxide is used as a propellant. Hydrogen peroxide is the object of diverse studies due to its useful properties. Although there are many varied applications of this substance, its usage remains limited. The main reason for this is high production costs. Moreover, in lower concentration it is chemically unstable and requires addition of stabilizers, which change the kinetics of reaction of its decomposition. A separate direction of research concerning hydrogen peroxide is its presence in the human body, which can have a significant influence on biochemical reactions that occur in our cells. Therefore, this simple substance is more important than it seems and further studies concerning its production, usage and appropriate concentration measurement can make a breakthrough in many areas of our lives.

Acknowledgments

This project would be impossible without help and support of our supervisors: M.Sc Konrad Gładyszewski and Ph.D Michał Tylman. We would like to thank them for their expert advice and encouragement throughout the whole "Najlepsi z najlepszych" project. We also would like to thank other members of Oktan Team for all of their work during ChemCar projects.

References

[1] https://pubchem.ncbi.nlm.nih.gov/compound/hydrogen_peroxide,Access data: 19.03.2017
[2] https://www.ncbi.nlm.nih.gov/mesh/68006861 , Access data: 19.03.2017
[3] Kirk-Othmer Encyclopedia of Chemical Technology. 4th ed. Volumes 1: New York, NY. John Wiley and Sons, 1991-Present., p. V13 (95) 962

[4] Abdollahi M., Hosseini A., ”Hydrogen Peroxide”, Encyclopedia of Toxicology (Third Edition)2014, Pages 967–970
[5] Mistik, S. I., Müge Yükseloğlu, S. "Hydrogen peroxide bleaching of cotton in ultrasonic energy." Ultrasonics 43.10 (2005): 811-814.
[6] Hitt, D.L., Zakrzewski, Ch.M. Thomas, M.A. "MEMS-based satellite micropropulsion via catalysed hydrogen peroxide decomposition." Smart Materials and Structures 10.6 (2001): 1163.
[7] Wang, Y. et al. "Bipolar electrochemical mechanism for the propulsion of catalytic nanomotors in hydrogen peroxide solutions." Langmuir 22.25 (2006): 10451-10456.
[8] Chuang, K.T., Bing, Z. "Production of hydrogen peroxide." U.S. Patent No. 5,338,531. 16 Aug. 1994.
[9] Rarata G., Surmacz P. „Nadtlenek wodoru klasy HTP jako uniwersalne medium napędowe oraz utleniacz”, Prace Instytutu Lotnictwa 2009, 202, p. 125-158
[10] Nicoll W.D. Smith A.F. Stability of Dilute Alkaline Solutions of Hydrogen Peroxide, Industrial and Engineering Chemistry 1955, 47, 12, p. 2548-2554
[11] Marzzacco C. The effect of a change in the catalyst on the enthalpy of decomposition of hydrogen peroxide, Chem 12 News 2008, p. 12-13
[12] Mok J.S., Welms W.J., Sisco J.C., Anderson W.E. Thermal Decomposition of Hydrogen Peroxide, Part 1: Experimental Results, Journal of Propulsion and Power 2005, 21, 5, p. 942-953
[13] Salem I.A., El-Maazawi M., Zaki A.B., Kinetics and mechanisms of decomposition reaction of hydrogen peroxide in presence of metal complexes, International Journal of Chemical Kinetics 2000, 32, 11, p. 643-666
[14] Schroeder J.E., Pouli D., Seim H.J., High surface area silver powder as an oxygen, Advances in Chemistry 2009, 90, p. 93-101
[15] Su-Lim L., Choong-Won L., Performance characteristics of silver catalyst bed for hydrogen peroxide, Aerospace Science and Technology 2009, 13, p.12-17
[16] Baumgartner H.J., Hood G.C., Monger J.M., Roberts R.M., Sanborn C.E., Decomposition of concentrated hydrogen peroxide on silver I. Low temperature reaction and kinetics, Journal of Catalysis 1963, 2, 5, p. 405-414
[17] Baumgartner H.J., Hood D. Hood G.C., Waver D.D., Catalyst for Hydrogen Peroxide Decomposition, United States Patent Office 1968, Patent number 3363982
[18] Garwing P.L., Heterogeneous decomposition of hydrogen peroxide by inorganic catalysts. A literature survey, Chemical Research and Development Center Princeton, New Jersey 1966
[19] Zhang, L., Lay, P. A., EPR spectroscopic studies on the formation of chromium (V) peroxo complexes in the reaction of chromium (VI) with hydrogen peroxide. Inorganic Chemistry, 37(8), 1729-1733. (1998).
[20] Dickman, M.H., Pope, M.T., "Peroxo and superoxo complexes of chromium, molybdenum, and tungsten." Chemical reviews 94.3 (1994): 569-584.
[21] Rarata, G., and P. Surmacz. "Nadtlenek wodoru klasy HTP jako uniwersalne medium napędowe oraz utleniacz." Prace Instytutu Lotnictwa (2009): 125-158.
[22] Wang, Z.J., et al. "Impacts of potassium permanganate (KMnO 4) catalyst on properties of hydrogen peroxide (H 2 O 2) foamed porous cement slurry." Construction and Building Materials 111 (2016): 72-76.
[23] Frikha, N., =Schaer E., Houzelot, J.L., "Experimental study and modelling of thermal runaway: Application to dichromate catalysed hydrogen peroxide decomposition." Thermochimica Acta 449.1 (2006): 47-54.
[24] Do, S.-H. et al. "Hydrogen peroxide decomposition on manganese oxide (pyrolusite): kinetics, intermediates, and mechanism." Chemosphere 75.1 (2009): 8-12.
[25] Simoyi, R.H. et al. "Reaction between Permanganate Ion and Hydrogen Peroxide: Kinetics and Mechanism of the Initial Phase of the Reaction'." Inorganic Chemistry 25.4 (1986): 538-542.
[26] Lin, S.S., Gurol, M.D. (1998). Catalytic decomposition of hydrogen peroxide on iron oxide: kinetics, mechanism, and implications. Environmental Science & Technology, 32(10), 1417-1423.
[27] http://rspa.royalsocietypublishing.org/content/royprsa/147/861/332.full.pdf, 15.03.2017
[28] Huang, H. H., Lu, M. C., Chen, J. N. (2001). Catalytic decomposition of hydrogen peroxide and 2-chlorophenol with iron oxides. Water Research, 35(9), 2291-2299.
[29] Barbusiński, K. (2009). Fenton reaction-controversy concerning the chemistry. Ecological Chemistry and Engineering. S, 16(3), 347-358.
[30] Markowski, J. (2011). Dyspersja tlenków żelaza – aktualny stan wiedzy. Nafta-Gaz, 67(4), 282-287.
[31] Machulek Jr., A., Quina, F.H. Gozzi, F., Silva, V.O., Riedrich, L.C., Moraes, J.E.F., (2013), Fundamental Mechanistic Studies of the Photo-Fenton Reaction for the Degradation of Organic Pollutants, Environmental and Analytical Update 25, 271-294
[32] Quiroz, M.A., Bandala, E.R., Martínez-Huitle, C.A. (2011). Advanced Oxidation Processes (AOPs) for Removal of Pesticides from Aqueous Media. Pesticides - Formulations, Effects, Fate, 687-730 (2011)

[33] Tseng, D. H., Juang, L. C., Huang, H. H. (2012). Effect of oxygen and hydrogen peroxide on the photocatalytic degradation of monochlorobenzene in aqueous suspension. International Journal of Photoenergy, 2012.
[34] Riga, A., Soutsas, K., Ntampegliotis, K., Karayannis, V., Papapolymerou, G. (2007). Effect of system parameters and of inorganic salts on the decolorization and degradation of Procion H-exldyes.Comparison of H2O2/UV, Fenton, UV/Fenton, TiO2/UV and TiO2/UV/H2O2 processes. Desalination, 211(1-3), 72-86.
[35] Malato, S., Blanco, J., Cáceres, J., Fernández-Alba, A. R., Agüera, A., Rodrıguez, A. (2002). Photocatalytic treatment of water-soluble pesticides by photo-Fenton and TiO 2 using solar energy. Catalysis Today, 76(2), 209-220.
[36] Halliwell, B., Clement, M. V., Long, L. H. (2000). Hydrogen peroxide in the human body. FEBS letters, 486(1), 10-13.
[37] Forman, H. J., Bernardo, A., Davies, K. J. (2016). What is the concentration of hydrogen peroxide in blood and plasma? Archives of biochemistry and biophysics, 603, 48-53.
[38] Popularna Encyklopedia Powszechna, wyd. Fogra (1994-1998)
[39]http://www.houstonisd.org/cms/lib2/TX01001591/Centricity/Domain/5363/07%20The%20Hydrogen%20Peroxide%20Breakdown.pdf , 10.03.2017

Katarzyna Pieklarz, Alicja Zawadzka
Technical University of Lodz, Faculty of Process and Environmental Engineering
213 Wolczanska Str., 90-924 Lodz, Poland, katarzyna.pieklarz@dokt.p.lodz.pl, alicja.zawadzka@p.lodz.pl

THE USE OF BIOFILTRATION PROCESS TO REMOVE MALODOROUS GASES FROM THE WASTEWATER TREATMENT PLANT

Abstract
Odorous substances emitted to ambient air from wastewater treatment plants cause a serious nuisance to inhabitants in the direct vicinity of such emitters. The solutions currently used to remove malodorous gases in the Wastewater Treatment Plant in Belchatow do not fulfill their function properly. This article presents the test results of the composition and concentrations of odorous compounds emitted from the above-mentioned plant. In addition, the paper introduces the concept of eliminating substances by the biofiltration process. Due to the applied method, one can expect to reduce the odor by at least 90%.

Key words
Biofiltration process, biofilter, microorganisms, malodorous gases, wastewater treatment plant

Introduction

Over the past few decades, enormous quantities of pollutants have been released into the environment, mainly into the air. Due to high emission of a wide variety of pollutants, there has been an increase in the number of environment-related problems. These compounds are usually removed slowly and tend to accumulate in the environment. Because of the high degree of toxicity, their accumulation can cause severe environmental problems. Therefore, scientists are conducting research to introduce new methods for removing odorous substances emitted mainly from wastewater treatment plants [4, 5, 8, 9].

Particularly promising solutions include biological methods, especially the biofiltration process. It is a complex biological process of removing malodorous substances consisting in the biodegradation of pollutants, whose products are non-toxic compounds inert to the environment. Both physical and biological processes occur during biofiltration [15].

Odorous contaminants occurring in the exhaust gases are subjected to the process of adsorption on the surface of the liquid bioactive layer (Figure 1.) that surrounds the grain fill - the filter material [1, 14, 15].

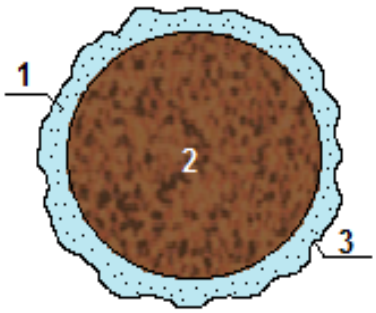

Fig. 1. Schematic of a biofilm covering the filter material
1 – microorganisms, 2 – filter material, 3 – bioactive layer
Source: Author's

The particles of odor adsorbed on the surface of the biofilm pass into the liquid phase and then diffuse into microorganisms colonizing the bioactive layer. In this layer, the microorganisms bring about the biodegradation of odorous pollutants to carbon dioxide, water and other organic compounds (biomass). The biomass causes the growth of microorganisms capable of increased distribution of impurities in mineralization involving

mainly bacteria of the genus: *Pseudomonas*, *Micrococcus*, *Corynebacterium*, *Hyphomicrobium*, *Rhodococcus*, *Xanthobacter*, *Arthrobacter*, *Methylomonas* or *Thiobacillus* and fungi [2, 6, 10, 11].

The biofiltration process is conducted in a biofilter, which comprises a housing and a layer of filling of the porous filter material. The material is inhabited by microorganisms capable of biological decomposition of the pollutant gas. The shape of biological filters depends mainly on the spatial potential and the scale of their use. Therefore, there are different types of biofilters in terms of construction, and types of fillers or additives and treatments that enhance the effectiveness of gas purification. In the case of laboratory testing, biofilters are very simple devices - usually pipes with a length of several tens of centimeters. Currently, both open and closed surface and container biofilters are used on a technical scale worldwide, and their height ranges from several tens of centimeters to several meters [3, 15, 16].

The diagram below (Figure 2) illustrates the treatment process of waste gases by biofiltration.

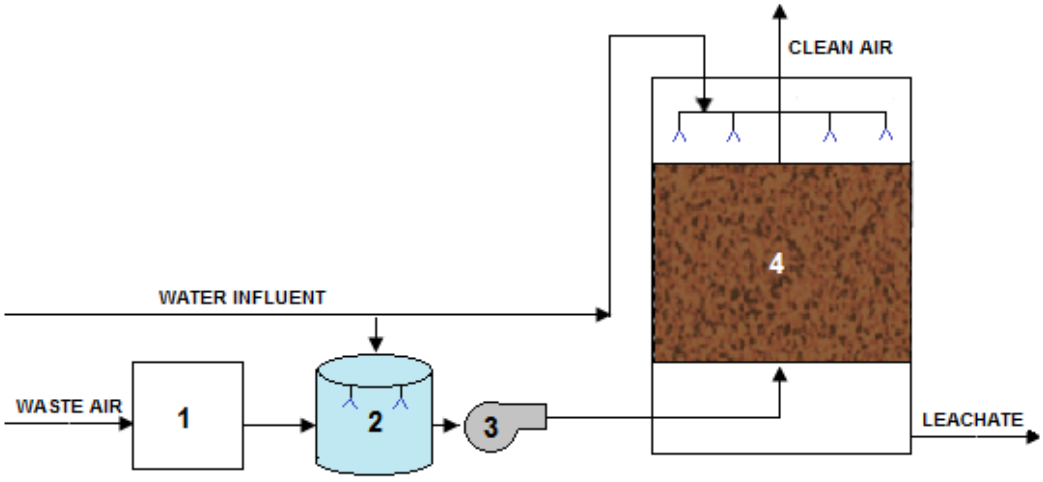

Fig. 2. Schematic diagram of a biofilter unit
1 – preconditioner for particulate removal, 2 – humidifier, 3 – blower, 4 – biofilter reactor
Source: Author's

As the schematic shows, the contaminated off-gas is passed through a preconditioner for particulate removal and humidification. The conditioned gas stream is then passed from the bottom of a filter bed with, for example, soil, peat, composted organic material or activated carbon. These media provide a surface for the attachment and growth of microorganisms. The bed and air stream are kept moist to encourage microbial activity. Humidification is the most influential parameter affecting the sorptive capacity [5, 12, 13].

The aim of this research was to perform analyzes of the composition and concentrations of malodorous substances (organic and inorganic ones) emitted from the Wastewater Treatment Plant in Belchatow.

Material and methods

To carry out the measurements, five representative research points located in the mechanical and biological facilities of the Wastewater Treatment Plant in Belchatow were selected (the primary settling tank, outdoor pool fermentation No. 1, outdoor pool fermentation No. 2, the phosphorus removal chamber and the nitrification chamber).

Samples for analytical testing were taken with the low flow suction pump equipped with a flow meter and a flow controller made by SENSIDYNE Co.

The identification and measurement of the concentration of inorganic compounds such as carbon monoxide, hydrogen sulfide, aliphatic hydrocarbons and ammonia were performed with the exhaust gas analyzer "LANCOM Series II" made by LAND Instruments Co.

The analysis of organic impurities was performed by gas chromatography with a mass detector made by VARIAN Co. after desorption from activated carbon. Before the analysis, the compounds were concentrated in short columns filled with activated carbon. Coal, before being placed in columns, was washed of 1.0 M HCl and heated to the boiling point to remove the compounds adsorbed on its surface. Thus, prepared activated carbon was placed in columns (100 mm in length and 5 mm in diameter each), in two portions. The first layer had a weight of 200 mg, and the second weighed 100 mg. Then, within 30 minutes, the test air was passed through the columns at a rate of 40 $L \cdot h^{-1}$. The next step of the study involved an independent extraction of layers of activated carbon with used carbon disulphide, and the chromatographic analysis of obtained extracts.

The acquired chromatographic image detected about 36 - 42 compounds (depending on the sample) which could not be identified. The surface area of the peaks of unidentified compounds was converted to the field of pentane, and was recognized as the sum of aliphatic hydrocarbons (ΣC_xH_y).

Results and discussion

The test results are presented in Table 1 and compared with the permissible concentrations of pollutants in the air specified in the Regulation of the Minister of the Environment of 26 January 2010 on reference values for certain substances in the air [7].

Table 1. The results of air samples analyze

Component of the air	Unit	Results for primary settling tank	Results for outdoor pool fermentation No. 1	Results for outdoor pool fermentation No. 2	Results for phosphorus removal chamber	Results for nitrification chamber	Permissible value
SO_2	$mg \cdot m^{-3}$	**63.0**	**11.0**	**69.0**	**1.6**	**1.2**	0.35
CO	$mg \cdot m^{-3}$	24.0	**40.0**	18.0	3.6	3.9	30.0
H_2S	$\mu g \cdot m^{-3}$	**126.0**	**100.0**	**151.0**	**28.0**	19.0	20.0
ΣC_xH_y	$mg \cdot m^{-3}$	**1043.0**	**768.0**	**1289.0**	**202.0**	**198.0**	3.0
Σ mercaptans	$\mu g \cdot m^{-3}$	**81.0**	**70.5**	**97.0**	18.0	**23.1**	20.0
Dimethylamine	$\mu g \cdot m^{-3}$	**105.0**	**84.0**	**116.0**	**20.0**	**15.0**	10.0
Trimethylamine	$\mu g \cdot m^{-3}$	**163.0**	**110.5**	**179.0**	**28.0**	**36.0**	20.0
Ammonia	$\mu g \cdot m^{-3}$	126.0	100.0	141.0	39.0	47.0	400.0
Isobutyric acid	$\mu g \cdot m^{-3}$	87.0	81.0	96.0	28.0	14.0	-
Formaldehyde	$\mu g \cdot m^{-3}$	**691.0**	**412.0**	**738.0**	**147.0**	**129.0**	50.0
Skatole	$mg \cdot m^{-3}$	1.6	1.2	1.7	<1.0	<1.0	-

Source: Author's

Completed analytical research shows that polymer gel mats and foggers used in the Wastewater Treatment Plant in Belchatow do not produce the expected results.

Several odorous compounds, including SO_2, CO, H_2S, NH_3, mercaptans, di- and trimethylamine, formaldehyde and other unidentified compounds presented as ΣC_xH_y, have been detected in the studied air samples. The concentration of the identified compounds has been exceeded several times, and sometimes hundreds of times the permissible concentrations of pollutants in the air. The air over the analyzed object also contains isobutyric acid and skatole, for which the Regulation of the Minister of the Environment of 26 January 2010 on reference values for certain substances in the air does not provide concentration limits, and the presence of which greatly affects the odor nuisance around the plant.

Due to the continuously high level of substances emitted into the atmosphere from the Wastewater Treatment Plant in Belchatow, this plant is a threat to the environment. The undesirable substances emitted into the atmosphere pollute the air not only in the plant itself, but also in the surrounding neighborhoods, which lowers the quality of life of residents of nearby settlements. For this reason, it is necessary to arrange air treatment, modernize the facility and expand the treatment system.

Concept of elimination of odorous substances

The preferred method proposed here is to enter the air purification system using the biological method of biofiltration. This requires additional encapsulation of the wastewater treatment plant (sealing processes) with laminate covered roofs. The encapsulation process will focus on the following wastewater treatment plant facilities:

- primary settling tank,
- outdoor pool fermentation No. 1,
- outdoor pool fermentation No. 2,
- three technological strings of the biological part (each consisting of: one phosphorus removal chamber, two denitrification chambers and two nitrification chambers).

The size of the installation for deodorizing the air has been determined based on the balance of air for each biofilter, as shown in Table 2 (assuming the height of the roof in the central point of each of the facilities equals to 0.5 m and the air change rate of 5 exchanges·h^{-1}).

Table 2. The balance of air for each biofilter

Name of the facility	Volume [m^3]	Multiplicity of air exchange [exchanges · h^{-1}]	Stream air ventilation [$m^3 \cdot h^{-1}$]
Primary settling tank	471.24	5	2356.2
Outdoor pool fermentation No. 1	2094.4	5	10472.0
Outdoor pool fermentation No. 2	2094.4	5	10472.0
Total - balance for the biofilter 1			**23300.2**
One technological sequence of biological part			
Phosphorus removal chamber	72.0	5	360.0
Denitrification chamber No. 1	150.0	5	750.0
Denitrification chamber No. 2	615.0	5	3075.0
Nitrification chamber No. 1	288.0	5	1440.0
Nitrification chamber No. 2	288.0	5	1440.0
Total - balance for one technological sequence			7065.0
Balance for three technological sequences – biofilter 2			**21195.0**

Source: Author's

The results of the calculations compiled in Table 2 indicate that the minimum capacity of biofilter No. 1 is 23300.2 $m^3 \cdot h^{-1}$, and biofilter No. 2 is 21195.0 $m^3 \cdot h^{-1}$.

The "BIO" type biofilters made by Laminopol Co. were proposed for purifying the exhaust air from the Wastewater Treatment Plant in Belchatow. Device No. 1 is a BIO24000 biofilter with a capacity of 24.000 $m^3 \cdot h^{-1}$, which will handle the primary settling tank and outdoor pools fermentation. Device No. 2 is a BIO22000 biofilter with a capacity of 22.000 $m^3 \cdot h^{-1}$, which is used to purify the air from the chambers of the biological part. The proposed biofilters are expected to use a filling made of coconut fibers with a porosity of 95% and a filter bed of 1.0 m in height.

The biofilters of the "BIO" type are modular units consisting of a biomass tank made of polyester-glass laminate, which is resistant to the condensate of contaminated air, and a machine compartment equipped with an air humidifier and a blower. The material used to build the above mentioned biological filters ensures long-term operation of the equipment without maintenance work [19].

The location of biofilters in the wastewater treatment plant is shown in Figure 3. Biofilter No. 1 is proposed to be located about 30.0 m east of the primary settling tank, while biofilter No. 2 is proposed to be located about 15.0 m south of the denitrification chambers.

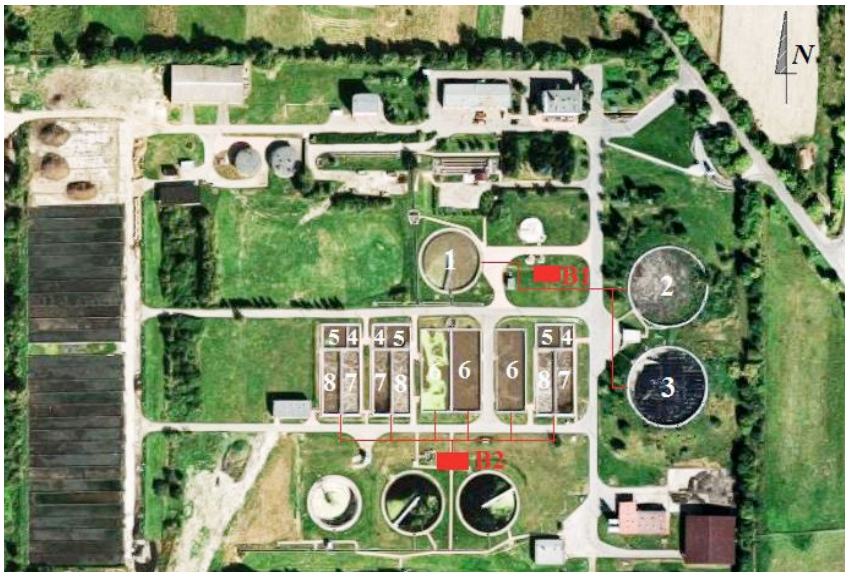

Fig. 3. The facilities of the Wastewater Treatment Plant in Belchatow
have been encapsulated and proposed location of biofilters [18]:
1 – primary settling tank, 2 - outdoor pool fermentation No. 1, 3 - outdoor pool fermentation No. 2, 4 - phosphorus removal chamber, 5 - denitrification chamber No. 1, 6 - denitrification chamber No. 2, 7 - nitrification chamber No. 1, 8 - nitrification chamber No. 2, B1 - biofilter No. 1, B2 - biofilter No. 2
Source: Author's

Expected effects of the biofiltration system

It has been assumed that the installation of biofilters after commissioning will have the following air cleaning effects:

- the effectiveness of the reduction of odors will be ensured at the level of at least 95% with respect to H_2S and Σ mercaptans,
- the effectiveness of the reduction of the remaining odor compounds will reach the level of at least 90% [17].

The results of the calculations of odorous substances obtained after the biofiltration process are summarized in Tables 3 and 4, and the example of the calculations for sulfur dioxide (biofilter No. 1) is shown by the following equations.

- Calculation of SO_2 concentration before the biofilter

$$c_{SO_2} = \frac{c_{SO_2(PST)} \cdot V_{(PST)} + c_{SO_2(OPF1)} \cdot V_{(OPF1)} + c_{SO_2(OPF2)} \cdot V_{(OPF2)}}{\sum V_{(BIOFILTER1)}} \quad [mg \cdot m^{-3}] \qquad (1)$$

where: $c_{SO_2(PST)}$ - SO_2 concentration in the air above the primary settling tank,

$c_{SO_2(PST)}$ = 63.0 mg·m^{-3},

$V_{(PST)}$ - ventilation air stream above the primary settling tank,

$V_{(PST)}$ = 2356.2 $m^3 \cdot h^{-1}$

$c_{SO_2(OPF1)}$ - SO_2 concentration in the air above the outdoor pool fermentation No. 1,

$c_{SO_2(OPF1)}$=11.0 $mg \cdot m^{-3}$

$V_{(OPF1)}$ - ventilation air stream above the outdoor pool fermentation No. 1,

$V_{(OPF1)}$ = 10472.0 $m^3 \cdot h^{-1}$

$c_{SO_2(OPF2)}$ - SO_2 concentration in the air above the outdoor pool fermentation No. 2,

$c_{SO_2(OPF2)}$=69.0 $mg \cdot m^{-3}$

$V_{(OPF2)}$ - ventilation air stream above the outdoor pool fermentation No. 2,

$V_{(OPF2)}$ = 10472.0 $m^3 \cdot h^{-1}$

$\sum V_{(BIOFILTER1)}$ - total air flow before the biofilter No. 1,

$\sum V_{(BIOFILTER1)}$ = 23300.2 $m^3 \cdot h^{-1}$.

$$c_{SO_2} = \frac{63.0 \cdot 2356.2 + 11.0 \cdot 10472.0 + 69.0 \cdot 10472.0}{23300.2} = \mathbf{42.33}\ [mg \cdot m^{-3}]$$

- Calculation of SO_2 concentration behind the biofilter, with assumed reduction rate = 90%

$$c'_{SO_2} = c_{SO_2} - 0.9 \cdot c_{SO_2}\ [mg \cdot m^{-3}] \quad (2)$$

$$c'_{SO_2} = 42.33 - 0.9 \cdot 42.33 = \mathbf{4.23}\ [mg \cdot m^{-3}]$$

Table 3. Concentration values of odorous substances obtained after air purification in biofilter No. 1

Component of the air	Unit	Concentration before the biofilter	Degree of pollutions reduction [%]	Concentration behind the biofilter	Permissible value
SO_2	$mg \cdot m^{-3}$	42.33	90.0	**4.23**	0.35
CO	$mg \cdot m^{-3}$	28.49	90.0	2.85	30.0
H_2S	$\mu g \cdot m^{-3}$	125.55	95.0	6.28	20.0
Σ C_xH_y	$mg \cdot m^{-3}$	1029.97	90.0	**103.0**	3.0
Σ mercaptans	$\mu g \cdot m^{-3}$	83.47	95.0	4.17	20.0
Dimethylamine	$\mu g \cdot m^{-3}$	100.51	90.0	10.05	10.0
Trimethylamine	$\mu g \cdot m^{-3}$	146.6	90.0	14.66	20.0
Ammonia	$\mu g \cdot m^{-3}$	121.06	90.0	12.11	400.0
Isobutyric acid	$\mu g \cdot m^{-3}$	88.35	90.0	8.84	-
Formaldehyde	$\mu g \cdot m^{-3}$	586.73	90.0	**58.67**	50.0
Skatole	$mg \cdot m^{-3}$	1.44	90.0	0.14	-

Source: Author's

Moreover, it has been assumed that:

- the concentrations of odorous substances emitted from nitrification chamber No. 1 are equal to the concentrations in chamber No. 2,
- the concentrations in the denitrification chambers are mean concentrations in the phosphorus removal chambers and nitrification chambers;
- the concentration of the compounds was calculated before entering biofilter No. 2 and after exiting the machine, and the results are summarized in Table 4.

Table 4. Concentration values of odorous substances obtained after air purification in biofilter No. 2

Component of the air	Unit	Concentration before biofilter	Degree of pollutions reduction [%]	Concentration behind biofilter	Permissible value
SO_2	$mg \cdot m^{-3}$	1.33	90.0	0.13	0.35
CO	$mg \cdot m^{-3}$	3.80	90.0	0.38	30.0
H_2S	$\mu g \cdot m^{-3}$	21.89	95.0	1.09	20.0
ΣC_xH_y	$mg \cdot m^{-3}$	199.29	90.0	**19.93**	3.0
Σ mercaptans	$\mu g \cdot m^{-3}$	21.46	95.0	1.07	20.0
Dimethylamine	$\mu g \cdot m^{-3}$	16.61	90.0	1.66	10.0
Trimethylamine	$\mu g \cdot m^{-3}$	33.43	90.0	3.34	20.0
Ammonia	$\mu g \cdot m^{-3}$	44.43	90.0	4.44	400.0
Isobutyric acid	$\mu g \cdot m^{-3}$	18.50	90.0	1.85	-
Formaldehyde	$\mu g \cdot m^{-3}$	134.79	90.0	13.48	50.0
Skatole	$mg \cdot m^{-3}$	< 1.0	90.0	< 0.1	-

Source: Author's

The results of the calculations presented in Tables 3 and 4 show that the biofiltration method is a highly effective solution to eliminate of odorous substances from the Wastewater Treatment Plant in Belchatow. The vast majority of contaminants such as CO, H_2S, Σ mercaptans, di- and trimethylamine, contained in the exhaust air from the analyzed plant have reached concentrations below the permissible standards for these compounds.

Only in the case of SO_2 and ΣC_xH_y did biofiltration not fully yield the expected results. In the present situation, it is recommended to enrich the filter bed with stimulators that promote the development of selected microorganisms, such as the *Drummond* strain bacteria, capable of removing undesired compounds from the gases.

Another way is to introduce preparations such as Ferrox or Nutriox into the wastewater collectors. They oxidize odorous substances, which results in transforming these compounds into more stable forms. In this case, however, the effluent should be continuously controlled to prevent the disturbance of the wastewater treatment plant.

Summary and conclusions

Municipal facilities are particularly troublesome source of emission of malodorous gases. The reason for this is a specific set of odorants emitted (for example, aldehydes, ketones, hydrogen sulphide and mercaptans) as well as the location of facilities in urban or a short distance from the buildings.

The most important sources of odor emissions from wastewater treatment plants are among other: grit chambers, pumping stations, precipitators, aeration chambers and sludge drying beds. The nuisance of the wastewater treatment plant is therefore the reason for taking appropriate measures, among which the most popular are biological methods, mainly biofiltration.

Based on the performed research and analysis, it was found that biofiltration is the optimum deodorization technology for use in the Wastewater Treatment in Belchatow. The biofiltration method is in fact a modern and innovative solution. It is relatively inexpensive and environmentally friendly. Moreover, it does not generate waste that cannot be managed naturally. The worn filter material is often used as a high-quality compost for horticultural crops. Also, biofiltration does not require large amounts of chemicals whose production is energy intensive, and which would contaminate the environment in the event of a leak. Another positive aspect of biofiltration is the fact that the installations used in this method are constantly being improved, which increases not only the performance of the equipment but also the extent of their use. In addition, it is possible to create an individual biofilter system depending on the needs of the analyzed municipal facilities.

References

[1] J.S. Devinny, J. Ramesh, A phenomenological review of biofilter models, *Chemical Engineering Journal*. 2-3 (2005), 188 – 189.

[2] Y.-T. Hung, L.K. Wang, N.K. Shammas, Handbook of environment and waste management. Air and Water Pollution Control, *World Scientific Publishing*, Singapore, 2012.

[3] U. Kita et al., Analysis of trends and solutions in the field of gas deodorization by biofiltration, 277 – 283, http://www.eko-dok.pl/2013/33.pdf [accessed on February 5, 2017] ”Analiza trendów i rozwiązań w zakresie dezodoryzacji gazów metodą biofiltracji”.

[4] J. Kośmider, B. Mazur – Chrzanowska, B. Wyszyński, Odors, PWN, Warsaw, 2012 ”Odory”.

[5] T.K. Kumar, Biofiltration of Volatile Organic Compounds (VOCs) – An Overview, *Research Journal of Chemical Sciences*. 8 (2011), 86.

[6] M. Łebkowska, A. Tabernacka, Biotechnological methods of removing pollutants from waste gases, *Biotechnologia*. 3 (2000), 148 – 149 ”Biotechnologiczne metody usuwania zanieczyszczeń z gazów odlotowych”.

[7] Regulation of the Minister of the Environment of 26 January 2010 on reference values for certain substances in the air (Dz. U. 2010 nr 16 poz. 87).

[8] J.D. Rutkowski, Odorous substances and their nuisance, *Przegląd Komunalny*. 10 (2005), 67–69 ”Substancje odorotwórcze i ich uciążliwość”.

[9] I. Sówka et al., The problems of odor nuisance selected of municipal facilities, 409 – 413, http://www.pzits.not.pl/docs/ksiazki/Ekotoks_2008/Sowka%20409-414.pdf [accessed on February 2, 2017] ”Problemy uciążliwości zapachowej wybranych obiektów gospodarki komunalnej”.

[10] J. Suschka, Beds and biological filters, Wyd. Politechniki Łódzkiej Filii w Bielsku – Białej, Bielsko – Biała, 2000 ”Złoża i filtry biologiczne”.

[11] M. Szklarczyk, Biological treatment of waste gases, Wyd. Politechniki Wrocławskiej, Wroclaw, 1991 ”Biologiczne oczyszczanie gazów odlotowych”.

[12] M. Szklarczyk, Structure, function and advantages of biological filters, *Ochrona Powietrza.* 1 (1992), 6 – 8 ”Budowa, działanie i zalety filtrów biologicznych”.

[13] M. Szklarczyk, Methods of deodorizing gases in wastewater treatment plants, *Przegląd Komunalny*. 11 (2005), 119 – 122 ”Metody dezodoryzacji gazów w oczyszczalniach ścieków”.

[14] J. Warych, Treatment of waste gases. Processes and apparatus, WNT, Warsaw, 1998 ”Oczyszczanie gazów. Procesy i aparatura”.

[15] M. Wierzbińska, Application of the biofiltration method for the deodorization of waste gases using fibrous deposits. Part I. Introduction to biofiltration, *Ochrona Powietrza i Problemy Odpadów*. 2 (2010), 49 – 51 ”Zastosowanie metody biofiltracji do dezodoryzacji gazów odlotowych przy wykorzystaniu złóż włóknistych. Część I. Wprowadzenie do procesu biofiltracji”.

[16] M. Wierzbińska, Application of the biofiltration method for the deodorization of waste gases using fibrous deposits. Part III. Studies on the effectiveness of biofiltration of odors using mixture of selected materials of natural origin, *Ochrona Powietrza i Problemy Odpadów*. 3 (2010), 98 ”Zastosowanie metody biofiltracji do dezodoryzacji gazów odlotowych przy wykorzystaniu złóż włóknistych. Część III. Badania efektywności biofiltracji odorów przy zastosowaniu złóż będących mieszaniną wybranych materiałów pochodzenia naturalnego”.

[17] M. Wierzbińska, W.E. Modrzelewski, Application of biofilters for deodorization of harmful gases, Ecological Engineering. 41 (2015), 125-132 ”Zastosowanie biofiltrów do dezodoryzacji uciążliwych gazów”.

[18] http://geoportal.gov.pl/ [accessed on November 28, 2016].

[19] http://www.laminopol.com.pl/pl/72/biofiltry_modulowe [accessed on November 20, 2016].

Paulina Sawicka-Chudy
Department of Biophysics, Faculty of Mathematics and Natural Sciences, University of Rzeszow
Pigonia 1, 35-317 Rzeszow, Poland, sawicka61@wp.pl

Maciej Sibiński
Department of Semiconductor and Optoelectronics, Lodz University of Technology
Wólczańska 211/215, 90-924 Lodz, Poland

Marian Cholewa
Department of Biophysics, Faculty of Mathematics and Natural Sciences, University of Rzeszow
Pigonia 1, 35-317 Rzeszow, Poland

Maciej Klein
Centre for Plasma and Laser Engineering, The Szewalski Institute of Fluid-Flow Machinery, Polish Academy of Science
Fiszera 14, 80-231 Gdansk, Poland
Faculty of Applied Physics and Mathematics, Gdansk University of Technology
Narutowicza 11/12, 80-233 Gdansk, Poland

Katarzyna Znajdek
Department of Semiconductor and Optoelectronics, Lodz University of Technology
Wólczańska 211/215, 90-924 Lodz, Poland

Adam Cenian
Centre for Plasma and Laser Engineering, The Szewalski Institute of Fluid-Flow Machinery, Polish Academy of Science
Fiszera 14, 80-231 Gdansk, Poland

TESTS AND THEORETICAL ANALYSIS OF A PVT HYBRID COLLECTOR OPERATING UNDER VARIOUS INSOLATION CONDITIONS

Abstract
The main goal of the study was to investigate the relationship between the orientation of the PVT (PhotoVoltaic Thermal) collector and the thermal and electric power generated. Extensive research was performed to find optimal tilt angles for hybrid solar thermal collectors, which combine photovoltaic as well as thermal collection in a single unit, known as PVT (PhotoVoltaic Thermal) modules for an office building with working hours between 7.00 and 16.00. The comprehensive study included field measurements of the modules in central Poland and tests under AM (air mass) 1.5 conditions in a certified laboratory KEZO (Centre for Energy Conversion and Renewable Resources) Polish Academy of Sciences in Jablonna. Furthermore, a PVT system was investigated using the simulation method based on the dedicated *Polysun* software. The PV characteristics and efficiency of the PV module and the relation between power or efficiency of the PVT module and incidence angle of solar-irradiance were studied. Optimal work conditions for commercial PVT modules were ascertained. In addition, it was found that the maximum efficiencies of PV module (η_{PV}), solar thermal-collector (η_c) and PVT hybrid collector (η_{PVT}) registered under field conditions were higher than the ones measured under laboratory conditions.

Key words
Conversion of solar energy, Photovoltaics, Silicon solar cells, PVT collector.

Introduction

Energy plays a vital role in daily human needs. Worldwide, energy consumption has shown rapid growth, which is the important global energy problem. PV modules generate clean electricity, reducing air pollution and having only little environmental impact. Now, typical efficiency of PV modules is in the range 15%÷20% [1]. The conversion of solar energy into electric power depends on the location, orientation, and type of photovoltaic

(PV) system. PVT hybrid collector works with even higher efficiency than sum of the solar thermal collector and PV module efficiencies [2] and simultaneously produces electrical and thermal power. The thermal efficiency of the flat-plate thermal collector is 40–60%. Therefore, the estimated efficiency of the PVT collector is the range from 60 to 80% [3]. In 1979 the first PVT model was demonstrated in Ref. [4]. Until now the PVT systems have been studied from various aspects: system design, performance analysis, simulation models, field or indoor experimental validation, economic and cost-effective analysis [2, 5-8]. Coventry [9] has developed and tested a PVT with a geometric concentration ratio of 37. Chow et al. [10] developed a prototype thermosyphon PVT collector made of aluminum alloy flat box. Dupeyrat et al. [11] tested the design of a prototype single glazed flat plate PVT collector focusing on the heat transfer between PV cells and fluid [3].

Nevertheless PVT hybrid collectors presents numerous advantages, specific work conditions and often contradictory requirements of both technologies cause extensive need for further technology investigation. Considering above facts, this paper aims on ~~to~~ studies of the relationship between orientation of PVT collectors and their thermal and electric power generation. Extensive research was performed to determine the optimal working angle for practical PVT installations. The parameters of the PVT system were measured in field and laboratory conditions. The results were confirmed using specialized computer program Polysun. Acquired results are useful for the design and construction of functional PVT systems.

1. Description of experiments

The research subject was a commercially available photovoltaic thermal hybrid solar collector manufactured by Volther Power Therm measuring 1640 x 870 x 105 mm. Fig. 1 presents the operation parameters of the collector for STC (Standard Test Conditions) [12].

Parameter	Value
Absorber type (PV)	Mono-crystalline
Absorber surface (T)	Copper
Nominal current I_{mp}	5.43 A
Short circuit current I_{sc}	5.67 A
Nominal voltage V_{mp}	36.8 V
Open circuit voltage V_{oc}	45.43 V
Cell efficiency	18%
Collector area	1.4 m^2
Nominal power	200 W
Efficiency (absorber)	49%
Peak power (at 1000 W/m^2)	680 W
Capacity	1.2 dm^3

Fig. 1. Outlook and parameters of investigated PVT collectors.
Source: Author's

Initial studies were performed under field conditions. Field experiments were conducted at the Technology Transfer Centre for Renewable Energy in Lodz (Φ = 51° 44' N, ϕ = 19° 21' E). The PVT hybrid collectors were located on the roof of the building and were inclined at 30º from the horizontal axis in a southern orientation: (E = +90°, S = 0°, W = -90°). Figure 2 presents a schematic diagram of the installation.

Research was done during the autumnal equinox at the beginning of October, during daytime between 8.00 and 16.00. It is assumed that the results obtained at the equinox will correspond well to the annual average values. The weather station on the roof of the building allowed determination of the meteorological conditions.

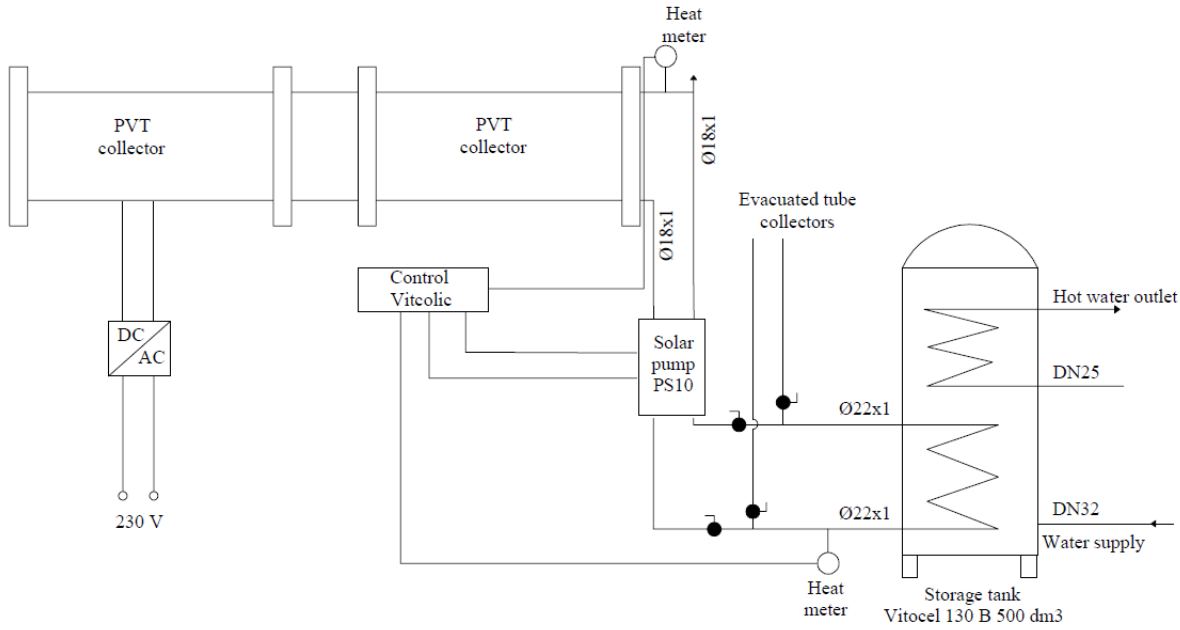

Fig. 2. Schematic diagram of installation PVT collectors.
Source: Author's

Figures 3 presents weather conditions on 2 October 2015 (solar irradiance on a horizontal surface, I_{rr} (right axis), solar elevation (it is the angle between the direction of the geometric center of the Sun and the horizon), S_e [13], the solar altitude angle (it is the angle between solar radiation which falls for receiver and receiver) for positioning the receiver at angles of 30° $S_{a30º}$ and 60º $S_{a60º}$ (left axis). Table 1 shows ambient temperature, T_a, wind speed, v, and values of solar elevation, S_e.

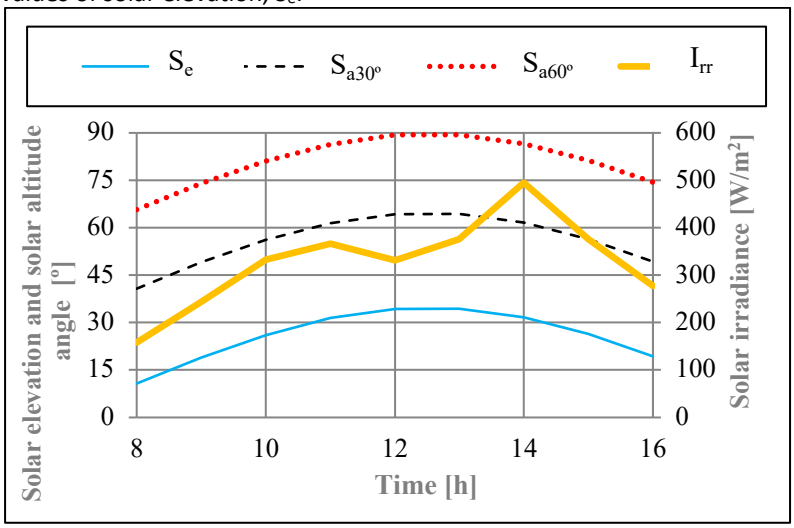

Fig. 3. The solar irradiance measured during field experiment, solar elevation and calculated solar altitude angle.
Source: Author's

Table 1. Ambient temperature, wind speed, values of solar elevation on 2 October 2015.

Time	T_a [ºC]	S_e [º]	v [m/s]
8.00	4.3	10.73	1.1
9.00	5.3	19.03	2.4
10.00	10.8	26.10	2.2
11.00	13.9	31.42	2.0
12.00	15.8	34.33	3.0
13.00	17.4	34.39	2.2
14.00	19.3	31.60	2.9
15.00	19.4	26.38	2.4
16.00	20.3	19.33	2.1
The average	14.07	–	2.3

Source: Author's

All electrical data were determined using a multifunction I-V Curve Tracer (HT IV 400). The acquired data included voltage-current characteristics (I-V curve), maximum power point (MPP) and power at MPP (P_{max}), the current ($I_{mp,}$ accuracy ±0.5%) and voltage ($V_{mp,}$ uncertainty ±0.5%) at maximum power point, the short circuit current (I_{sc}) and the open circuit voltage (V_{oc}) - see I-V curves at various module temperatures at Fig. 11a in Appendix. Solar irradiance was determined using a pyranometer SP Lite2 KIPP& ZONEN (uncertainty ±0.05%). Solar circuit systems was control by solar controller VI ECO SOL 200 (uncertainty ±1ºC).

Later, PVT tests were conducted under laboratory conditions. Clean water was used as a solar working fluid. The photovoltaic characteristics of the PVT module were measured under STC conditions using a class AAA steady-state solar simulator (LA150200, Eternal Sun) equipped with an AM 1.5 G filter. The light intensity was determined by a silicon reference cell (ReRa Solutions) and corrected to 1000 W/m^2. I-V curves were recorded on IV-System Pro (ReRa Solutions) and a Tracer IV-curve software (ReRa Solutions). The IV-System Pro consist of an EL 9000A (Elektro Automatik) electronic DC load connected with two 34410A (Agilent) multimeters, for PV panels measurements, and a 2401 SourceMeter Keithley (uncertainty ±0.012%), for I-V measurements of a reference cell. During measurements the temperature difference between the inlet fluid and the ambient air was set to: ΔT = 5 K and ΔT = 30 K. Temperatures were measured by PT100 (class A, uncertainty ±0,15 °C) temperature sensors connected to a 34970A (Agilent) data acquisition control unit. Afterwards, solar thermal collector tests were carried out. During measurements, in order to better reflect the natural conditions, the solar simulator was operated in ST1000 mode wherein infrared radiation intensity is higher. Therefore, the light intensity was determined using an IR02 pyrgeometer Hukseflux (uncertainty ±15 °C) and a SR11 pyranometer Hukseflux (uncertainty ±8%) connected to a 34970A (Agilent) data acquisition control unit. The mass flow rate of fluid through the solar thermal collector was set to 1.3 kg/min and was determined by an Optimass 6400 C Krohne (uncertainty ±0.1%) mass flow meter.

2. Model description

The measured energy characteristics and the PVT system efficiency were verified using the *Polysun* software from the company VELA SOLARIS [14]. This part is mostly for comparative and demonstration use rather than for reliably justified conclusions, as the applied meteorological conditions do not refer to the specific test localization (due to known limitation regarding the license of this software version). The program provides dynamic simulations of thermal, photovoltaic and PVT systems and enables their optimization [16]. *Polysun* 8.1. Simulation Software Designer Demo is available now [14]. For prediction or estimation of efficiency of PVT collector (ε_{sys}) the following equation is considered in this study [15]:

$$\varepsilon_{sys} = (Q_{use} + E_{inv})/(E_{aux} + E_{par}), \% \quad (1)$$

where Q_{use} is the effective energy consumption [kWh], E_{inv} is energy supplied to the grid from the inverter [kWh], E_{aux} is auxiliary energy, E_{par} is parasitic energy of the respective system [kWh].

The parameters of the PVT system used in our simulations are listed down in Table 2.

Table 2. The parameters values of PVT system.

Parameters	Value
Number of residents	4
Orientation of PVT collectors	South
Number of PVT modules	6
System specification	Commercial system
Hydronic system template	Hybrid Solar PV and solar hot water residential 1 tank system
Auxiliary heating	Oil

Source: Author's

The setup of the solar PVT system used in this research is depicted in Figure 4. On the left side of the picture is the PVT collector, and in the center is the APU (auxiliary power unit). Both components are connected to the heat exchangers. Number of PVT modules was dedicated by program *Polysun* for 4 residents.

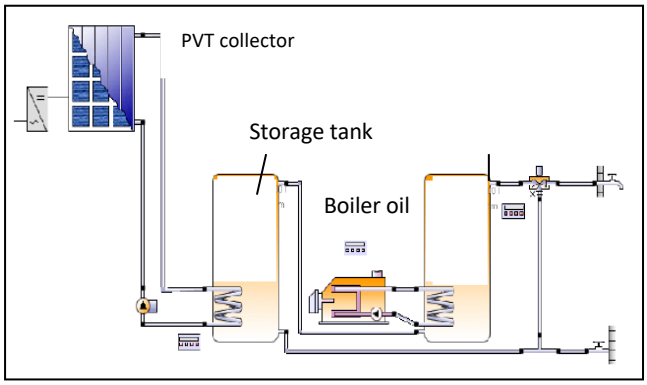

Fig. 4. A solar PVT system designed using Polysun program.
Source: Author's

3. Results and discussion

3.1. PVT measurements in field conditions

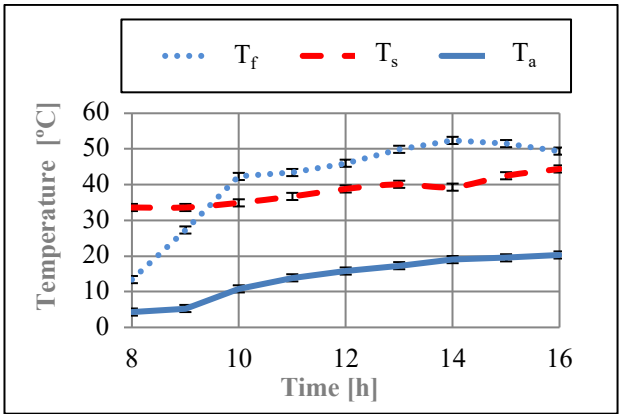

Fig. 5a. Field test results of ambient temperature, the fluid temperature at the collector outlet, and the water temperature in the storage tank during daylight operation time.
Source: Author's

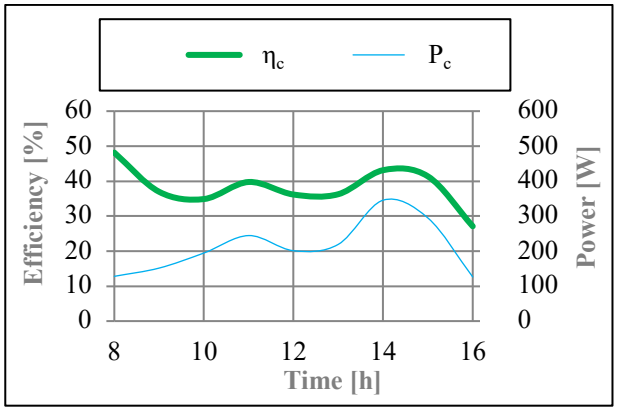

Fig. 5b. Instantaneous power and efficiency values of solar thermal collector.
Source: Author's

Initially, measurements related to thermal-collector operation were performed under field conditions (described in Figures 3). Performance data was not STC-corrected. Authors showed "raw" data to analyzed real work of PVT

system. Figure 5a summarizes the data related to the temperatures of ambient air (T_a), of the cooling water at the collector outlet (T_f) and of water in the storage tank (T_s). The daytime operation of a solar thermal collector can be divided into two periods. First, between 8.00 and 10.00, the cooling water temperature of the solar thermal collector, T_f, rises from 13 to 42ºC. At that moment, a circulation pump is activated leading to a heat exchange between water from the heat collector and water in the storage tank (see red curve in Fig. 5a). The temperature of the water in the storage tank, T_s, slowly increases but the temperature of the water in the collector holds steady for one hour (see plateau on T_f curve). Later, between 11.00 and 14.00 the water temperature in the collector increases quasi linearly. Although the temperature T_f decreases after 14.00 due to a strong decrease of solar irradiance and heat exchange with colder water in storage tank, the heat energy collected at the storage tank increases even after 16.00. At 16.00 the controller turns off the circulation pump to prevent possible heat losses from the water in the storage tank. The temperature difference of water collected in the solar collector and water in the storage tank approaches "zero" and later goes negative. The thermal heat energy accumulated in the storage tank (Q) was ~ 10 MJ. It can be calculated using the measured temperatures and model described in Ref. [16] given by the following equation:

$$Q = V\rho k_c(T_z - T_p), [J] \quad (2)$$

where V is the fluid capacity flow rate during the day (m^3), ρ is density (kg/m^3), k_c is the heat capacity of water J/(kg·K), T_z is the inlet fluid temperature to storage tank (K), T_p is the outlet fluid temperature to the storage tank (K).

Figure 6b shows the instantaneous power (P_c) and efficiency (η_c) of the thermal collector calculated using the model [17]. The power P_c is given by the following equation:

$$P_c = A_c[\beta\tau I_{rr} - k(T_{ab} - T_a)], [W], \quad (3)$$

where A_c is total collector aperture area (m^2), βτ is transmittance–absorptance product, k is solar-collector heat-transfer loss-coefficient ($W/m^2 \cdot ºC$), T_{ab} is average temperature of the absorbing surface (ºC), T_a is ambient temperature (ºC), I_{rr} is instantaneous solar irradiance (W/m^2).

The PV electric performance was also studied. Figure 6a shows how the module electric parameters (I_{mp}, V_{mp}) at maximum power point changes during the chosen day. The interrelation between the instantaneous solar irradiance (I_{rr}) and instantaneous, PV power at MPP (P_{max}) and efficiency (η_{PV}) is shown in Figure 7b.

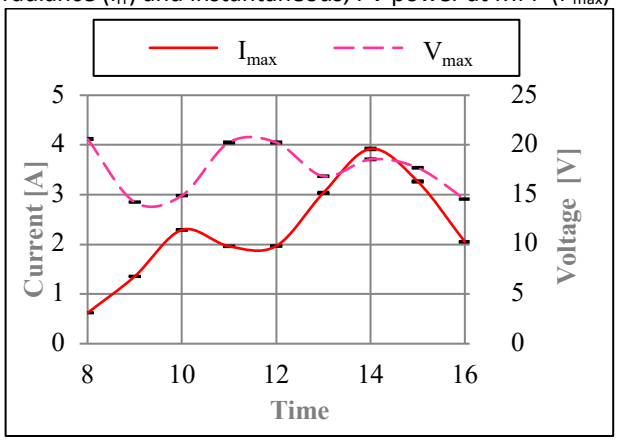

Fig. 6a. Current and Voltage at MPP of PV module.
Source: Author's

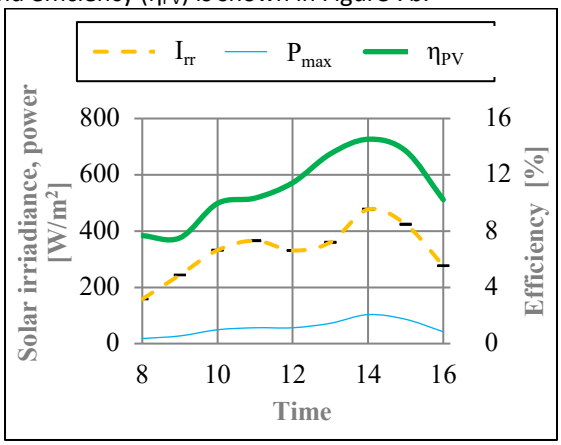

Fig. 6b. P_{max}, I_{rr}, η_{PV} values of PV panel.
Source: Author's

Figure 6a shows that the I_{mp} current strongly depends on irradiance (compare with I_{rr} at Fig. 6b), while voltage varies in a small range 14÷21 V. The black lines represent error bars. The PV current in the range 0.8÷ 3.9 A was measured. As solar irradiance increases three times, the current grows ~400%. Figure 7b shows that as the solar irradiance increases, the values of P_{max} and η_{PV} also increase. The instantaneous efficiency was found in the range from about 8% (morning hours, S_e = 10.73º) to 14% (irradiation about 600 W/m^2, S_e = 33.14º). The amount of power generated and voltage by PVT system was consistent with the solar irradiance. The maximum values were achieved at 14.00. The electric energy production-density, 475 Wh/m^2, was determined using formula in Ref. [18]. The instantaneous maximum output-power MPP, 143 W (S_e = 33.14º) was about 28% lower than the nominal power of the PV module (200 W).

3.2. PVT tests under laboratory conditions

The relation of PVT module performance and solar-simulator altitude-angle were investigated under laboratory conditions. First, the PV module and later thermal collector performance was studied.

Impact of solar-simulator altitude-angles on performance of PV module and thermal collector

The photovoltaic electric characteristics were measured for different solar-simulator altitude-angles α and temperature difference ΔT = 5ºC and ΔT = 30ºC (between the temperature of water at the inlet to thermal collector and the ambient air). The light intensity was adjusted to 1000 W/m^2. The altitude angle was varied between 30 º and 90º (for 90º the solar simulator was situated parallel to the PVT module).

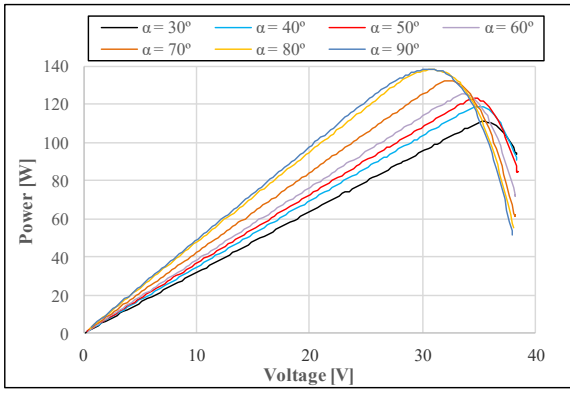

Fig. 7a. The P–V characteristics of PV module for different angles of radiation incidence for ΔT = 5ºC.
Source: Author's

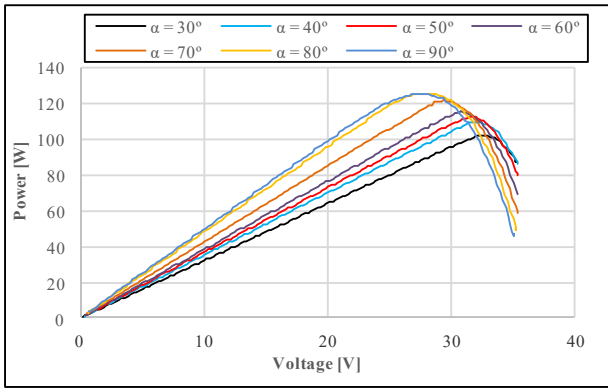

Fig. 7b. The P–V characteristics of PV module for different angles of radiation incidence for ΔT = 30ºC.
Source: Author's

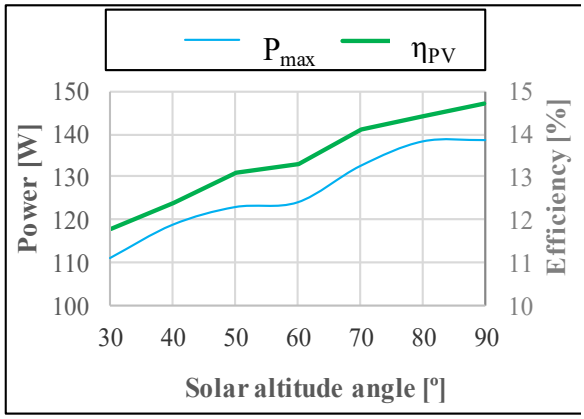

Fig. 8a. The power (P_{max}) and efficiency (η_{PV}) as function of altitude angle for ΔT = 5ºC.
Source: Author's

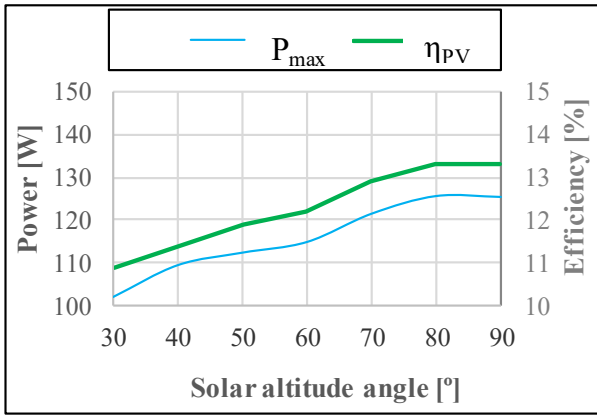

Fig. 8b The power (P_{max}) and efficiency (η_{PV}) as function of altitude angle for ΔT = 30ºC.
Source: Author's

Figures 8a and 8b show that the PV power at MPP and efficiency increases when the solar altitude angle increases, both for ΔT = 5°C and 30°C. As the temperature difference ΔT rises from 5 to 30°C the power at MPP, P_{max}, decreases about 7 W. The maximum value of P_{max} was registered for α = 80-90°; it was 138 W (at V_{mp} ~ 32V) and 125 W (V_{mp} ~27V), for ΔT = 5 and 30°C, respectively. As altitude angle, α, decreases P_{max} decreases but V_{mp} increases (from 32 to 36V) for ΔT= 5°C. The open circuit Voltage, Voc, increases as well. The dip at 60º could be caused by absorption and reflection.

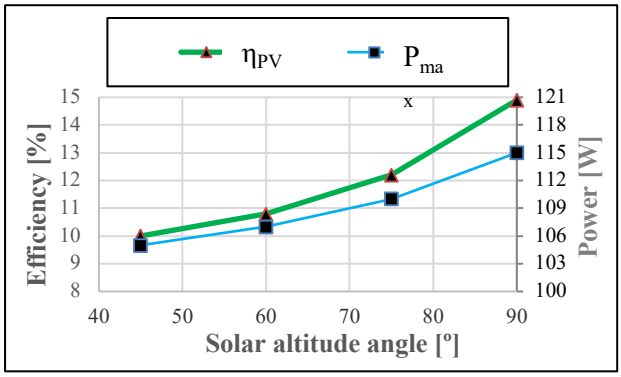

Fig. 8c. The power (P_{max}) and efficiency (η_{PV}) as function of altitude angle for ΔT = 10ºC.
Source: Author's

Then, the PV module and the solar thermal collector were also studied for ΔT = 10ºC. Figure 9c shows that the PV power at MPP and efficiency increases when the solar altitude angle increases, from 104 to 115 W and 10 to 15%, respectively.

The performance of the thermal part of PVT and its dependence on solar-altitude angles was also investigated. The relation between instantaneous thermal power of solar collector (P_c) calculated based on eq. (3), (as well as efficiency) and the solar altitude angle was studied (see results in Table 3 and Figure 9). Table 3 shows solar-simulator irradiance and measured difference between cooling fluid temperature at the collector outlet and at the inlet (T_{outlet} -T_{inlet}) as function of the solar-altitude angle. As the solar-altitude angle increases from 45-75° the temperature difference, T_{outlet} -T_{inlet} , falls 3 times (from 0.64 to 0.21 K). As the altitude angle of the solar simulator increases, solar irradiance and the solar collector output-power also increase.

The efficiency (in contrast to power) of the thermal collector varies differently in relation to the solar altitude angle; it decreases slightly and then increases with the solar altitude angle following the tendency of T_{outlet} -T_{inlet}. Moreover, the efficiency drops only ~6%, whilst power increases by 75% of initial value (Fig. 9). This is important for electric-thermal power balancing under real installation conditions.

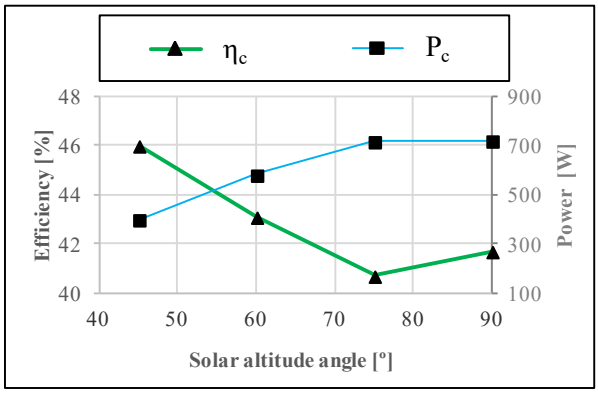

Fig. 9. Power output and total efficiency as function of solar-altitude angle for solar thermal collector for ΔT =10ºC.
Source: Author's

Table. 3. Interrelation between the solar altitude angle, irradiance and T_{outlet} -T_{inlet}.

Solar altitude angle [º]	Irradiance [W/m²]	T_{outlet} -T_{inlet} [K]
45	588	0.64
60	937	0.59
75	1204	0.21
90	1225	0.48

Source: Author's

4. Comparison of results

The efficiency of PVT (η_{PVT}) collectors under both field (during the autumnal equinox) and laboratory conditions as a function of the solar-altitude angle was calculated using equation [19]:

$$\eta_{PVT} = \eta_{PV} + \eta_c \quad . \tag{4}$$

In the case of the field experiment, the values of efficiency for the thermal collector (η_c) (see Figure 10a) were deduced from data presented in Figure 6b, where the solar-altitude angle as a function of time was determined using the data shown in Figure 3 for a module positioned under 30° angle ($S_{a30º}$). The same was done for efficiency of PV module (η_{PV}) under field conditions, but this time using the data presented in Figure 6b. The rather erratic character of the field experiment data should be related to changing weather conditions, such as wind and air temperature. The variation of the solar altitude angle is limited to range 40-65º achievable for the chosen position of the solar panel during the autumnal equinox.

In the case of the laboratory experiment, the efficiency of the thermal collector (presented in Figure 10b) was assumed from the data presented in Figure 10c. The values of PV module efficiency were derived from the data presented in Figure 10, as ~ΔT = 10ºC was observed during the field experiment.

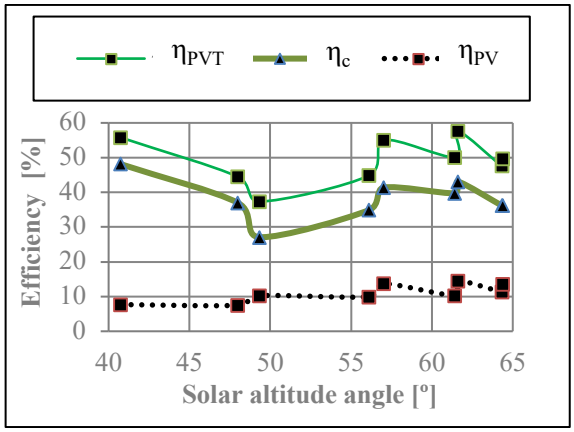

Fig. 10a. Efficiency measured under field conditions.
Source: Author's

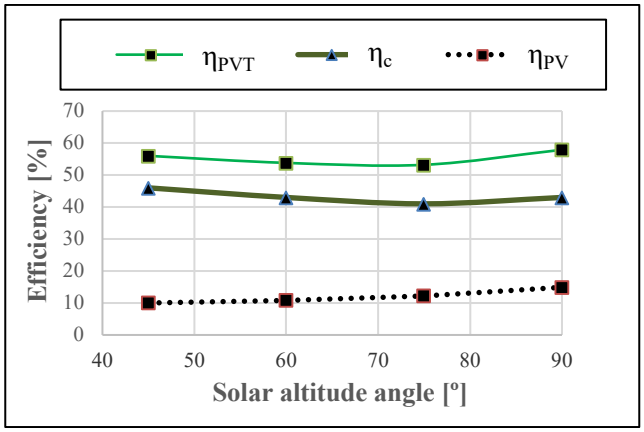

Fig. 10b. Efficiency measured under laboratory conditions.
Source: Author's

The calculated maximum values of η_{PV}, η_c and η_{PVT} efficiencies and optimal (i.e. corresponding to the maximum value) solar altitude angle, α, for a PVT collector are shown at Table 4. It should be underlined that the values of PVT efficiency do not vary much under laboratory conditions and are close to the maximal values under field conditions. Generally good agreement between the maximal values of efficiencies can be observed, however significant difference in the optimal tilt angle needs to be investigated and addressed in the future. The optimal value of the solar altitude angle for η_c is the smallest considered in this study, both under field and laboratory conditions. In both cases, the PV efficiency grows with α. We recalculated altitude angle to the tilt angle (it is the angle between receiver and horizontal position) to compare results in literature. In the literature there are only tilt angle of receivers. The results are in agreement with the earlier reported works [20].

Table 4. Maximum efficiency of PV module (η_{PV}), solar thermal-collector (η_c) and PVT hybrid collector (η_{PVT}) as well as related optimum solar altitude-angles measured.

	Maximum efficiency (respective solar altitude angle)	
	Field conditions	**Laboratory conditions**
η_{PV}	14.5% (62º)	14.9% (90º)
η_c	48.0% (40º)	46.0% (45º)
η_{PVT}	57.7% (62º)	57.9% (90º)

Source: Author's

Calculated values of PVT collector efficiency (η_{PVT}) were compared with the values obtained from the computer program *Polysun* for *the period* during the autumnal equinox at 12.00 for solar altitude angles in the range 45 - 90º. The PVT module efficiency reaches its maximum at α = 90º; the results under laboratory conditions show a similar tendency, although this is screened by oscillations due to weather conditions (e.g. wind and rain). This fact indicates the need for longer-term outdoor observation, necessary for temporary disturbances elimination Nevertheless one may confirm that, the simulated values do not vary much in the range of the considered solar altitude angle, α.

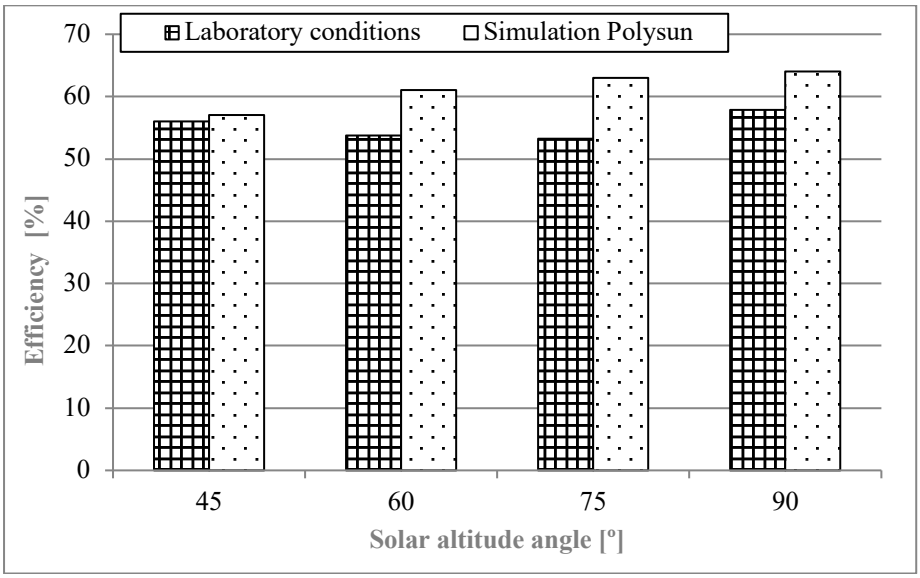

Fig. 10c. PVT collector efficiency under laboratory conditions and corresponding Polysun simulation results

Source: Author's

5. Conclusions

In this study, a PVT collector under field and laboratory conditions was examined. Furthermore, a PVT system was simulated using the demonstration version of *Polysun* software. Through the research, the relationship between orientation of the PVT collector and thermal and electric power generated was investigated. The maximum values of efficiencies for PV module (η_{PV}), solar thermal-collector (η_c) and PVT hybrid collector (η_{PVT}) under different conditions were determined. It was found that the efficiency of the PV module increases with the altitude angle both in laboratory and field experiments. In the case of field experiments, the range of altitude angle was limited (40º;65º). The efficiency of the thermal collector varies slightly in the considered range of altitudes angles and peaks at the lowest considered angle. However, the efficiency of the PV module is more significant overall. Furthermore maximum values of efficiencies for PV, PVT and thermal collector corresponds at the satisfactory level in experiments performed under field and laboratory conditions. The results are in agreement with the earlier reported work on the relation of the tilt angle and efficiencies of PVT modules [21–23]. The simulation results using the *Polysun* software agree reasonably well with experimental data received under laboratory conditions.

Acknowledgments

The authors would like to thank the Technology Transfer Centre for Renewable Energy and Energy Conversion in Lodz and Research Center in Jablonna for allowing them to perform their research.

Nomenclature

A_c	total collector aperture area, m^2
AM	air mass
I_{max}	current point of maximum power, A
I_{mp}	current point of maximum power in standard test conditions, A
I_{sc}	short circuit current, A

I_{rr}	instantaneous solar irradiance, W/m^2
k	solar-collector heat-transfer loss-coefficient, W/m^2 ºC
P_c	instantaneous power of the thermal solar collector, W
P_{max}	maximum nominal power of module, W
PVT	photovoltaic thermal hybrid solar collector,
STC	standard test conditions,
S_e	solar elevation (altitude angle), º
$S_{a30º}$	solar altitude angle for positioning the receiver at angles of 30°, º
$S_{a60º}$	solar altitude angle for positioning the receiver at angles of 60º, º
T_a	ambient temperature, ºC
T_{ab}	average temperature of the absorbing surface, ºC
T_f	fluid temperature at the collector outlet, ºC
T_{inlet}	cooling fluid temperature at the collector inlet, ºC
T_{outlet}	collector outlet temperature, ºC
T_s	water temperature in the storage tank, ºC
Q	energy accumulated in storage tank, kJ
v	wind speed, m/s
V	fluid capacity flow rate during day, m^3
V_{max}	voltage on point of maximum power, V
V_{mp}	voltage on point of maximum power in standard test conditions, V
V_{oc}	open voltage, V

Greek Letters

α	angle of incidence, º
βτ	transmittance–absorptance product,
ε_{sys}	solar yield, %
ΔT	difference between collector inlet fluid temperature and the ambient air temperature, K
η_c	efficiency of solar thermal collector, %
η_{PV}	efficiency of the PV module, %
η_{PVT}	efficiency of PVT hybrid collector, %

References

[1] M. Lämmle, A. Oliva, M. Hermann, K. Kramer, W. Kramer, PVT collector technologies in solar thermal systems: A systematic assessment of electrical and thermal yields with the novel characteristic temperature approach. Solar Energy, Volume 155, October 2017, Pages 867-879

[2] Proekologiczne odnawialne źródła energii Witold M. Lewandowski 2012.

[3] E. Yandri, The effect of Joule heating to thermal performance of hybrid PVT collector during electricity generation, Renewable Energy, Volume 111, October 2017, Pages 344-352

[4] L.W. Florschuetz, Extension of the Hottel-Whillier model to the analysis of combined photovoltaic/thermal flat plate collectors Sol. Energy, 22 (1979), pp. 361-366

[5] N.Aste, C. Del Pero, F.Leonforte, Water PVT Collectors Performance Comparison, Energy Procedia Volume 105, May 2017, Pages 961-966,

[6] A.H. Besheer, M. Smyth, A. Zacharopoulos, J. Mondol, A. Pugsley Review on Recent Approaches for Hybrid PV/T Solar Technology (2016)

[7] Niccolò Aste, Claudio Del Pero, Fabrizio Leonforte, Massimiliano Manfren, Performance monitoring and modeling of an uncovered photovoltaic-thermal (PVT) water collector, Solar Energy, Volume 135, October 2016, Pages 551-568

[8] Lovedeep Sahota, G.N. Tiwari Review on series connected photovoltaic thermal (PVT) systems: Analytical and experimental studies, Solar Energy, Volume 150, 2017, pp. 96-127

[9] J.S. Coventry Performance of a concentrating photovoltaic/thermal solar collector Sol. Energy, 78 (2005), pp. 211-222,

[10] T.T. Chow, J. Ji, W. He Photovoltaic-thermal collector system for domestic application J. Sol. Energy Eng., 129 (2007), p. 205.

[11] Dupeyrat Patrick, Menezo Christophe, M. Rommel, H. Henning Efficient single glazed flat plate photovoltaic – thermal hybrid collector for domestic hot water system Sol. Energy, 85 (2011), pp. 1457-1468,

[12] www.vitechnology.pl, version 2.01.2016.

[13] www.esrl.noaa.gov, version 2.01.2016.
[14]
[15] http://www.velasolaris.com, version 2.01.2016.
[16] Polysun: User's manual for Polysun 3.3, SPF. Switzerland, 2000.
[17] J. Dąbrowski: Solar collectors to heat water efficiency and profitability of the installation, Publisher University of Life Sciences in Wroclaw, 2009.
[18] S. A. Kalogirou: Progress in Energy and Combustion Science, 30 (2004) p. 231-295,
[19] A. Lisowski: Conversion of renewable energy sources, Publisher Village of Tomorrow, 2009.
[20] Klugman E., Radziemska E., Lewandowski W.M.: Influence of temperature on conversion efficiency of a solar module working in photovoltaic PV/T integrated system, 16th European Photovoltaic Solar Energy Conference and Exhibition, United Kingdom Glasgow, 1-5 May 2000, p. 2406-2409.
[21] Kaya M. Thermal and electrical performance evaluation of PV/T collectors in UAE; 2013.
[22] T.T. Chow, W. He, J. Ji An experimental study of facade-integrated photovoltaic/water-heating system Appl. Therm. Eng. 27 (2007), p. 37–45.
[23] T.T. Chow, A.L.S. Chan, K.F. Fong, Z. Lin, J. Ji Annual performance of building-integrated photovoltaic water-heating system for warm climate application Appl. Energy 86 (2009), p. 689–696.
[24] W. He, X.Q. Hong, X.D. Zhao, X.X. Zhang, J.C. Shen, J. Ji Operational performance of a novel heat pump assisted solar facade loop-heat-pipe water heating system Appl. Energy 146 (2015), p. 371–382.
[25] Subhash Chander, A. Purohit, Anshu Sharma, S.P. Nehra, M.S. Dhaka: Impact of temperature on performance of series and parallel connected mono-crystalline silicon solar cells, Energy Reports 1 (2015) p. 175–180.
[26] R. Tripathi, G.N. Tiwari, Energetic and exergetic analysis of N partially covered photovoltaic thermal-compound parabolic concentrator (PVT-CPC) collectors connected in series. Solar Energy 137 (2016) p. 441–451.
[27] R. Tripathi, G.N. Tiwari, Annual performance evaluation (energy and exergy) of fully covered concentrated photovoltaic thermal (PVT) water collector: An experimental validation Solar Energy 146 (2017) p. 180-190.
[28] Shyam, G.N. Tiwari, Olivier Fischer, R.K. Mishra, I. M. Al-Helal, Performance evaluation of N-photovoltaic thermal (PVT) water collectors partially covered by photovoltaic module connected in series: An experimental study. Solar Energy 134 (2016) p. 302-313.
[29] R. Tripathi, G.N. Tiwari, Energy matrices evaluation and exergoeconomic analysis of series connected N partially covered (glass to glass PV module) concentrated-photovoltaic thermal collector: At constant flow rate mode. Energy Conversion and Management 145 (2017) p. 353-370.
[30] K. Znajdek, M. Sibiński Practical Realization of a Hybrid Solution for Photovoltaic and Photothermal Conversion, Journal of Power and Energy Engineering 7 (2013).

Appendix

As stated in the Introduction, increase in PV module temperature results in a significant efficiency drop. In order to check the impact of temperature on performance of the studied PV, experiments were carried out using a constant light intensity source of 1000 W/m^2 with cell temperature in the range 20-60ºC. From Figs 12a and 12b it is clearly seen that the temperature of the PV module significantly influences the current–voltage characteristic and module efficiency. It was calculated that the forward voltage of the solar cell decreases ~2 mV/K, with temperature increase. The results are in agreement with the earlier data for silicon solar cells [24-29].

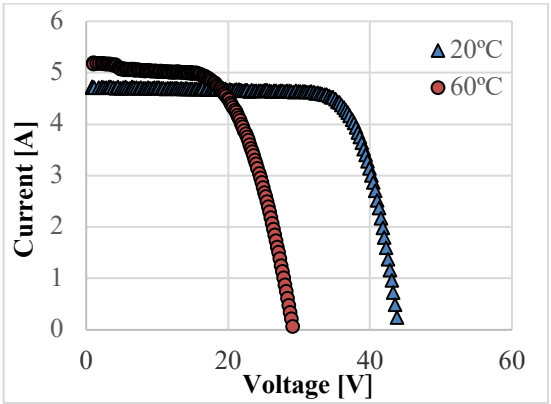

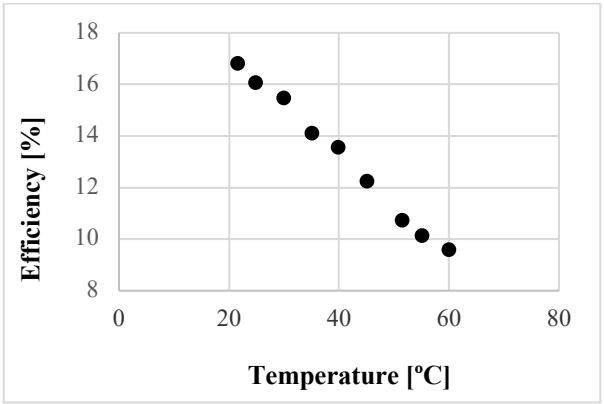

Fig. 11a. The I–V characteristics of PV module under different cell temperatures (20 and 60°C) for light concentration of 1000 W/m^2.
Source: Author's

Fig. 11b. The effect of temperature increase on PV module efficiency for light intensity 1000 W/m^2.
Source: Author's

Figure 11c shows a thermogram of the surface temperature after measurements when the solar thermal system was turned on (left) and off (right).

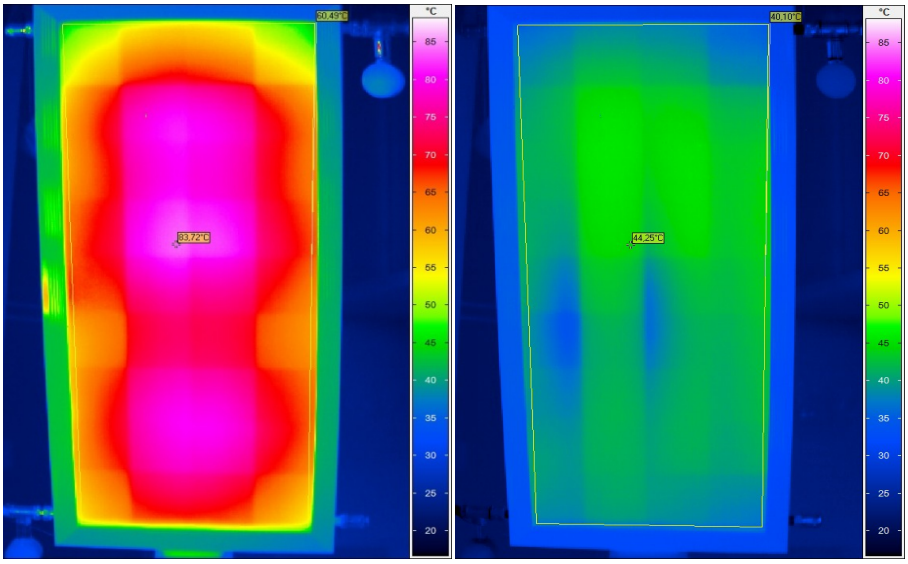

Fig. 11c. Solar hybrid system working without liquid flow (left) solar hybrid system after 15 minutes of liquid flow (right).
Source: Author's

This experiment was conducted at the Department of Semiconductor and Optoelectronic Devices, Lodz University of Technology [30]. Average surface temperature of the solar hybrid system working without liquid flow is ~82 ºC and average surface temperature the same solar hybrid system after 15 minutes of liquid flow is ~42 ºC.

Kinga Korniejenko
Cracow University of Technology, Faculty of Mechanical Engineering, Institute of Materials Engineering
al. Jana Pawła II 37, 31-867 Kraków, Poland, kinga.korniejenko@mech.pk.edu.pl

AN ASSESSMENT OF THE EFFECTIVENESS OF SUPPORT FOR UNIVERSITY PROGRAMS FROM THE HUMAN CAPITAL OPERATIONAL PROGRAM IN YEARS 2013-2015 IN THE DEVELOPMENT OF STUDENTS COMPETENCES IN ENTREPRENEURSHIP

Abstract
The article presents the ways of support from European funds in the development of student competencies and organizational innovation in the field education. It is based on a case study of the project 'Inżynieria materiałowa – inżynieria przyszłości' (Material engineering – engineering of the future'), financed by the European Social Fund in Poland. The project was implemented at the Faculty of Mechanical Engineering of the Cracow University of Technology in the years 2012-15. The research methods used are critical analysis of literature sources, surveys and a case study of the project mentioned above.

Key words
enterprise and entrepreneurship education, innovation in education, student competencies, European Social Fund

Introduction

Education, especially in the field of engineering, is the spine of development and economic growth of a country. STEM (Science, Technology, Engineering and Mathematics) fields are the most critical sciences for a nation and are key to strengthening the global economy [1]. For those reasons it is essential to develop a new, modern way of supporting education that meets contemporary market requirements and predicts future trends. Entrepreneurship is an important element of innovative education, especially for engineering/STEM graduates. They are not only demanded for technical and scientific careers, but also in other sectors such as finance, where they very often hold managerial positions [1, 2].

Entrepreneurship is also complex problem because there are many definitions in the literature and many theoretical and practical cases connected with this topic. Based on literature review, for the purpose of this article, entrepreneurship is defined as a way of thinking and acting by the author of article. Entrepreneurs are people who can notice opportunities or face problems responsibly [3]. They are people who can create new values and are agents of change that have impact on others. They are also creators of companies or projects and possess the basic skills of creativity and innovation [3, 4]. This kind of education is crucial for the engineering profession, where complexity and interdisciplinary cooperation increase together with the development of the world economy. Most companies require equipping engineering graduates with a set of non-technical skills such as communication, decision making, management, and leadership [5, 6, 7]. Entrepreneurial training can enhance the acquisition of relevant skills for graduates. It is important because research shows that engineering students and graduates in the US, Europe, and the Asia Pacific region have these skills at a very low level [5, 6, 7]. This kind of problem applies to Polish students and graduates as well [8, 9, 10].

Development of enterprise and entrepreneurship education

Enterprise and entrepreneurship education can help students to succeed in their future career by learning to think like entrepreneurs, facilitating corporate entrepreneurship and to address global competition and technological changes [3, 11]. These classes also develop other soft skills such as creativity and divergent thinking that are important for identifying new business opportunities [12]. In this case, creativity is especially important because it is perceived as the prime source for innovation [13]. They should give the proper knowledge and skills as well as create positive attitudes to entrepreneurship [14]. Thanks to this course, students may learn how to recognize the opportunities and follow them through with new ideas and determine the necessary resources. This is important not only in private business but also in project applications in many areas, including scientific activities. Enterprise and entrepreneurship education also give them the possibility to improve their critical

thought and managing abilities [11]. Implementing differential learning experiences into the educational process is crucial for enterprise and entrepreneurship education, such as business exhibitions, conferences of successful entrepreneurs, and company visits. Such experiences increase the effectiveness of this kind of education [3, 15].

It is also worth pointing out that entrepreneurship education is relatively a new topic for university courses. It was born in the United States of America in the 1940s and 1950s. The first academic course on entrepreneurship was launched in 1947 at Harvard Business School [16]. For many years, enterprise and entrepreneurship education has evolved significantly. Today, most universities offer the courses of entrepreneurship and many of them are focused on innovation topics [17]. Moreover, the development of enterprise and entrepreneurship education is supported by national and international policies, especially in the field of STEM education. The entrepreneurship initiatives in this area are very important for economic development. Grants funded by the National Science Foundation (U.S.A.) for North Carolina Central University launched in 2014 are exemplary of this sort of education. They are implemented as 'DREAM STEM'. The main goal of this program is to identify scientists and integrate entrepreneurship into scientific education. This program is worth over $1.75 million [18]. Other exemplary came from Latin America is Fondo Emprender (Entrepreneurship Fund). This fund was created to finance business projects, having as beneficiaries students who are about to finish their undergraduate or postgraduate programs and with no more than two years after completing their studies. Between 2003 and 2015, 3,494,185 companies in 607 municipalities have been created per year with public funds, with 102 million dollars and generate 39,817 jobs [3]. The calculation shows that average number generated jobs per 1 company was about 0.011 work position.

Entrepreneurship education should empower post-graduation opportunities in modern society. It should also ameliorate some socio-economic problems, especially unemployment [19]. The article shows how enterprise and entrepreneurship education is supported from European funds. Thanks to a grant from the Human Capital Operational Program in years 2013-2015 it was possible to develop students' competencies in this area and at the same time the development organizational innovation in the area of education.

Research methods

The article based on the case study of the project 'Inżynieria materiałowa – inżynieria przyszłości' (Materials engineering – engineering of the future'), especially research activities undertaken during the project such as surveys. The questionnaires (with open, semi open and closed questions) were given to the students and also to potential employers (during student's internships) in the framework of the project.

The project 'Inżynieria materiałowa – inżynieria przyszłości' (Materials engineering – engineering of the future') was supported from European funds in the development of student competencies. It was financed by the European Social Fund in Poland under the Human Capital Operational Program in years 2013-2015. The main aim of the project was to encourage young people to study Materials Engineering. The background of this national program was to persuade young people to choose engineering studies as more profitable for their future. In this time, many young people chose humanities because they were perceived as easier. It cased lack of technical competencies in the Polish economy. The project was implemented at the Faculty of Mechanical Engineering of the Cracow University of Technology in the years 2012-15. The students supported by this project had an opportunity to learn the skills required on the labour market. The project was focused on developing competencies needed in the job market, collaboration with enterprises in education and creating opportunities for students to develop practical skills through internships. The project was focused on BA students. In Poland, the duration of these studies is three and half years for engineering disciplines. The students have complex support programs that include [20] the following:

- An additional subsidy for the best students (about half of students each year)
- Additional classes in mathematics, physics and chemistry on the first year
- Lectures conducted by visiting professors
- Practical classes conducted by practitioners from industry
- Study visits to foreign organizations and domestic companies
- An additional course in the field of environmental protection in the second year
- An additional course in the field of computer methods for engineers (AutoCAD)
- Workshops on research methods such as thermal analysis and scanning microscopy
- Additional course entitled Internal Auditor Environmental Management System according to ISO requirements

- Internships in companies (1 month)
- An additional course in the field of environmentally-friendly solutions for production in the third year
- Participation of the best students in conferences
- Internships in companies
- Internships at foreign universities for the bests students (Japan and Germany)
- An additional course entitled International Welding Engineer (IWE
- A course in the field of entrepreneurship in the third year

In addition to the benefits that students have achieved enriching their portfolio, the project made it possible to prepare teaching materials and purchase equipment that was necessary to carry out the activities of modernized curricula.

One of the important elements of the complex program for students was enterprise and entrepreneurship education. It was organized as an additional class in the third year of study. This period was chosen because of the study organization. After the three and a half years the students received the title of engineer and some of them decided to start a professional career. The form of classes had an innovative character and were focused on skills based education. The course included three parts: lectures and workshops as a base to prepare a business plan step-by-step, classes with practitioners (entrepreneurs) and student work on business plans. The students were divided in groups of about 17 people. Each group had 20 hours of lectures and workshops and 10 hours of classes with practitioners. The classes ended with a competition for the best business plan and had a valuable prize. The main goal was to raise the self-motivation of the students to attend classes and work on business plans.

The results present information from three kinds of surveys. The first are those made at the beginning of each year of the three and half year study program. They were conducted on 71 students in the first year (2012/13), 54 students in the second year (2013/14), 56 students in third year (2014/15) and 20 students in the fourth year (2015/16). The surveys included closed and semi-opened questions and were modified each year depending on the project activities. Below are selected answers to the questions connected with entrepreneurial aspects. The second one are results after the class evaluation. It was made using a questionnaire with closed and semi-opened questions regarding the utility of additional course in the students' opinion. The questionnaire had 16 items.

The questionnaire were filled out by 32 of the 68 students participating in the classes, and 49 prepared business plans. Below are selected answers regarding the students' opinions about the classes. Students as well as employers participated completed questionnaires after the internships. In the project, 49 students participated in the internship program, and 47 of those had a minimum of 3 months of internships. After each internship was an evaluation. It based on questionnaires filled by student and employer. The questions were connected with the effectiveness of this kind of support and the skills required by the labour marked. The chosen opinions are presented below.

Results

The surveys were made at the beginning of each year of study. The results show the change in attitude of the students to enterprise and entrepreneurship education and their plans for the future. The charts (Figure 1 and Figure 2) are based on questions from the surveys and the students' answers.

Figure 1 presents the results of how the students' opinion changed regarding the entrepreneurship classes. On the vertical axis there are presented year of study. On the horizontal axis there are presented amount of students that chosen the variant of answer in the questionnaire. The numbers were transferred into percentage. Since the classes were organized during the third year of study, there were no questions about the classes for the first-year students. The results have the character of a Gauss chart. Many students perceived this topic as 'quite interesting' or 'interesting' before the classes. After the entrepreneurship classes, the responses changed. The students have basic knowledge, so a small group was interested to continue the topic. It is worth saying that the classes were made during the third year and they had a positive opinion. The students identified the appropriate adjustment of the amount of material for the classes, the appropriate form and the content, the appropriate range of material and the timeliness of the course.

Figure 2 shows the change in opinions related to the future place of work. On the vertical axis there are presented amount of students that chosen the variant of answer in the questionnaire. The numbers were transferred into percentage. On the horizontal axis there are presented possibilities of answer (multiple chose). The years of study for each variant are presented in columns (as Roman numbers in legend). The students were asked where they would like to work after the completing their studies. The results of the questionnaires show that only a small group of students is interested in conducting their own business, and that group decreased during the project. The correlation between this chart and Figure 1 is very interesting, especially the large decrease in those who would like to be entrepreneurs after the classes. The course gave the students an awareness not only about the advantages of entrepreneurship, but also about the disadvantages and barriers connected with conducing their own business. Looking at the results, the question is about the meaning of guidance enterprise and entrepreneurship education. The answers show the results of the questionnaires after internships. About 75% students claimed to lack the 'soft skills' needed in their future jobs. Participation in enterprise and entrepreneurship education gave them the opportunity to enforce it. It may be especially useful in other career types such as work in small and medium enterprise or global corporations. Student opinions confirm employer opinions that students lack 'soft competencies', including those related to enterprises.

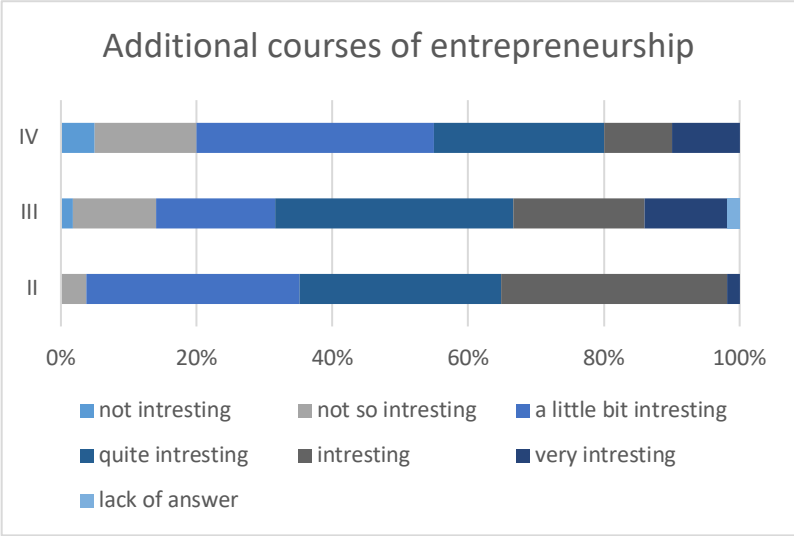

Fig. 1. The assessment of the usefulness of the entrepreneurship curse developing students' skills
Source: Author's

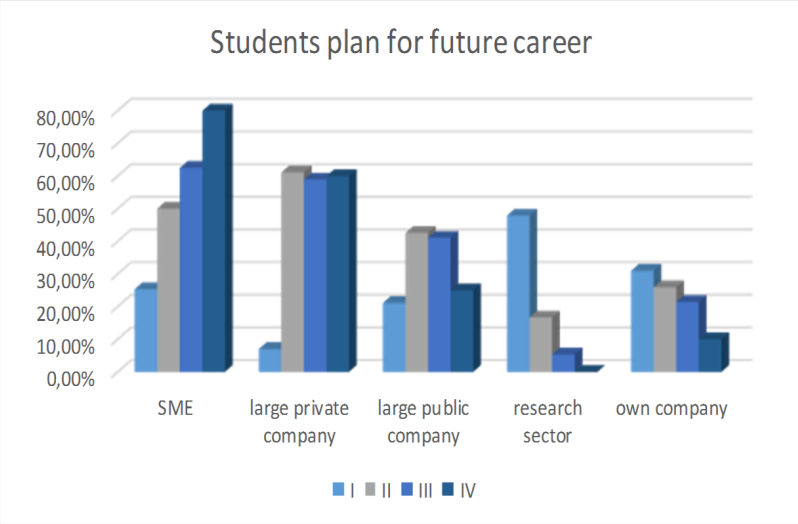

Fig. 2. The organizations where the students would like to work in the future
Source: Author's

Summary and conclusions

The article presents selected results connected with developing entrepreneurships competencies. The case study of the project 'Inżynieria materiałowa – inżynieria przyszłości' (Material engineering – engineering of the future'),

financed by the European Social Fund in Poland shows the possibility of supporting enterprise and entrepreneurship education. The students supported by this project have a large opportunity to learn the skills that are required on the labour market. The project was focused on development competences needed in today's job market, collaboration with enterprises and creating opportunities for students to develop practical skills (internships). The students had a complex support program, including entrepreneurship competencies. The results of the questionnaires show that only a small group of students is interested in conducting their own business, and that group decreased during the project. Reasons could be the increased awareness of students regarding the difficulties linked running a company. However, the entrepreneurship classes included in engineering curricula have other advantages for the students. Participation in this kind of class may be also useful other types of careers and helps to develop other 'soft skills' that are desired by labour market.

The research results shows that the support for enterprise and entrepreneurship education is desirable. The important thing is design the modern curricula for this type of education. The curricula should be strictly connected with current market situation. In this case the European financial support for the entrepreneurial education for students is crucial. The universities, especially technical ones, concentrate on specialist knowledge missing the others area of education such as entrepreneurship. The external support gives an opportunity to enforce this area of knowledge. The results could be very promising in long term perspective. This kind of education is not only better market adaptation of the graduates, but creating the basis for modern, innovative economy based on small and medium enterprises.

Acknowledgements
This research was part of the project 'Inżynieria materiałowa – inżynieria przyszłości' (Materials engineering – engineering of the future'), financed by the National Centre for Research and European Development under the Social Fund in Poland 2007-2013.

References

[1] M. Abdulwahed, Technology Innovation and Engineering' Education and Entrepreneurship (TIEE) in Engineering Schools: Novel Model for Elevating National Knowledge Based Economy and Socio-Economic Sustainable Development, Sustainability 9, 171 (2017) 1-21.

[2] M. Borrego, J. Bernhard, The emergence of engineering education research as an internationally connected field of inquiry, J. Eng. Educ. 100 (2011) 14–47.

[3] J.G. Gutiérrez, J.E.G. Baquero, New cross-proposal entrepreneurship and innovation in educational programs in third level (tertiary) education, Contaduría y Administración 62 (2017) 239–261.

[4] H. El-Gohary, H.M. Selim, R. Eid, Entrepreneurship Education and Employability of Arab HE Business Students: An Attempt for a Primary Investigation, International Journal of Business and Social Science 7, 2 (2016) 52-72.

[5] A. Patil, G. Codner, Accreditation of engineering education: Review, observations and proposal for global Accreditation, Eur. J. Eng. Educ. 32 (2007) 639–651.

[6] M. Abdulwahed, W. Balid, M.O. Hasna, S.A. Pokharel, Skills of engineers in knowledge based economies: A comprehensive literature review, and model development, in Proceedings of the 2013 IEEE International Conference on Teaching, Assessment and Learning for Engineering (TALE), Kuta, Indonesia, 26–29 August 2013, 759–765.

[7] J.A. Hamad, M. Hasanain, M. Abdulwahed, R. Al-Ammari, Ethics in engineering education: A literature review, in Proceedings of the 2013 IEEE Frontiers in Education Conference (FIE), Oklahoma City, OK, USA, 23–26 October 2013, 1554–1560.

[8] T. Rachwał, K. Wach, Badanie intencji przedsiębiorczych młodego pokolenia: wyniki ankietyzacji wśród studentów kierunków nieekonomicznych, Przedsiębiorczość – Edukacja 12 (2016) 405–415.

[9] A. Andrzejczyk, Przedsiębiorczość studentów województwa podlaskiego, Optimum. Studia Ekonomiczne 6 (84) (2016) 142-170.

[10] T. Kusio, Podnoszenie kompetencji przedsiębiorczych przed wejściem na rynek pracy, Nierówności Społeczne a Wzrost Gospodarczy 50 (2/2017) (2017) 403-412.

[11] S. Ojaghi, B. Rezaee, N. Naderi, H. Jafari, Conceptual – Analytical Model Challenges of Entrepreneurship Education in Higher Education Institutions (Case Study: Universities in the Kermanshah City), Pal. Jour. 16 (2017) 95-104.

[12] S. Karimi, H.J.A. Biemans, T. Lans, M. Aazami, M. Mulder, Fostering students' competence in identifying business opportunities in entrepreneurship education, Innovations in Education and Teaching International 5, 2 (2016) 215–229.

[13] R. Cachia, A. Ferrari, K. Ala-Mutka, Y. Punie, Creative Learning and Innovative Teaching. Final Report on the Study on Creativity and Innovation in Education in the EU Member States, Luxembourg: Publications Office of the European Union, 2010.

[14] T. Garvan, B. Ocinneide, Entrepreneurship Education and Training Programmes: A Review and Valution, Journal of European Industrial Training 18, 11 (1994) 13-21.

[15] S. Robinson, H. A. Stubberud, Elements of entrepreneurial orientation and their relationship to entrepreneurialintent, Journal of Entrepreneurial Education 17, 2 , (2014) 1–11.

[16] K. Wach, Edukacja na rzecz przedsiębiorczości wobec współczesnych wyzwań cywilizacyjno-gospodarczych, Przedsiębiorczość – Edukacja 9 (2013) 246 – 257.

[17] A. Mohanty, D. Dash, Engineering Education in India: Preparation of Professional Engineering Educators, Journal of Human Resource and Sustainability Studies, 4 (2016) 92-101.

[18] A. Chatterji, E. Glaeser, W. Kerr, Clusters of Entrepreneurship and Innovation, Innovation Policy and the Economy 14 (2014) 129-166.

[19] N. Onuma, Entrepreneurship Education in Nigerian Tertiary Institutions: A Remedy to Graduates Unemployment, British Journal of Education 4, 5 (2016) 16-28.

[20] K. Korniejenko, J. Mikula, Development of Polytechnic Education by Using the Projects Funding from External Sources, proceedings of the International scientific conference 'Modern technologies and the development of polytechnic education', Far Eastern Federal University, Vladivostok, 14-18 September 2015, 772 – 776.

Monika Smaga
Research and Innovation Centre Pro-Akademia
Innowacyjna 9/11, 95-050 Konstantynów Łódzki, Poland, monikaturek@op.pl

Grzegorz Wielgosiński
Lodz University of Technology, Faculty of Process and Environmental Engineering,
Wólczańska 213, 90-924 Lódź, Poland, grzegorz.wielgosinski@p.lodz.pl

Aleksander Kochański
Research and Innovation Centre Pro-Akademia
Innowacyjna 9/11, 95-050 Konstantynów Łódzki, Poland, aleksander.kochanski@proakademia.eu

Katarzyna Korczak
Research and Innovation Centre Pro-Akademia
Warsaw University of Technology, Faculty of Power and Aeronautical Engineering, Institute of Heat Engineering
Nowowiejska 21/25, 00-665 Warszawa, Poland, katarzyna.korczak@proakademia.eu

BIOMASS AS A MAJOR COMPONENT OF PELLETS

Abstract
The article describes the quality parameters of the selected elements of biomass as a potential ecological biofuel. Several selected elements of a type of biomass were tested to determine the calorific value, humidity, content of sulfur and amount of ash produced in burning process. The concept of biomass and the legal aspects of its combustion are described. The research of biomass samples revealed that they may be turned into a high-energy, ecologically solid biofuel. Production of biofuel from the tested biomass does not require any additional binders. Studies have shown that the tested material can also act as a component of composite pellets. The quality parameters of such pellets can be determined with the composite calculator that is described in this article. The article also describes the technical aspects of the pellet production line, which should be applied to produce good-quality pellets from the tested types of biomass.

Key words
biomass, bio waste, pellet, composite calculator, pellet production lines

Introduction

Currently, there are three definitions of "biomass" that have been formulated in several legal acts. Although these definitions are often consistent with one another, they represent a different approach to biomass itself. The first definition states that biomass is the entire organic matter that exists on earth, including all materials of plant or animal origin that are biodegradable. The second definition describes biomass as the biodegradable parts of products, waste or residues of biological origin from agriculture, including plant and animal materials that result from forestry, fisheries and from other related industries, including aquaculture and fish farming. They also include the biodegradable fraction of industrial and municipal wastes, including installations for waste management, water treatment and sewage treatment. The third definition of biomass assumes that it is solid or liquid materials of plant or animal origin that are biodegradable and derived from products, waste and residues from agriculture and forestry and other related industries. They could also be from other wastes that are biodegradable or from cereal grains that do not meet the quality requirements for cereal [1-8].

Biomass is described by many laws and regulations, both in Polish and European law. The greatest concern related to biomass, however, is that it is often mistakenly treated as a waste. This is due to the meaning of the word "waste", which indicates all the useless substances and materials disposed of. Biomass may also match this description. However, waste is treated mainly as substances or materials that need to be disposed of and could be hazardous to the environment. While biomass is environmentally friendly and can be used to produce energy, it could also become a super-efficient ecological or alternative fuel.

Properties of pellets and briquettes made from biomass has been investigated by many Polish research teams. Niedziółka et al. assessed in [9] the energetic and mechanical properties of pellets produced from agricultural biomass, mainly wheat straw, rape straw, maize straw and its combinations. Obidziński presents in [10-11] the results of a research on the influence of potato pulp content in a mixture with cereal residuals (oat bran, buckwheat hulls) on the pellets quality and its elemental composition. Stolarski et al. investigated the quality and cost of small-scale production of briquettes, made from agricultural and forest biomass in north-eastern Poland [12]. Kijo-Kleczkowska et al. on the other hand performed experimental studies from a comparative analysis of on the mechanisms and kinetics of the combustion of pellets of sewage sludge, coal and biomass [13-14]. Some alternative pellets substrates were investigated as well: Ciesielczuk et al. checked the possibility of using spent coffee ground in energy recycling using a combustion process [15], while Cichy et al. investigated properties of pellets made from Pruning Operations in Fruit Orchards [16]

Alternative fuel, also known as non-conventional fuel, is a fuel of standardized quality properties, such as calorific value, humidity or content of certain chemical elements. This kind of fuel is made from non-hazardous waste and is used as a source of energy in incineration or co-incineration processes of waste. Biomass and its components are not hazardous. Biomass does not contain any harmful chemicals and it does not pollute the environment in any way, even if it is burned, because it consists of organic matter of plant or animal origin.

Fuel produced from biomass is ecological and has solid briquettes or pellets, burns well, is highly energetic and produces a small amount of ash in the combustion process. The production of such fuel does not require any additional chemical substances. Pellets are produced by drying and compressing biomass in special pellet production lines. Since no additional binder is needed to produce the pellets, they are a clean, dried and compressed biomass. Additionally, if the calorific values of all the components of biomass are known, then it is possible to create a high calorific mixture. The composite biomass calculator allows creating a biomass mixture by combining low energy compounds with high energy compounds in the proper proportions to produce a good quality pellet. Besides determining the calorific value of a composite pellet, the biomass calculator will also determine the humidity, content of sulfur, carbon, hydrogen, and the percentage of ash. It appears that biomass, which is frequently treated as waste to be disposed of, can be successfully used to produce a high-quality ecological fuel.

Definition of biomass and the legal aspects in the processes of its incineration

Biomass, according to the encyclopedic definition, is the whole organic matter, all vegetable- or animal-derived biodegradable substances existing on Earth. It has been known to and used by man since the dawn of time. Historically, it was the first source of energy used by man.

Today, biomass is often the source of primary energy. In poorer countries it is the primary source of thermal energy, while in richer countries it a renewable energy source (RES) that partially displaces non-renewable fossil fuels such as coal, lignite, crude oil or natural gas whose global resources have been steadily shrinking. The use of biomass as a renewable energy source is also the result of a globally-implemented policy of climate protection and systematic reduction of greenhouse gas emissions, including carbon dioxide (CO_2). This is based on the belief that carbon dioxide, which is inevitably emitted during the combustion of hydrocarbons, has already been collected from the atmosphere by plants and converted in the process of photosynthesis into biomass. This means CO_2 circulates in the environment without increasing its amount. Hence, biomass is commonly regarded as an emission-free CO_2.

Biomass is the third largest natural source of energy in the world. The global energy potential of biomass is estimated at approximately 100-440 EJ/year, which corresponds to roughly 30% of the global energy demand. According to available data, the current consumption of biomass in the world produces approximately 40 EJ per year [17-20]. In Poland, approximately 212 PJ is produced annually from biomass, and with the mean demand for primary energy amounts to approximately 4 480 PJ, or 4.7% [21]. To obtain energy, biomass is used both in unprocessed and processed forms into the so-called biofuels, which are used for both generation of power and heat as well as in transport.

The formal definition of biomass was included in several legal acts, including the act on waste (art. 162 and art. 2) [1], the act on bio-components and liquid biofuels (art. 2) [2], the Regulation of the Minister of Economy on

the detailed scope of obligations for the obtainment and presentation for remission of certificates of origin, payment of the substitute fee, purchase of electricity and heat generated from renewable energy sources and the obligation to confirm the data concerning the amount of electricity generated from a renewable energy source (§ 2) [3], Regulation of the Minister of Environment on the emission standards from installations (§ 2) [4], as well as in European law - Directive of the European Parliament and of the Council 2010/75/EC on industrial emissions [5]Directive of the European Parliament and of the Council 2009/28/EC on the promotion of the use of energy from renewable sources [6] and the Regulation of the European Parliament and of the Council 1099/2008/EC on energy statistics [7].

In European law, the concept of biomass shall be understood as the biodegradable fraction of products, waste or residues of biological origin from agriculture (including vegetable and animal substances), forestry and the associated industries, including fishery and aquaculture, as well as the biodegradable fraction of industrial and urban waste [6]. Biomass also means products consisting of any vegetable substances from agriculture or forestry that can be used as fuel to recover their energy and the following waste [5]:

- vegetable waste from agriculture and forestry;
- vegetable waste from the food processing industry, if the generated heat is recovered;
- fibrous vegetable waste from the process of production of primary wood pulp and from production of paper from pulp, if such waste is co-incinerated at the place of production and the generated heat is recovered;
- cork waste;
- wood waste, except wood waste that may contain halogenated hydrocarbon derivatives of organic compounds or heavy metals introduced as a result of the application of agents for wood preservation or coating, including wood waste originating from construction and demolition works.

In Polish law, however, biomass has been defined as the biodegradable fractions of products, waste or residues of biological origin from agriculture, including vegetable and animal substances, from forestry and fishery and the associated industries, including breeding of fish and aquaculture, as well as the biodegradable fraction of industrial and municipal waste, including waste from installations for the management of waste as well as water treatment and wastewater treatment [2]. The scope of the concept of biomass has recently been extended in the Regulation of the Minister of Economy [3], according to which biomass is a solid or liquid vegetable or animal substance that is biodegradable, derived from products, waste and residues from agriculture and forestry as well as the associated industries. They should also contain fractions of other wastes that are biodegradable, and cereal grains that do not meet the quality requirements for intervention purchases.

As can be seen, a clear definition of what can be considered biomass is quite difficult. Determination of what could theoretically be considered to have satisfied the above-mentioned definitions and be treated as biomass, but what should not be considered as biomass, seems slightly easier. The list of types of waste that can be considered as biomass is specified both by the act on waste [1] and the Regulation of the Minister of Environment [4]. In line with the act on waste, biomass in the form of animal manure, which is subject to the provisions of the Regulation of the European Parliament and of the Council specifying health rules concerning animal by-products and derived products not intended for human consumption [7]. In addition, straw and other non-hazardous natural substances derived from agricultural or forestry production used in agriculture, forestry or for energy production from such biomass with the use of processes or methods that do not harm the environment or endanger human life and health are not considered to be waste.

The following are also not regarded as waste (e.g. in the processes of thermal treatment):

- vegetable waste from agriculture and forestry;
- vegetable waste from the food processing industry, where the generated thermal energy is recovered;
- fibrous vegetable waste from the process of production of primary cellulose mass and from production of paper from mass, if such waste is incinerated at the place of production and the generated thermal energy is recovered;
- cork waste;
- wood waste, except that which is contaminated with impregnating agents and protective coatings that may contain halogenated organic compounds or heavy metals, the content of which includes wood waste from construction, overhauls and demolitions of structures and road infrastructure.

Despite the existence of the above-mentioned legal definitions, the problem of distinguishing between biomass and wood waste is a very frequent one. Generally, the concept of biomass in all legal acts shall be understood as uncontaminated wood that originates from sawmills or, more broadly, is delivered directly by the forestry and agricultural sectors (firewood, brushwood, wood chips, wood pellets, bark, sawdust, shavings, chips, scrap, or energy crops), as well as waste such as straw, rice husks, nut shells, poultry litter, and crushed citrus dregs. There are also many other wooden materials that are the product of certain industrial processes, particularly in the wood and paper industry. In contrast, contaminated wood originating in furniture factories and demolitions cannot be considered biomass [8].

Proper classification of combustible material, whether biomass or waste, is of paramount importance in the use of its fuel properties. Biomass is treated the same way as fossil fuels (Chapter 2), while incineration and co-incineration of waste is described in Chapter 3. In combustion for energy generation purposes, only the emission of dust, sulfur dioxide and nitrogen oxide is subject to limitation, while in the case of waste, the emission of carbon monoxide, hydrogen chloride, hydrogen fluoride, total organic compounds and heavy metals as well as polychlorinated dibenzo-p-dioxins and polychlorinated furans are subject to limitation. Although from the chemical standpoint, the process of combustion of solid fossil fuels (coal, lignite, peat) biomass or waste is similar [22] and similar contaminations are generated, their quantities will vary depending on the quality of the combustion process, and it is closely connected with the uniformity and the homogeneity of the incinerated material.

Despite many undeniable advantages, such as the widespread availability, renewability, or CO_2 "zero-emission", biomass as fuel also has many flaws, which could include [23-26]:

- relatively low density, which causes difficulties with transport and storage,
- high variability of moisture content, which is the source of numerous problems in the process of combustion,
- calorific value lower than in the case of fossil fuels (particularly coal),
- high variability of properties and elemental composition.

The use of biomass as an energy source has been the subject of many studies during the recent years. They concerned both the fuel properties of biomass [27-30] and the technology of energy use, whether directly through incineration [31-34], or as fuel for co-incineration with coal [35-40]. However, regardless of the adopted technology of incineration or co-incineration, in recent years we have been observing more and more widespread use of biomass as a fuel for energy purposes [41-43].

The argument frequently raised with the burning of biomass is the small emissions of sulfur dioxide and particulate matter, which is much smaller than in the case of coal. This obviously involves much lower sulfur content in the biomass and much lower content of flame retardants. However, due to the high content of volatile substances and the presence of chlorine, biomass burns differently than carbon, producing much higher emissions of the so-called products of incomplete combustion (i.e. PICs) hydrocarbons resulting from numerous chemical reactions taking place outside of the combustion zone. Of those, one will find a long list of aromatic hydrocarbons, simple aliphatic hydrocarbons (including formaldehyde), as well as polycyclic aromatic hydrocarbons (PAHs) and polychlorinated dibenzo-p-dioxins (PCDDs) and polychlorinated dibenzofurans (PCDFs) [44-52]. Also, sometimes the emission of carbon monoxide and hydrocarbons from combustion of biomass is higher than in the case of coal combustion [53].

Quality indexes of the biomass components

The most common component of pellets is an organic matter derived from plants. Pellet is a biofuel made in special presses called pellet mills, from compressed under high pressure wood waste such as sawdust, shavings, wood chips, bark, energy crops, or straw. Pellet is a kind of a small briquette with the form of granules shaped like spheres or cylinders, with a diameter of 6-25 mm and a length of several centimeters. Pellets have a calorific value similar to wood, low humidity (4,3-10%), and during the combustion process they produce a low amount of ash. For these reasons, their use is convenient in the private central heating boilers and fireplaces equipped with a pellet tank, dispenser and feeder [54-55]. Such pellets can be composed entirely of a plant organic biomass, which so far was often treated as waste that needed to be disposed of. The composition of such biofuel may include, for example, grass cuttings, fallen leaves, fragments of cut down trees and shrubs, weeds or plant

origin waste from the production of food, such as fruit stones, nut shells and inedible peels from fruits and vegetables.

Pellet produced from such biomass can meet the quality requirements for the solid organic fuels. Moreover, it does not contain any harmful chemicals and does not pollute the environment in any way, even if it is burned, because it consists of organic matter of vegetable or animal origin.

Production of such fuels does not require any additional chemicals. Pellets are formed by drying and compacting a biomass in special pellet production lines. There is no need to add any additional binders to produce such biofuels. Pellet is a pure, dried and compacted biomass. It's a bio fuel made of wood waste such as sawdust, woodchips and bark or energy plants. Pellet is a kind of a good quality briquette, having the form of granules in the shape of spheres or cylinders that are the size of a few centimeters [56].

Due to its composition, pellets have a calorific value similar to wood (16,00-19,00MJ/kg), low humidity (<%), low sulfur content (<1%), and produce a small amount of ash (<1.00%). These attributes make them a convenient fuel to use in the individual boilers and stoves that are equipped with a reservoir, dispenser and feeder [57].

It appears that the majority of pellets available on the market consist only of timber that comes from sawmills or from energy plants that are specially bred for this purpose. There is also a pellet produced from straw, but it is not so common because such pellet produces more ash than pellets from wood (3-5%), which causes users to clean and service their boilers more frequently.

Recently, agripellets are also becoming a popular biofuel on the energy market. There are no specific standards for quality requirements of agripellets. Although agripellets lag wooden pellets in terms of calorific value, they are becoming more widely used by industry. The calorific value of agripellets oscillates between 12 and 18MJ/kg, and the ash content is relatively high (over 1%).

Nowadays, the biomass that is being "produced" by the people becomes an issue and begins to transform into troublesome waste. Getting rid of unwanted biomass may be a problem for municipalities (e.g. mown grass), forestry management (e.g. material left after deforestation), orchards owners (e.g. waste from fruits and cut down trees), and food manufacturers (e.g. post-production waste, such as peels, seeds and stones). The idea to produce biofuel from such biomass, seems very interesting. Production of such biofuels may solve the problem of a bio-waste disposal and places a new environmentally friendly product on the energy market. Such composite pellet could be produced from grasses, straw, twigs, peels from fruits, vegetables and mushrooms, nutshells, weeds, or fallen leaves.

The study material consisted of samples from:

1. Mowed grass
2. Weeds
3. Walnut shells
4. Pistachio shells
5. Peels of citrus fruits (orange, lemon, lime)
6. Straw
7. Peels of vegetables (beets, carrots, potato)
8. Fallen leaves
9. Peels of fruits (banana, apple, pear)
10. Onion skins
11. Champignons skins
12. Plum seeds

In the first stage of the study, samples were dried in a laboratory oven for 5 hours at 105^{o}C. After that, quality parameters used to describe solid fuels were measured in tested samples. The aim of the study was to determine the quality parameters of the biomass samples, including the calorific value, to confirm whether such biomass is suitable as a component of pellets or other solid biofuels. To determine the calorific value, the following parameters had to be measured for each sample:

1. humidity content

2. content of hydrogen
3. Higher heating value

The following formula has been used to calculate the Lower heating value:

LHV = HHV – r*(a*h + w) [MJ/kg]

LHV – Higher heating value
HHV – Lower heating value
r – heat of vaporization of water (2,455 MJ/kg)
a – hydrogen to water conversion rate 8,94
h – hydrogen content [kg]
w – humidity content [kg]

Additionally, the percentage content of sulfur and the percentage content of ash left after combustion were determined.

Tests were carried out on 3 different measuring devices:

1. Calorimeter Parr 6400 CALORIMETER – Higher heating value
2. Thermogravimetric Analyzer TGA ELTRA THERMOSEPT – humidity, ashes
3. Carbon Hydrogen Sulfur Determinator PC Controlled ELTRA CHS 580 – sulfur, hydrogen

Tests were carried out at room temperature (ca 25^{o}C). Each measurement was carried out in three repetitions. It was assumed that the tested material has a high calorific value, but it may also have a higher content of sulfur in comparison to wood pellets and thus can produce more ash after combustion (Table 1).

Table 1. The quality parameters measured from samples of selected elements of biomass

No.	**Tested material**	**Lower heating value [MJ/kg] (after drying)**	**Humidity [%] (after drying)**	**Ash content [%]**	**Sulfur content [%]**
1.	Mowed grass	15.92	10.0	1.70	0.45
2.	Weeds	1.23	7.47	2.50	0.79
3.	Walnut shells	18.20	7.90	0.59	0.64
4	Pistachio shells	16.54	6.65	0.75	0.99
5.	Peels of citrus fruits (orange, lemon, lime)	18.05	3.13	3.04	0.84
6.	Straw	16.10	9.14	4.89	0.52
7.	Peels of vegetables (beets, carrots, potato)	16.43	1.58	6.76	0.69
8.	Peels of fruits (banana, apple, pear)	16.37	4.19	4.80	0.96
9.	Fallen leaves	18.70	7.78	4.73	0.54
10.	Onion skins	15.89	9.99	6.15	0.57
11.	Mushroom skins (champignons)	14.81	8.19	7.63	0.40
12.	Plum seeds	19.58	7.34	0.46	0.62

Source: Author's

Studies have shown that quality parameters of tested samples of biomass are slightly below the average quality of wooden pellets available on the market, but they are very similar to agripellets. The calorific values of tested materials oscillate between 13.23 and 19.58 MJ/kg. As samples were pre-dried before examination, they also met humidity requirements of wooden pellets. Drying components is one of the steps of pellet production in pellet mills, so humidity value of the examined samples should be consistent with the humidity of pellets produced from the examined material.

Research showed that the tested biomass contains sulfur in the amount that meets the criteria of the standards for wood pellets. Besides that, the presence of sulfur is a natural consequence of sulfur content in the vegetable proteins, which is a building material of tested biomass.

It appears that the greatest issue of the tested samples is the high content of ash (even up to 7.6%). The high content of ash in the burned pellets results in the faster clogging of heating boilers and stoves. However, this is the only disadvantage of such fuel, which can be eliminated or reduced by applying a dedicated boiler that is suitable for this specific type of biomass. Additionally, various types of biomass mixtures can be created.

High- and low-energy biomass components can be combined in suitable proportions. Components that produce a high amount of ash can be mixed with components that produce a low amount of ash to create a good-quality pellet. Choosing the relevant ingredients and mixing them in adequate proportions adjusts the calorific value and moisture content as well as the ash content. Such biomass can be also mixed with other components, such as wood or coal dust to improve quality parameters.

It is important to note that plum seeds have very good energy parameters. They have high calorific value and very low ash content. Additionally, it turns out that such biomass does not need to be pelletized.

The possibility of forming pellets from biomass was also examined. The study was conducted in a laboratory conditions. Pellet granules were produced by the manual press for pellets - Parr Pellet Press. Research has shown that production of pellets from tested biomass components does not require any additional binder to form pellet granules. Figure 1 presents a sample of pellets made from straw.

Fig. 1. Pellets made of straw
Source: Author's

The composite biomass calculator

The composite biomass calculator is a tool used on a first step of a development of new composite pellet. It is used to make a preliminary assessment of properties of the composite, to estimate energy input required for the process as well as costs of production. It accounts for available mass flows of substrates and shows the effectiveness of the production in several production scales and on different pellet production lines. It also optimises the composition of a pellet before starting more complex research.

The structure of the calculator consists of four parts: (1) *input data*, (2) *energy properties*, (3) *production expenditures* and (4) *comparison to other fuels*. Calculations can be done in one of two levels of accuracy. For more general purposes, users only need to input mass flows/capacities and acquisition costs of available substrates. Implemented parameters (calorific value, moisture contents, ash content and sulfur content) for several examined components of biomass, energy plants and of course wood, proceed in further calculations. In more advanced research, the user can change these implemented parameters based on the results of actual substrates tests and add new substrates and their properties. Second, part of the calculator, *energy properties*,

calculates and shows the following properties of composite pellets: net mass of a composite pellet, calorific value, sulfur content, ash content, moisture content and total ash mass in a given pellet mass. Third, part of a calculator, *production expenditures,* calculates and shows all production costs. User needs to input following parameters: outcome moisture content of a pellet and cost rate of the electricity. Parameters like moisture content of input substrates and cost rate of biomass are taken from previous parts of a calculator. As a result, this part shows how much water is evaporated in a process and how much biomass is required to fuel the process and cannot be used for pellet production including the costs of biomass and electricity. The final result is a total cost of the production of the pellet, given as a total value for the total given capacity of a substrates, as well as a unit value for one tonne of a pellet and for one GJ of energy (Fig.). Fourth, part of the calculator, *comparison to other fuels*, compares parameters of a composite pellet and other popular fuels such as hard coal, oil, natural gas, traditional pellet, and firewood. The parameter that is compared is a unit price of the energy that is carried out by these fuels (PLN/GJ). For more complex analysis, the user can add new fuels. Parameters of fuels in this part need to be updated regularly, because of dynamic changes of prices of fuel on the market.

INPUT

Component	Higher heating value	Lower heating value	Sulfur content [%]	Ash content [%]	Humidity [%]	Cost [PLN]	Mass [kg]
Miscanthus		16,280	0,145%	6,896%	20,00%	560,00	1000,00
Jerusalem artichoke		15,320	0,060%	5,367%	23,00%	430,00	1000,00
Grass		14,820	0,145%	4,129%	50,00%	500,00	1000,00
Sawdust		17,140	0,079%	1,043%	45,00%	400,00	1000,00
TOTAL	-	-	-	-	-	1890,00	4000,00

OUTPUT

Mass of pellets [kg]	Average HHV [MJ/kg]	Average LHV [MJ/kg]	Average sulfur content [%]	Avrage ash content [%]	Average humidity [%]	Avrage ash content [kg]
2 647,00	-	15,89	0,11%	4,36%	34,50%	115,38

Fig. 2 Calculation of properties of hybrid biomass pellets made from Miscanthus, Jerusalem artichoke, grass and sawdust
Source: Author's

The calculator was already used in research on composite pellets. It gives accurate results for a pellet production line with an output of 1500 kg/h. A plan for further development of the calculator includes adding modules of several different size of production lines to improve results of the calculations for smaller and larger flows of biomass. We are also going to continuously validate all algorithms using the results of tests of new composite pellets, produced in different pellet production lines with different line sizes and substrates of the pellet.

At the current stage, the calculator is mainly used in industrial research to estimate the parameters of a pellet and to optimize its composition. It seems it would be valuable to develop a substrates database and add more components, including atypical ones like industrial wastes from the wood industry, paper industry, or textile industry, sewage sludge, or green waste from cities. This would apply the calculator not only to industrial research, but also for estimation of an energy potential of a given area, such as that of a city or an industrial park.

In sum, the Biomass Calculator estimates quality parameters of designed composite pellets. The input of the Biomass Calculator application are the quality parameters of tested biomass components, such as calorific value, moisture content, ash content and sulfur content.

The composition of tested biomass need to be updated in the application by entering the weight of individual biomass components (in kg). The outputs of the application are the quality parameters of pellet composed of input materials in given proportions. Input data can be modified or adjusted to determine the most suitable composition that meets the required quality parameters. Examples of calculations done in the biomass calculator are shown below. In these examples, the production of pellets composed of 25% wood, 25% miscanthus (energy plant) and 50% mown grass are proposed.

Technical aspects of pellet production lines

On the Polish market, there is a wide diversity of pellet producing technological lines. The most common division among them is based on the material they operate on and production capacities. Large technological lines are able to produce over a dozen of tones per hour, which is an impressive feature even if compared with western and American technologies, especially if one takes into account that this kind of facility was introduced in Poland almost 15 years later.

Two of the most common materials of which Polish pellet is made is straw and wood. Scientific studies are currently conducted on a 3rd type of fuel called urban biomass, such as branches, boughs, mown grass, weeds and other biomass found in cities. Thus far, the economical aspect of such pellet is questionable, and until the final report is ready it is impossible to elaborate on the economical aspect of this matter.

The first material that is commonly used in Poland in the process of pellet production is straw. Poland is a highly developed agriculture region that is rich in this kind of biomass. Another large part of the market belongs to wood pellets. These pellets are made either from leftovers of wood from mills or other production facilities. Due to the high competition on the market and growing market needs, producers often use forest wood, which is harder to process. The third category of pellet source material is urban biomass. This sector is rather unexplored and could potentially be very profitable, depending on the economical and caloric aspects of pellets.

There is hardly a typical pellet producing line, and lines designs are bases on the specific materials that the producer wants to process. Therefore, pellet producing lines destined to process forest wood shall be equipped with several devices that are not required by the enterprise producing furniture. For scientific reasons, we shall cover all the required devices below [56]:

1. Debarker- this device is useful for the production of pellets from forest wood. After the material is acquired from the forest it is very often dragged via forest roads for several hundred meters or even further. This enables sand to invade the bark. Sand is a highly undesired material in pellet production and bark makes the final pellets look darker, which is not welcomed by the buyers. The best way to avoid sand and bark is to remove it completely.
2. Wood chipper- this kind of machine is required to preprocess wood. There are sever kinds of chippers. depending on the cutting technology and scale of the material. As a desired product, pellet producers require the smallest clean wood chips as possible. On the picture below, one can observe operating a mobile wood chipper.
3. Wood crusher- this kind of device sometimes replaces the before mentioned wood chipper. The principle of operation is the same; however, if the material provided is small enough, investors can omit the expensive wood chipper by mounting a larger wood crusher into the pellet producing line.
4. Separator- device which separates proper fuel from undesired particles such as stones, rocks, metals, and glass. A separator is a mandatory device for processing weeds.
5. Strawchopper/grinder – before drying straw, it needs to be cut and ground into smaller particles. A commonly used device to archive this goal is a strawchopper/grinder, which is a variation of the strawchopper used in agriculture. The material is shredded and cut/ground into smaller bits to provide a more efficient drying process, and counter the possible problems that might occur in the dryer – small bits are more easily processed by the drying infrastructure. Depending on the size of provided material packages, a strawchopper/grinder might have significant dimensions and power consumption. The main reason for the production of large dimensions strawchoppers /grinders is the need to provide as compatible device as possible to most common solutions already operating on the agriculture market.
6. Dryer – When the material has desirable dimensions, it can be processed by the drying machinery. There are several types of dryers. However, the principal in all of them is alike: material is dried and when it is moisture free (10%-15%) it can be pelletized. As mentioned before, there are several kinds of dryers which operate on different bases. The mechanism of supplying a dryer in either heat or air might vary, as well as the method of material transportation within the drying facility. After the drying process material is either reground or if the dimensions are appropriate, it is directly transported into a pelletizer unit.
7. Pelletizers – These machines vary depend on size and construction. The idea of operation is to squeeze the disordered material thru a matrix that results in gaining the desired length and diameter pellet. To

archive this goal, operating staff needs to both provide proper material and have the pelletizer set to process material with strict parameters.

After the pellet is "produced" by the pelletizing unit it needs to be cleared from the dust and cooled. The cooling process can be done either mechanically by the blowers which blow air into the pellet that cools it or passively, for example by the long transportation conduct that is between the pelletizer and the storage unit.

Among the problems encountered during pelletizing mixed materials, the first question that arises is, "What is mixed material"? By the phrase mixed material, we understand weeds, grass, and wood bits. These materials are mixed together and induced in to the line. There are several difficult stages when mixed material is provided to the pellet production line. First, although pelletizing mixed materials is possible, if the process is to be conducted fast, an undisturbed proportion of the mix should be strictly maintained to avoid recalibrating the machines. This can prove to be quite difficult in non-laboratory conditions when several hundred kilograms or even more of material is processed on a daily basis. The mix should also contain up to 15-20% of added material. For example, the main 80-85% of material should be wood chips and 15-20% should be mown grass. Another problematic part of the drying unit which can cause many difficulties, since the particles of the mix and the humidity are different. Extreme lighter particles can stand over the dryer for an extended period of time and ignite.

If both the before mentioned difficulties are avoided, the pelletizing process should be conducted without obstacles. As the product is considered a mixed origin pellet, it is suspected to be less caloric than wooden pellets and the color of the material to be not as light, which can be a factor of choice for the final user.

Summary

Considering the quality parameters of selected elements of the biomass, production simplicity of pellets from such material and legal regulations related to processing and combustion of bio-waste and biomass, it can be stated that the production of such pellets is beneficial for the economy.

It not only solves the problem of unmanaged bio-waste, but also provides a new product on the energy market in the form of biocomposite pellets. Quality parameters of such pellets may be similar to parameters of wooden pellets available on the market and additionally do not pollute the environment.

The production of such pellets will require using a special matrix to form pellet granules in pellet production lines, which would be more suitable for soft vegetables, not for hard woods. However, that would be the only necessary modification of the existing pellet production lines needed.

There is no need for any additional binders or other chemicals to form such pellets. The only disadvantage of the pellets is the high content of ash produced during the combustion process. However, this can be eliminated or significantly reduced by applying dedicated stoves that are suitable for this specific type of pellet. It is possible that in the future such a pellet will revolutionize the European energy market and solve the problem of disposal of organic waste at the same time.

References

[1] Act dated December 14, 2012 on waste (Journal of Laws of 2013. item 21, 888, 1238, of 2014 item 695, 1101, 1322, of 2015 item 87, 122, 933, 1045, 1688, 1936, 2281).
[2] The Act of 25 August 2006 on biocomponents and liquid biofuels (consolidated text Journal of Laws of 2015, item 775, amendments in the Journal of Laws of 2016, item 266, 1165).
[3] Regulation of the Minister of Economy on the detailed scope of obligations for the obtainment and presentation for remission of certificates of origin, payment of the substitute fee, purchase of electricity and heat generated from renewable energy sources and the obligation to confirm the data concerning the amount of electricity generated from a renewable energy source (Journal of Laws of 2012. item 1229 of 2013 item 1362, of 2014 item 1688, 671, 1912).
[4] Regulation of the Minister of Environment of 4 November 2014 on emission standards for certain types of installations, sources of combustion of fuels and equipment for incineration or co-incineration of waste (Journal of Laws of 2014, item 1546).

[5] Directive of the European Parliament and of the Council 2010/75/EU of 24 November 2010 on industrial emissions (integrated pollution prevention and control) (Official Journal of the EU L 334 of 17.12.2010, 17-119).
[6] Directive of the European Parliament and of the Council 2009/28/EC of 23 April 2009 on the promotion of the use of energy from renewable sources and amending and subsequently repealing Directives 2001/77/EC and 2003/30/EC (Official Journal of the EU L 140 of 05.06.2009, 16-62).
[7] Regulation of the European Parliament and of the Council No 1069/2009 laying down health rules as regards animal by-products and derived products not intended for human consumption and repealing Regulation (EC) No 1774/2002 (Animal by-products Regulation) (Official Journal of the EU L 300 of 14.11.2009, 1-33, as amended).
[8] Regulation of the European Parliament and of the Council No 1099/2008 of 22 October 2008 on energy statistics (Official Journal of the EU L 304 of 14.11.2008, 1-62).
[9] I. Niedziółka, M. Szpryngiel, M. Kachel-Jakubowska, A. Kraszkiewicz, K. Zawiślak, P. Sobczak, R. Nadulski, Assessment of the energetic and mechanical properties of pellets produced from agricultural biomass, Renewable Energy 2015, 76, 312-317
[10] S. Obidziński, Pelletization of biomass waste with potato pulp content, International Agrophysics, Volume 28, Issue 1, 85–91
[11] S. Obidziński, J. Piekut, D. Dec, The influence of potato pulp content on the properties of pellets from buckwheat hulls, Renewable Energy 2016, 87, 289-297
[12] Mariusz J. Stolarski, Stefan Szczukowski, Józef Tworkowski, Michał Krzyżaniak, Paweł Gulczyński, Mirosław Mleczek, Comparison of quality and production cost of briquettes made from agricultural and forest origin biomass, In Renewable Energy, Volume 57, 2013, Pages 20-26
[13] Agnieszka Kijo-Kleczkowska, Katarzyna Środa, Monika Kosowska-Golachowska, Tomasz Musiał, Krzysztof Wolski, Combustion of pelleted sewage sludge with reference to coal and biomass, In Fuel, Volume 170, 2016, Pages 141-160
[14] Agnieszka Kijo-Kleczkowska, Katarzyna Środa, Monika Kosowska-Golachowska, Tomasz Musiał, Krzysztof Wolski, Experimental research of sewage sludge with coal and biomass co-combustion, in pellet form, In Waste Management, Volume 53, 2016, Pages 165-181
[15] Ciesielczuk, T. , Karwaczyńska, U. , Sporek, M., The Possibility of Disposing of Spent Coffee Ground With Energy Recycling, Journal of Ecological Engineering, 2015, Vol. 16, 133--138
[16] Wojciech Cichy, Magdalena Witczak, Małgorzata Walkowiak, Fuel Properties of Woody Biomass from Pruning Operations in Fruit Orchards, BioResources, 2017, Vol. 12, 6458-6470
[17] M. Parikka, Global biomass fuel resources, Biomass and Bioenergy, 2004, 27, 613-620.
[18] British Petroleum, BP Statistical Review of World Energy, London, June 2015.
[19] R. Slade, R. Saunders, R. Gross, A. Bauen, Energy from biomass: the size of the global resource, Imperial College Centre for Energy Policy and Technology and UK Energy Research Centre, London, 2011.
[20] World Energy Council, World Energy Issues Monitor, London, 2014.
[21] Central Statistical Office, Statistical Yearbook of Environmental Protection, Warsaw 2015.
[22] G. Wielgosiński, Pollutant Formation in Combustion Processes. - in: Advances in Chemical Engineering, Zeeshan Nawaz & Shahid Naveed (Ed.), InTech Rijeka 2012, 295-324.
[23] H.L. Chum, R.P. Overend, Biomass and renewable fuels, Fuel Processing Technology 2001, 71, 187-195.
[24] L.I. Darvell, J.M. Jones, B. Gudka, X.C. Baxter, A. Saddawi, A. Williams, A. Malmgren, Combustion properties of some power station biomass fuels, Fuel 2010, 89, 2881-2890.
[25] S.V. Vassilev, D. Baxter, L.K. Andersen, C.G. Vassileva, T.J. Morgan, An overview of the organic and inorganic phase composition of biomass, Fuel 2012, 94, 1-33.
[26] S.V. Vassilev, C.G. Vassileva, V.S. Vassilev, Advantages and disadvantages of composition and properties of biomass in comparison with coal: An overview, Fuel 2015, 158, 330-350.
[27] A. Demirbas, Combustion characteristics of different biomass fuels, Progress in Energy and Combustion Science 2004, 30, 219-230.
[28] B.M. Jenkins, L.L. Baxter, Jr.T.R. Miles, T.R. Miles, Combustion properties of biomass, Fuel Processing Technology 1998, 54, 17-46.
[29] A.M. Kanury, Combustion characteristics of biomass fuels, Combustion Science and Technology 1994, 97, 469-491.
[30] H. Heykiri-Acma, Combustion characteristics of different biomass materials, Energy Conversion Management 2003, 44, 155-162.
[31] R. van den Broek, A. Faaij, A.D. van Wijk, Biomass combustion for power generation, Biomass and Bioenergy 1996, 11, 271-281.

[32] C. Yin, L.A. Rosendahl, S.K. Kær, Grate firing of biomass for heat and power production, Progress in Energy and Combustion Science 2008, 34, 725-754.
[33] A.A Kahn, W. de Jong, P.J. Jansens, H. Spliethoff, Biomass combustion in fluidized bed boilers: potential problems and remedies, Fuel Processing Technology 2009, 90, 21-50.
[34] D.I. Barnes, Understanding pulverised coal, biomass and waste combustion – A brief overview, Applied Thermal Engineering 2015, 74, 89-95.
[35] D.A. Tillman, Biomass cofiring: the technology, the experience, the contribution consequences, Biomass and Bioenergy 2000, 19, 365-384.
[36] R. Garcia, C. Pizarro, A. Alvarez, A.G. Lavin, J.L. Bueno, Study of biomass combustion wastes, Fuel 2015, 148, 152-159.
[37] A. Demirbas, Sustainable cofiring of biomass with coal, Energy Conservation and Management 2003, 44, 1465-1479.
[38] M. Sami, K. Annamalai, M. Wooldridge, A review of cofiring of coal: bio-solid fuels cofiring, Progress in Energy and Combustion Science 2001, 27, 171-214.
[39] L. Baxter, Biomass-coal co-combustion: opportunity for affordable renewable energy, Fuel 2005, 84, 1295-1302.
[40] S.G. Sahu, N. Chakraborty, P. Sarkar, Coal-biomass co-combustion: An overview, Renewable and Sustainable Energy Reviews 2014, 575-586.
[41] E.A. Sondreal, S.A. Benson, J.P. Hurley, M.D. Mann, J.H. Pavlish, M.L. Swanson, Review of advances in combustion technology and biomass cofiring, Fuel Processing Technology 2001, 71, 7-38.
[42] T. Nussbaumer, Combustion and co-combustion of biomass: fundamentals, technologies and primary measures for emission reduction, Energy and Fuels 2003, 17, 1510-1521.
[43] E. Hughes, Biomass co-firing: economics, policy and opportunities, Biomass Bioenergy 2000, 19, 457-65.
[44] J.M. Jones, A.R. Lae-Langton, L. Ma, M. Pourkashanian, A. Williams, Pollutants generated by combustion of solid biomass fuels, Springer Verlag London 2014.
[45] P. Samaras, G. Skodras, G.P. Sakellaropoulos, M. Blumenstock, K.W. Schramm, A. Kettrup, Toxic emission during co-combustion of biomass-waste wood-lignite blends in an industrial boiler, Chemosphere 2001, 43, 751-755.
[46] J.M. Williams, L.M. Jones, M. Pourkashanian, Pollutants from the combustion of solid biomass fuels, Progress in Energy and Combustion Science 2012, 38, 113-137.
[47] M. Cerqueira, L. Gomes, L. Tarelho, C. Pio, Formaldehyde and acetaldehyde emissions from residential wood combustion in Portugal, Atmospheric Environment 2013, 72, 171-176.
[48] A. Musialik-Piotrowska, W. Kordylewski, J. Ciołek, K. Mościcki, Characteristics of air pollutants emitter from biomass combustion in small retort boiler, Environment Protection Engineering 2010, 36, 123-131.
[49] A. Demirbas, Hazardous Emissions from Combustion of Biomass, Energy Sources, Part A 2008, 30, 170-178.
[50] C.K.W. Ndiema, F.M. Mpendazoe, A. Williams, Emission of pollutants from a biomass stove, Energy Conversion and Management 1998, 39, 1357-1367.
[51] E.D. Lavric, A.A. Konnov, J. De Ruyck, Dioxin levels in wood combustion – a review, Biomass Bioenergy 2004, 26, 115-145.
[52] B. Schatowitz, G. Brandt, F. Gafner, E. Schlumpf, R. Bühler, P. Hasler, T. Nussbaumer, Dioxin emissions from wood combustion, Chemosphere 1994, 29, 2005-2013.
[53] G. Wielgosiński, P. Łechtańska, O. Namiecińska, Emission of some pollutants from biomass combustion in comparison to hard coal combustion, Journal of the Energy Institute 2016, 89, in press.
[54] J. Morell, K. Hill, All About Pellet Stoves, This Old House Magazine, 2012.
[55] P. Frederick, 2012 VT Wood Chip & Pellet Heating Conference, Biomass Energy Resource Center, January 2012.
[56] R. Fuller, Pelleting Process, University of Illinois, December 2011.
[57] Wood pellets standard EN 14961-2.